Teresa De Cicco, M.Sc.

“The role of the actin-remodeling proteins Cap2 and Cttn in the development of the neuromuscular synapse”

Ph.D. thesis

Completed at the Łukasiewicz Research Network - PORT
Polish Center for Technology Development and

Nencki Institute of Experimental Biology

Supervisor Dr hab. Tomasz J. Prószyński

Institute of Immunology and Experimental Therapy
Polish Academy of Sciences

Acknowledgements

I would like to thank:

My supervisor, Dr. hab. Tomasz J. Prószyński, for the years of mentoring that enabled me to grow professionally and for the limitless enthusiasm in science that supported my PhD projects.

The Hirszfeld Institute, for giving me the chance to defend this thesis.

Professor Dr. Marco Rust and Dr. Lara-Jane Kepser from the University of Marburg, for the possibility to collaborate on the study of CAP2, share passion to science, and their help in developing and shaping my own project.

Professor Dr. Klemens Rottner, from Technische Universität Braunschweig, for the share of precious tools to develop Cttn project.

Members of the lab of Synaptogenesis at PORT, present and former, for the support in new challenges and the scientific discussions.

Members of the lab of Synaptogenesis at the Nencki Institute for the unforgettable good times in a happy lab and for the team spirit during difficulties. Special thanks to Agata Błażewicz and Agata Litwinowicz for the infinite human understanding and compassion that I could have never imagined to experience in a competitive work environment and for their precious friendship that still lasts.

The next-door lab mates for their salvific presence during my PhD studies as international student:

Roberto Pagano for sharing reagents, expertise, honest opinions at work, and deep friendship afterwork.

Giuseppe Giuffrida, known as Simon, for the revelation of the golden rules to deal with failed experiments: "Run around the building", "It's fiiiiine", "Breath-in/beath-out", and "Pontious Pilate", for the politically committed talks during lunch breaks, and the amazing friendship afterwork.

Anastasiia Bohush, Izabella Jasyk, Niels André, Miguel Lermo, Shila Mitra for the special good times together.

My family, for giving me the freedom to make my own choices and learn from my own mistakes. For instilling the values of education, knowledge, and respect of the others.

Artur, for the IT devices that facilitated my home-writing and the moral support during the final stages of my PhD.

My sister Chiara, for bringing brightness to each visit paid me in Poland.

My old friends Alessandra, Nina, Hanna, and Maria, for being always close during these long years I've been away.

This thesis is dedicated to all PhD students whose passion for science and integrity endured numerous vicissitudes of their PhD path.

Achievements

Kepser, L.J., Damar, F., **De Cicco, T.**, Chaponnier, C., Prószyński, T.J., Pagenstecher, A. and Rust, M.B. (2019). "CAP2 deficiency delays myofibril actin cytoskeleton differentiation and disturbs skeletal muscle architecture and function". Proceedings of the National Academy of Sciences, 116(17), pp.8397-8402.

Bernadzki, K.M., Daszczuk, P., Rojek, K.O., Pęziński, M., Gawor, M., Pradhan, B.S., **De Cicco, T.**, Bijata, M., Bijata, K., Włodarczyk, J. and Prószyński, T.J., (2020). "Arhgef5 binds α-dystrobrevin 1 and regulates neuromuscular junction integrity". Frontiers in Molecular Neuroscience, 13, pp.104.

The National Science Center Research Preludium19 Grant (2020/37/N/NZ3/03855): "The role of the Cap2 protein in the organization of neuromuscular synapses".

Abbreviations

AAV	Adeno-associated virus
ABP	Actin-binding proteins
ACh	Acetylcholine
AChR(s)	Acetylcholine receptor(s)
AChE	Acetylcholine esterase
α-DB1	Alpha-dystrobrevin1
ADP	Adenosine di-phosphate
AIS	Axonal initial segment
AP	Action potential
ATP	Adenosine tri-phosphate
AZ	Active zone
BiFC	Bimolecular complementation fluorescence
BTX	Bungarotoxin
DGC	Dystrophin glycoprotein complex
IF(s)	Intermediate filament(s)
CAP	Cyclase-associated protein
CNS	Central nervous system
Cttn	Cortactin
Dok7	Docking protein 7
ECM	Extracellular matrix
LRP4	Lipoprotein receptor-related protein 4
MACF1	Microtubule-actin cross-linking factor 1
MHC	Myosin heavy chain
MN(s)	Motoneuron(s)
MuSK	Muscle-specific kinase

MT(s)	Mictrotubule(s)
NGS	Normal goat serum
NF	Neurofilament
NPF(s)	Nucleation promoting factor(s)
N-Wasp	Wiscott-Aldrich Syndrome protein
PFA	Paraformaldehyde
PNS	Peripheral nervous system
SDS-PAGE	Sodium dodecyl sulfate polyacrylamide gel electrophoresis
SEM	Standard error of mean
Sol	Soleus
SM	Sternomastoid
SV	Synaptic vesicles
SV2A	synaptic vesicle protein 2
TA	Tibialis anterior
Tn	Troponin
Tm	Tropomyosin
Tris-HCl	Hydroxymethyl aminomethane hydrochloride
VN	Venus

Abstract

The neuromuscular junction (NMJ) is a peripheral synapse that connects motor neurons with a highly specialized zone of skeletal muscle fibers and governs essential life functions such as movements and breathing. Structurally, the NMJ is a tripartite functional unit where motoneurons, post-synaptic specialization, and terminal Schwann cells participate to the neuromuscular signaling. The development of NMJ is a multi-stage process that is crucial for the healthy functioning of the synapses.

The cyclase-associated protein 2 (CAP2) and Cortactin (Cttn) are actin-binding proteins (ABPs) that participate to the dynamics of actin-cytoskeleton remodeling by sustaining separate mechanisms. CAP2 is known to be involved in "actin-treadmilling" by promoting the disassembly of filamentous actin (F-actin) at its pointed-end. Furthermore, CAP2 participates in parallel to the mechanism of globular actin (G-actin) recharging, an essential step for the re-incorporation of actin monomers within the filaments. Whereas, Cttn, participates to the action of Arp2/3 complex, thus it is implicated in remodeling mechanism that polymerases branches of actin from a pre-existing filament and increases the complexity of actin-meshwork.

Actin cytoskeleton underpins multiple stages of synaptic formation, participating to both pre-synaptic and post-synaptic events. Furthermore, actin-cytoskeleton is important for maintenance of synaptic integrity through lifespan. The disruption of actin dynamics impairs the healthy functioning of these synapses. In vertebrates, CAP2 is expressed in muscles and the heart and the brain, suggesting a specific role in these organs. My study provide in-depth characterization of CAP2 phenotype at the peripheral synapses and I reported that CAP2 is a novel key organizer of NMJ.

The dystrophin-glycoprotein complex (DGC) is a transmembrane multi-protein complex that stabilizes the post-synaptic apparatus of NMJ by linking the extracellular matrix (ECM) to the intracellular cytoskeleton. Our long-term studies focus on the understanding the molecular functions of one core DGC cytoplasmic components, named α-Dystrobrevin 1 (αDB1), which plays a role in synaptic stabilization. αDB1 functions as a recruiter for peripheral partners of the DGC at the NMJ and Cttn emerged as interactor of αDB1 from our preliminary screening based on mass spectrometry. In my study revolving around the role of Cttn at NMJ, I confirmed that Cttn is interactor of αDB1 at NMJ and provided deep characterization *in vivo*.

Streszczenie

Złącze nerwowo-mięśniowe (NMJ) to wyspecjalizowany typ synapsy w obwodowym układzie nerwowym, łączący aksony neuronów ruchowych z włóknami mięśni szkieletowych. Przekazywanie sygnałów na tych połączeniach umożliwia skurcz mięśni, a tym samym podstawowe funkcje życiowe, takie jak ruch i oddychanie. Strukturalnie NMJ składa się z zakończenia presynaptycznego na neuronie, maszynerii postsynaptycznej na włóknach mięśniowych oraz z komórek Schwanna, które pokrywają aksony neuronów motorycznych. Rozwój NMJ to wieloetapowy proces, który ma kluczowe znaczenie dla prawidłowego funkcjonowania synaps.

Cytoszkielet aktynowy pełni ważne funkcje w tworzeniu i funkcjonowaniu synaps, regulując zarówno maszynerię presynaptyczną, jak i postsynaptyczną. Zakłócenie dynamiki aktyny upośledza prawidłowe funkcjonowanie złącz nerwowo-mięśniowych i zdolności lokomotoryczne organizmu. Przedstawione w niniejszej rozprawie badania dotyczą poznania funkcji dwóch białek regulujących cytoszkielet aktynowy, białka 2 związanego z cyklazą adeninową (CAP2) oraz kortaktyny (Cttn), w rozwoju NMJ.

CAP2 bierze udział w przebudowie szkieletu aktynowego, poprzez odłączanie cząsteczek globularnej aktyny (G-aktyny) od aktyny fibrylarnej (F-aktyny), na jednym z jej końców. Równolegle uczestniczy w przyłączaniu nowych cząsteczek G-aktyny na drugim końcu F-aktynowego łańcucha. Proces ten umożliwia ponowne włączanie monomerów aktynowych do włókien. U kręgowców CAP2 ulega ekspresji w mięśniach szkieletowych, sercu i mózgu, co sugeruje jego specyficzną rolę w tych narządach. Moje badania wykazały, że białko CAP2 pełni ważną funkcję w regulacji rozwoju złącz nerwowo-mięśniowych. Myszy z delecją genu kodującego CAP2 wykazują morfologiczne zaburzenia w organizacji zarówno części presynaptycznej złącza, jak i aksonów neuronów motorycznych. Zatem CAP2 jest nowym, kluczowym organizatorem NMJ.

Białko Cttn, natomiast, zostało zidentyfikowane przez nasz zespół badawczy jako potencjalnie wiążące się do α-dystrobrewiny 1 (αDB1), cytoplazmatycznego składnika kompleksu dystroglikanu (DGC). DGC jest transbłonowym kompleksem wielobiałkowym, który stabilizuje maszynerię synaptyczną NMJ poprzez oddziaływanie z macierzą zewnątrzkomórkową (ECM) oraz z cytoszkieletem wewnątrzkomórkowym. Białko αDB1 wydaje się działać na zasadzie rusztowania dla peryferyjnych partnerów DGC, w tym dla białka Cttn. W moich badaniach potwierdziłam, że Cttn wiąże się z αDB1 w obrębie NMJ oraz że białko to występuje na NMJ. Używając myszy pozbawionych ekspresji Cttn, pokazałam, że białko to pełni ważną funkcję w organizacji morfologii synaps nerwowo-mięśniowych.

This work was supported by the National Science Centre Research Grants:

UMO-2018/29/B/NZ3/02675 (TJP)

2020/37/N/NZ3/03855 Preludium19 grant (TDC)

1. Introduction……...14
1.1. Nervous system…….....14
1.1.1. Central nervous system……..14
1.1.2. Peripheral nervous system……..14
1.1.3. Neurons……..16
1.1.4. Synapses…….16
1.1.5. Types of neurons……17
1.1.6. Glial cells……...17
1.1.6.1. The astrocytes……...17
1.1.6.2. The oligodendrocytes……...18
1.2. Neuromuscular junction…….19
1.2.1. The structure of NMJ……..19
1.2.1.1. Pre-synaptic terminal……...20
1.2.1.2. Myelinating and non-myelinating Schwann cells…….21
1.2.1.3. Synaptic cleft……22
1.2.1.4. Post-synaptic terminal……..23
1.2.1.4.1. AChR and Rapsyn…….23
1.2.1.4.2. $Na_{v1.4}$ and Ankyrins……...24
1.2.2. Neuromuscular transmission……..25
1.2.2.1. Cholinergic signal transmission……...25
1.2.2.2. Excitation-contraction coupling……...25
1.2.2.3. Sarcomere contraction……..26
1.2.3. NMJ development……..28
1.2.3.1. Embryonic development……..28
1.2.3.2. Post-natal development……30
1.2.3.2.1. Synaptic elimination…….30
1.2.3.2.2. Fetal to adult AChR maturation……30
1.2.3.2.3. Plaque-to-pretzel transition……...31
1.2.3.2.4. Formation of synaptic folds……..31
1.2.4. Dystrophin-glycoprotein complex…….33
1.2.5. Cultured myotubes as a model to study post-synaptic machinery……...35
1.3. Cytoskeleton……..38
1.3.1. Microtubules (MTs)……...38
1.3.2. Intermediate filaments (IF)…….38
1.3.3. Actin……...38

1.3.3.1. Sarcomere components and structure……...39
1.3.4. Actin-binding proteins (ABPs)……...41
1.3.5. Cortactin……41
1.3.6. Cyclase associate proteins (CAPs)……43
1.3.6.1. Structure of CAPs……43
1.3.6.2. The origin of the name CAP……44
1.3.6.3. Functions of CAPs in actin dynamics……...44
1.3.6.4. CAP2……45
1.3.6.5. CAP2 is a multitask protein……..45

2. Hypothesis……47
2.1. CAP2 is a key NMJ organizer……47
2.2. Cttn is a peripheral partner recruited at the NMJ via αDB1……47

3. Materials and Methods……..49
3.1. Materials……49
3.2. Animal models……...52
3.2.1. CAP2 mouse line genotyping……53
3.2.2. Cttn mice lines genotyping……54
3.2.3. Electrophoresis……...56
3.3. Immunofluorescence……..57
3.3.1. Tissue preparation……..57
3.3.2. Muscle cross-sections……58
3.3.3. Immunostaining……58
3.4. Bimolecular fluorescence complementation (BiFC)……59
3.4.1. Cloning Strategy NEBuilder Hifi assembly……59
3.4.2. αDB1-VN173 construct for BiFC……..60
3.4.3. Cttn-VC155 constructs for BiFC……60
3.4.4. Competent bacteria transformation……63
3.4.5. Cloning verification……...63
3.5. Animal Procedures……64
3.5.1. Mice anesthesia……..64
3.5.2. Plasmid electroporation of TA……...64
3.5.3. Denervation……66
3.5.4. Newborn mice AAV injection……66
3.6. Cell culture……67

3.6.1. Cells transfection……67
3.6.2. Cells lysis……...67
3.7. Co-immunoprecipitation……67
3.7.1. Proteins isolation from cells……...67
3.7.2. Proteins isolation from tissues……68
3.7.3. Magnetic beads preparation……68
3.7.4. Antibody binding……...…68
3.7.5. Coimmunoprecipitation……68
3.7.6. Target protein complex elution……...68
3.7.7. SDS-PAGE……69
3.7.8. Western-blot……...69
3.8. Behavioral experiments……69
3.8.1. The "grip strength" test……...70
3.8.2. The "voluntary wheel" test……70
3.8.3. The "exhaustion" test……71
3.9. Microscopy……72
3.10. Statistics……...72

4. Results……...…73
4.1. CAP2 project……..73
4.1.1. Adult CAP2-KO NMJs are abnormal in size……..73
4.1.2. NMJs fragmentation in CAP2-KO……76
4.1.3. Developmental study of NMJ in CAP2-KO……...77
4.1.4. The small NMJs lay on single fibers……...78
4.1.5. Localization of CAP2 at NMJ……79
4.1.6. Re-expression of CAP2 in CAP2-KO muscles fails to rescue the NMJ phenotype……80
4.1.7. Poly-innervation in CAP2-KO……...…81
4.1.8. Motoneuron defects in CAP2-KO……..82
4.1.9. Axon regeneration after nerve crush……...84
4.2. Cttn project……87
4.2.1. Cttn is enriched at the NMJ……87
4.2.2. Cttn is αDB1 interactor……...88
4.2.3. Cttn interacts with at αDB1 NMJ……89
4.2.4. Cttn-KO phenotype *in vivo*……...*91*
4.2.5. Lack of phenotype in muscle-specific Cttn-KO……..94

4.2.6. Cttn is dispensable for skeletal muscle integrity……95
4.2.7. Locomotion is not affected by Cttn-loss……96

5. Discussion……97
5.1. Summary on molecular functions of CAP2……97
5.2. Summary of the role of CAP2 in muscles and neurons……...97
5.3. CAP2 in human diseases……98
5.4. Summary of NMJ phenotype in CAP2-KO mice……98
5.5. Summary of MNs phenotype in CAP2-KO mice……99
5.6. NMJ phenotype is separate from "ring-fibers"……100
5.7. Elements of developmental delay……100
5.8. Signs of premature aging in CAP2-KO NMJs……..101
5.9. The cross-talk of cytoskeleton networks……..102
5.10. Limitation of the study and future directions……..103
5.11. Highlights of Cttn study……103
5.12. Summary of the role of Cttn at NMJ……...105
5.13. Impact of Cttn in Type I *versus* Type II contractile fibers…...105
5.14. Impact of Cttn at the synapses……106
5.15. Conclusions……107

6. References……...109

1. Introduction

1.1. Nervous system

The vertebrates' nervous system (NS) is divided into central (CNS) and peripheral (PNS), with the CNS consisting of two parts: the brain and the spinal cord (see **Figure 1.1 A**).

1.1.1. Central nervous system

The brain is a complex organ that acquires, integrates, and elaborates information coming from the outside and inside of the organism. Consisting of approximately 100 billion neurons, the brain performs several complex computational tasks that require high levels of organization from specialized brain regions and types of neurons, to local circuits and specific precise neuronal connectivity[1].
The spinal cord of the CNS allows communication between the brain and the body through ascending and descending pathways. The ascending pathways transmit the sensory inputs from the body to the brain such as pain, whereas the descending pathways direct the transmission from the brain to the body, and control voluntary movements (see **Figure 1.1 B)**. Furthermore, the spinal cord is the center of coordination of many reflexes[2].

1.1.2. Peripheral nervous system

The peripheral nervous system (PNS) consists of nerves and ganglia that connect the primary motor cortex of CNS to the rest of the body and mediate the relationship between the environment and the body. Anatomically, the nerves (spinal and cranial) are bundles of neuronal axons that can target muscles, glands, and other organs whereas the ganglia are clusters of cell bodies of the nerves[3].
Functionally, the PNS can be divided into two parts: the somatic nervous system and the autonomic nervous system. The somatic nervous system controls voluntary movements, by targeting the skeletal muscle and consists of both afferent (sensory) and efferent (motor) nerves. The cell bodies of lower motoneurons (efferent bundles) are positioned in the anterior horn of the spinal cord while the cell bodies of sensory neurons (afferent bundles) lie in the dorsal root ganglia. The autonomic system governs the internal organ homeostasis[3].

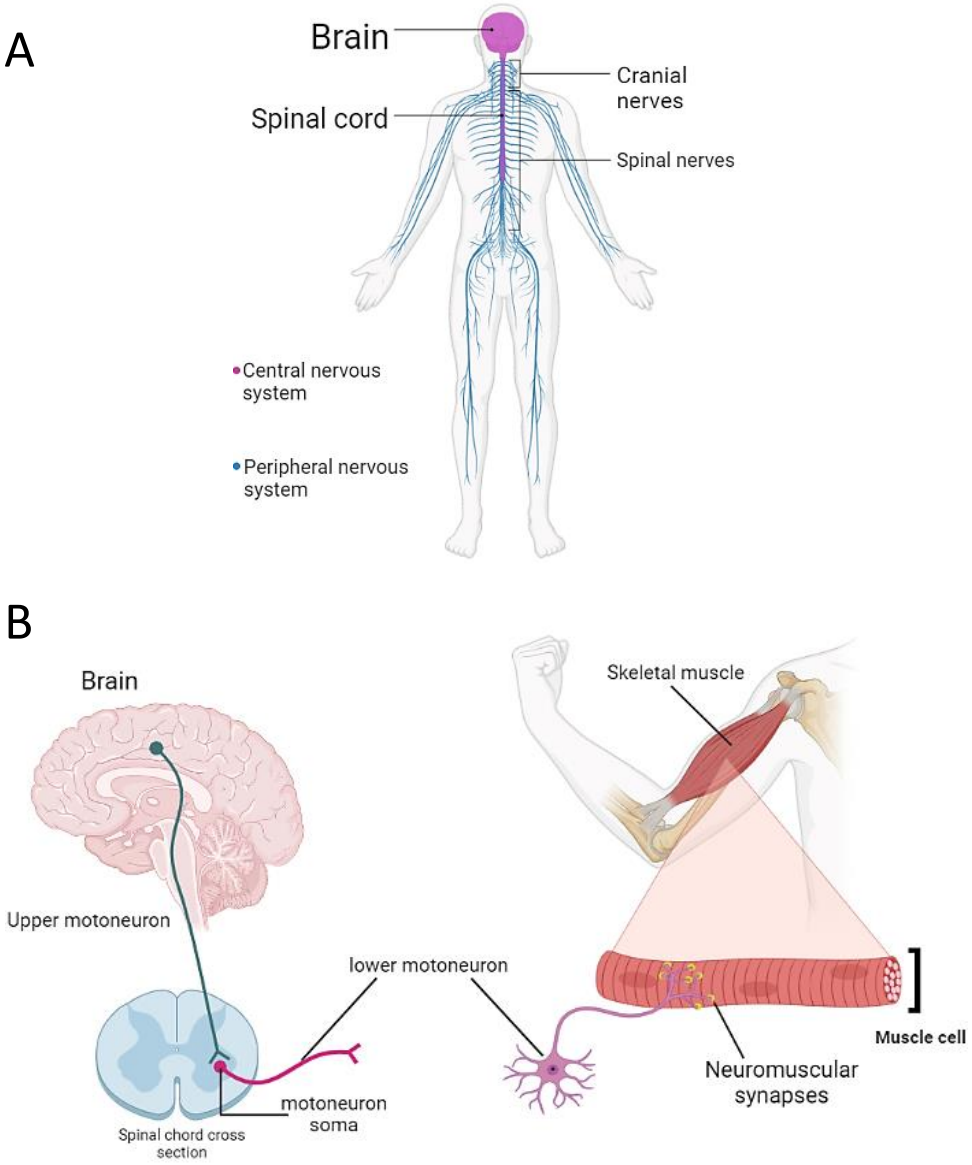

Figure 1.1. Nervous system. A) Illustration of human central and peripheral nervous system. **B**) Motoneurons carry the motor information from the brain to the muscles. Upper motoneurons in the brain connect to lower motoneurons, whose soma is located in the ventral horn of the spinal cord. The soma of lower motoneuron projects its axon to the periphery and takes contact to the muscle fibers. Neuromuscular synapses connect the motoneurons of PNS to the muscle and control voluntary movements (image created in Biorender).

1.1.3. Neurons

Neurons represent the functional cells of the nervous system that form complex circuits through intricate interactions. Neurons are highly polarized cells with specialized cellular domains: cell body, axon, and dendrites, and each part allows them to play specific functions. Termed soma, the neuronal cell body consists of a nucleus surrounded by cytoplasm. The dendrites are branching projections from the soma that are specialized in receiving and processing of information from other cell[4]. On the other side, the axons are neuronal processes that are specialized in signal transmission to the other cells. Situated at the interface between the somatodendritic compartment and the proximal axon, the "axon-initial segment" (AIS) is a 20-60μm sized that separates these two neuronal compartments and it is crucial to maintain cellular polarity both physically and physiologically. The major hallmark of the AIS is high density of Na^+ channels, of which the major present subtypes are $Nav_{1.1}$, $Nav_{1.2}$ and $Nav_{1.6}$ and can differ according to neuron type and developmental stage[5]. At AIS, the Na^+ channels outnumber those of the soma by approximately 50 folds, thus this confers asymmetrical channel distribution. Consequently, this confers lower action potential (AP) threshold to the membrane compared to the somatodendritic domain, which represents the AP firing zone within the neuron. Restricted at the AIS, AnkyrinG (AnkG) is a scaffold protein playing a major in the clustering mechanisms of Na^+ channel clustering at the AIS and in the maintenance of neuronal cell-polarity. Upon lack of AnkG, the Na+ channels fail to aggregate at the AIS and also the proteins restricted to the somatodendritic domain invade the axon[5,6,7].

1.1.4. Synapses

The synapse is the neuronal domain where the cellular communication takes place. Structurally, the synapses are specialized gap junctions formed at site of contact between neurons or neurons and other target cells like skeletal muscles. For efficient signal transmission, the organization of synaptic structure is crucial and implicates close apposition of synaptic terminals. The terminal that sends signals is named "pre-synaptic" whereas the terminal which is targeted by these signals is called "post-synaptic"[4]. The signals in the form of AP travel down the axon and reaches the synapse, where it stimulates the release of the neurotransmitter molecules at the presynaptic sites. The neurotransmitter is captured by the postsynaptic neurotransmitter receptors enabling cellular communication[8,9]. Two types of synapses exist in the nervous system: electrical and chemical, exhibiting different characteristics.

1.1.5. Types of neurons

The nervous system is constituted by different types of neurons which differ for morphology, localization, function or secreted neurotransmitter. For instance, anatomically, motor neurons present a single axon and multiple dendrites, whereas sensory neurons lack dendrites but their axon splits into a central and peripheral branch heading to different environments[10]. Functionally, motoneurons govern voluntary and involuntary movement through the connection of the nervous system to the muscles or the target organs. Instead, sensory neurons are activated by physical (touch, heat) or chemical (taste, smell) stimuli coming from the environment and transmit the signal to the brain[11].

1.1.6. Glial cells

Besides the neurons, the nervous system is built by a second group of non-neuronal cells called glial cells and these are known to outnumber the neuronal cells[12]. The glial cells of the CNS are estimated to occupy a half of the brain volume and are subdivided into astrocytes and oligodendrocytes[12].

1.1.6.1. Astrocytes

The Astrocytes are the most numerous glial cells in CNS and are morphologically characterized by radial processes, which confers to them a typical a star-like shape, and are known to be implicated in a multitude of functions including neuronal metabolism, synaptogenesis and homeostasis. The astrocytes take direct contact with the capillaries within the brain, from which these cells absorb and store nutrients to sustain the brain nutritional needs; astrocytes function as protective barrier for the CNS and filter unwanted substances. Accumulating evidence rewrote the classical paradigm according to which the information flows directionally from pre- to post-synaptic neurons, and led to the conceptualization of "tripartite-synapse", according to which not only are the astrocytes important to maintain adequate environmental conditions for neurons, but these cells also actively participate to synaptic communication[13]. Indeed, the astrocyte processes unsheathe the synapses and establish a close physical interaction with neurons at the synaptic junctions, and this is the site where neuron-astrocyte information exchange occurs[13,14]. The astrocyte express a wide variety of neurotransmitters receptors, including glutamate, acetylcholine, GABA, and endocannabinoids, and this enables their engagement in the synaptic activities. Consequently, the astrocytes respond to the neurotransmitters by increasing the intracellular Ca^{2+}, which stimulates the release of gliotransmitters through which the synaptic signals are integrated and modulated[15,16].

1.1.6.2. Oligodendrocytes

The oligodendrocytes represent the second group of non-neuronal cells in the CNS and are important as they form a highly specialized structured named myelin sheath, which wraps around neuronal axons and creates electrical insulation which is essential for the rapid propagation of the electrical signals[15]. In PNS, Schwann represent the equivalent of oligodendrocytes and these types of cells are called cells, subdivided into myelinating and non-myelinating. The details of these cells will be described later.

1.2. Neuromuscular Junction

1.2.1. Structure of NMJ

The neuromuscular junctions (NMJs) are highly specialized chemical synapses established between the motor neurons in the PNS and skeletal muscle fibers (see **Figure 1.2**). In vertebrates, NMJs control key functions in daily life such as voluntary movement and breathing[17,18]. Easily accessible and large in size, the NMJ has been extensively studied in the past decades and not only has this allowed to explore the molecular mechanisms underlying the NMJ formation and functioning by itself, but it has also enabled to understand the basic principles of synaptic organization and functions that are relevant to synapses in the brain[19]. The NMJ is a occupies less than 0.01–0.1% of the entire muscle fiber surface and exhibits the typical features of a chemical synapses[17]. The neuromuscular synapses can be different between species; for example, NMJs of vertebrates and *C. elegans* are cholinergic synapses whereas fruit fly *Drosophila melanogaster* is glutamatergic. Furthermore, important NMJ's morphological differences exist among species: for example, the human NMJs significantly smaller in size and exhibit more fragmented architecture than murine synapses[20].

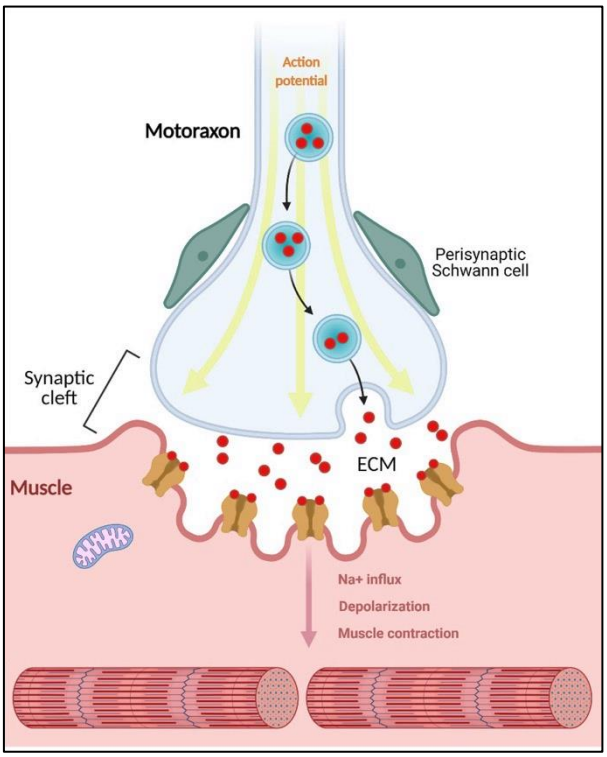

Figure 1.2. NMJ components. The NMJ is a tripartite structure consisting of motor axon (pre-synaptic terminal), post-synaptic machinery laying on a restricted area on the muscle fibers and perisynaptic Schwann cells (PSC) that envelope the synapse (image created by Biorender).

1.2.1.1. Pre-synaptic terminal

The pre-synaptic terminal of NMJ is the domain of motor axons where the electrical signal is turned into chemical (see **Figure 1.3**). Termed "active zone", this structure allows for efficient neurotransmitter exocytosis. The synaptic vesicles (SV) are synthesized at the cell-body, transported to the active-zone, where these are uploaded with ACh and docked beneath the pre-synaptic membrane. The synthesis ex-novo of SV in accompanied by a vesicle recycling system occurring at the axon tip, and this mechanism is responsible to maintain a pool of fusion-competent SV. Such refined organization ensures prompt availability and immediate release of neurotransmitter upon AP stimuli[21,22]. The ACh neurotransmitter is loaded into synaptic vesicles by an ATP-dependent mechanism promoted by the action of vesicular ACh transporters (VAChTs) located at the SV membrane. VAChTs promotes the influx of the neurotransmitter into the vesicles, utilizing the proton electrochemical gradient ($\Delta\mu H^+$) of the SV lumen, generated by action of the vacuolar-type H^+ –adenosine triphosphatase (ATPase)[23]. At the pre-synaptic terminal, the arrival of the AP depolarizes the pre-synaptic membrane, and this triggers the opening of the voltage-gated Ca^{2+}channels (VGCC) causing local influx of calcium ions (Ca^{2+}) into the cytosol. Ca^{2+} is a central signaling molecule as the local increase of the calcium level at the active zone stimulates the exocytosis of SV into the synaptic cleft. SV fusion events are mediated by the Synaptotagmin-1(Syt1), a member of a protein family with calcium-sensitive properties which is embedded at the membrane of SV. The calcium-sensing property of Syt1 resides at its cytoplasmic domains (C2A and C2B) and these domains are also responsible for the interaction with Syntaxin of the Soluble N-ethylmaleimide sensitive factor Attachment protein REceptor (SNARE) complex. Upon Ca^{2+} binding, Syt1 associates with the fusogenic SNARE complex, an heterotrimeric complex involving the vesicle-associated membrane protein (VAMP) Synaptobrevin and the membrane associated proteins called synaptosomal-associated protein of 25 kDa (SNAP-25) and Syntaxin[24,25,26]. Once activated, the SNARE complex promotes the formation of fusion pores at the membrane of the SVs, which then fuse to the pre-synaptic membrane of AZ thus the ACh is exocyted into the synaptic cleft[27].

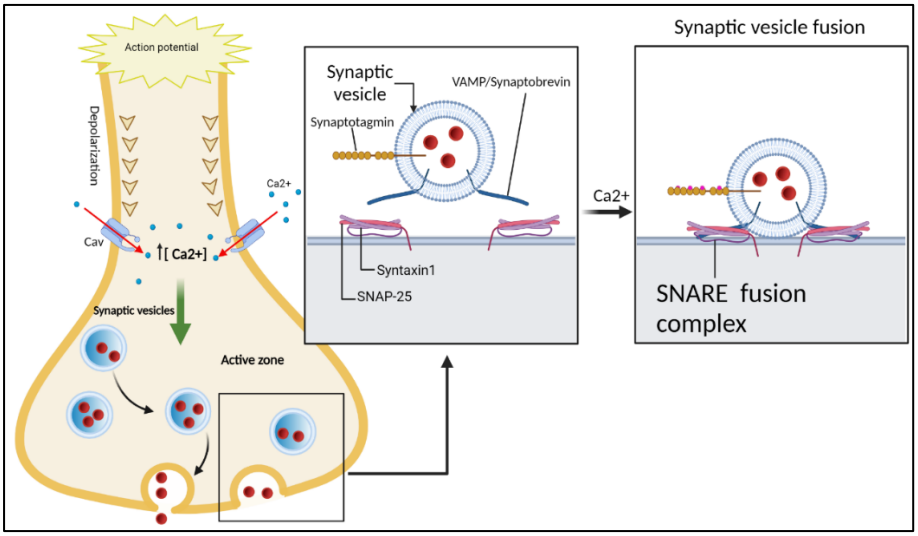

Figure 1.3. The" active zone" (illustration created by Biorender).

1.2.1.2. Myelinating and non-myelinating Schwann cells

Schwann cells are glial cells of PNS subgrouped into myelinating (M-) and non-myelinating (non-M). M-Schwann cells form the myelin sheath that wraps in spiral the motor axon and such evolutionary adaptation has optimized the speed of nerve conduction and enabled the development of a complex nervous system in vertebrates[28]. Along the axon, the myelin sheath, forming the "internodes" that insulate the axon and preventing the leakage of action potential, is discontinued with unmyelinated periodic gaps, called Ranvier's nodes. These nodes are rich of ion channels and at this site the depolarization is rejuvenated. The propagation of action potentials from node to node is called saltatory conduction, and represent an evolutionary adaptation[29]. The M-Schwann cells form multilamellar insulation sheath (internodes) and exhibit compartmentalized cytoplasm with proteins and channels sets differentially expressed in each domain. The cytoplasm of M-Schwann cells is radially organized in "abaxonal domain", which is the most peripheric domain being in contact with basal lamina (BL) and where the nucleus resides, the "compact myelin", representing internal layer of myelin sheath, and "adaxonal domain", the most internal domain separated from the axon by a 15 nm "periaxonal space". Longitudinally, the cytoplasm of M-Schwann cells is organized into: "internodal", that occupies 99% of the myelinating SC length, "paranodal" and "juxtaparanodal". The axon induces M-Schwann cells to myelinate, also dictating the amount of myelin sheath to form, and the neuregulin1 (NRG1) is the best characterized mediator of such axon-glia cells communication[30]. Perisynaptic Schwann cells (PSC or terminal Schwann cells) are non-myelinating glial cells located at the synaptic button and are increasingly emerging as key multiplayer during the development and maintenance of the

NMJs. It has been reported that at the early developmental stage, the PSCs are localized ahead of the axons' tip at the postsynaptic sites. At this site, the PSCs function as a guide for the axon's tip that mediates the contact with the postsynaptic terminals of the muscles. Later during the development, PSCs support the maintenance of the nerve-muscle connection by counteracting the axon destabilization occurring as an effect muscle contraction. Briefly, the neuromuscular signaling results into sarcoplasm [Ca^{2+}] increase, which is essential for myofiber contraction and this is also associated to production and secretion of thrombin. Thrombin is a factor that destabilizes the axon leading to retract from the NMJ[31]. The PSCs prevents axonal withdrawal and stabilize the nerve-muscle connection by secretion of Serpin C1/D1, a thrombin-inhibiting factor[32]. During the NMJ development, PSCs are involved in the process of "synaptic elimination". At the early stages of development, the axon terminals outnumber the synapses and compete to innervate a single post-synaptic endplate. In the context of this developmental process, PSCs promote the "winner" axon among the competitors and degrade the "loser" axons (details described in the next chapters)[31]. Furthermore, the PSCs play also a role in the acetylcholine receptors (ACh) organization and post-synaptic machinery maturation through the secretion of a plethora of factors. Among these, PSCs secrete a specific isoform of agrin that can stimulate the aggregation of receptors, although with lower impact compared to the neuronal isoform[33].

1.2.1.3. Synaptic cleft

NMJs exhibit the typical features of chemical synapses, thus the pre- and post-synaptic terminals of NMJ are interposed by a space called "synaptic cleft", consisting of the extracellular matrix (ECM) through which the acetylcholine neurotransmitter travels. The ECM of NMJ consists of the basal lamina (BL), where hallmark molecules are stably localized. Among these, laminins are muscle-synthesized components of the synaptic cleft, organized in heterotrimeric structures of α, β and γ subunits. The α4, α5 and β2 are specifically enriched at the synaptic cleft and are found to be essential for synaptic formation, development and transmission. Indeed, in α4/α5 laminin double-mutant mice, NMJs form normally but their developmental maturation is delayed. Furthermore, β2-laminin knock-out mice display severe phenotypes with reduced synaptic folding and impaired synaptic transmission[34]. Another well-characterized component enriched the synaptic cleft is Agrin, a nerve-secreted proteoglycan which mediates the aggregation of AChR at the post-synaptic terminal and stabilization (details described later)[35,36,37]. Also, the acetylcholinesterase (AChE) is a hallmark of synaptic cleft specialization: this enzyme hydrolyses the ACh into acetate and choline, thus terminating the transmission signal. For this reason, AChE is central regulator of cholinergic signal at this site (signaling mechanisms described later).

The inhibition of AChE activity increases the ACh persistence at the synaptic cleft and results into prolonged cholinergic signal transmission. In nature, toxins exist which target AChE blocking its activity, and leading to muscle paralysis and eventually death by asphyxiation[38]. However, AChE inhibitors (AChEI) have found successful clinical application in conditions such as Myasthenia gravis (MG), an autoimmune disease resulting from antibodies targeting AChR (most common), leading to the destruction or inactivation of these receptors[39]. AChE is anchored to the BL of the synaptic cleft via CollagenQ (ColQ), a collagenic tail that anchors three AChE tetramers at the synaptic cleft forming an hetero oligomer AChE-ColQ[40]. ColQ deficiency is correlated to AChE decrease at NMJ, which is cause of myastenic syndromes. However, the role of ColQ is not limited to a structural protein, and through the interaction with other partners, ColQ is implicated in NMJ differentiation. In details, ColQ contacts the Muscle-Specific Kinase (MuSK) by its C-terminal and interacts with the dystroglycan via perlecan-binding[41,42,43].

1.2.1.4. Post-synaptic terminal

1.2.1.4.1. AChR and Rapsyn

The postsynaptic terminal of NMJ is a highly specialized area that occupies <0.1% of the muscle fiber surface, that forms characteristic invaginations, termed "synaptic folds" whose function is to increase the total endplate area. Receptors and channels are disposed in specific and well-segregated domains of the synaptic folds (**Figure 1.4**)[21,44]. A high concentration of nicotinic acetylcholine receptors (nACh), situated at the crests of the synaptic folds, represents the major hallmark of the post-synaptic terminal. The estimated density of AChR at NMJ is >10,000/μm^2 against to the <10/μm^2 of the extra synaptic zone in mouse[21,45]. The nAChR is a heteropentameric ion channel consisting of two α1, β, δ, and the fetal γ subunit which is replaced by the adult ε subunit[46,47]. Each AChR subunit consists of an extracellular N- and C-terminal domains, 4 transmembrane segments and a cytoplasmic loop between segment 3 and 4, and this loop is an important regulation site. The mature receptor exhibits two binding sites for the ACh neurotransmitter located at the interface between the α/γ and the α/δ subunits. The AChR clusters juxtapose the motoneuron pre-synaptic AZ and such organization ensures that the site of neurotransmitter release is precisely mirrored by the site where its receptors are highly enriched, thus increasing signal transmission efficacy of the synapse[48,49]. The receptor-associated protein at the synapses (Rapsyn) is a 43 kDa scaffold and signaling protein, known since decades to be direct interactor of AChR and present at equimolar concentration as ACh[50,51]. Rapsyn is a key molecule for the formation of NMJ and in rapsyn-deficient mice the AChR clusters fail to form[52]. The mechanism through which Rapsyn governs the AChR clustering in dependent on the agrin-signalling pathway. Furthermore, Rapsyn anchors and stabilizes the

receptor at the post-synaptic membrane by bridging the receptors to the cortical cytoskeleton, however our insights of Rapsyn function are still limited[51,53,54].

1.2.1.4.2. $Nav_{1.4}$ and Ankyrins

The muscle-specific voltage-gated Na^+ channels ($Nav_{1.4}$) are situated at the folds of NMJ and represent the second important channel type responsible to initiate the depolarization events in muscle. Also enriched at the depths, the Ankyrins (Ank) are a family of scaffolding proteins and organizers of the membrane domains by linking integral membrane proteins to the cortical cytoskeleton. In vertebrates, the three genes ANK1, ANK2, ANK3 encode respectively for AnkR, AnkB, AnkG, generating multiple splicing variants and with different tissue-expression pattern and specific cellular localization[55]. The AnkG splicing variant, AnkG270, localizes at the depths of NMJ post-synaptic folds where it is responsible for Na1.4 channels aggregation and stabilization at the folds depths, along with its binding-partner β-spectrin[56,57]. To ensure proper stabilization, the post-synaptic components are linked to the cytoskeleton and ECM receptor, and this will be discussed in the next chapter[58].

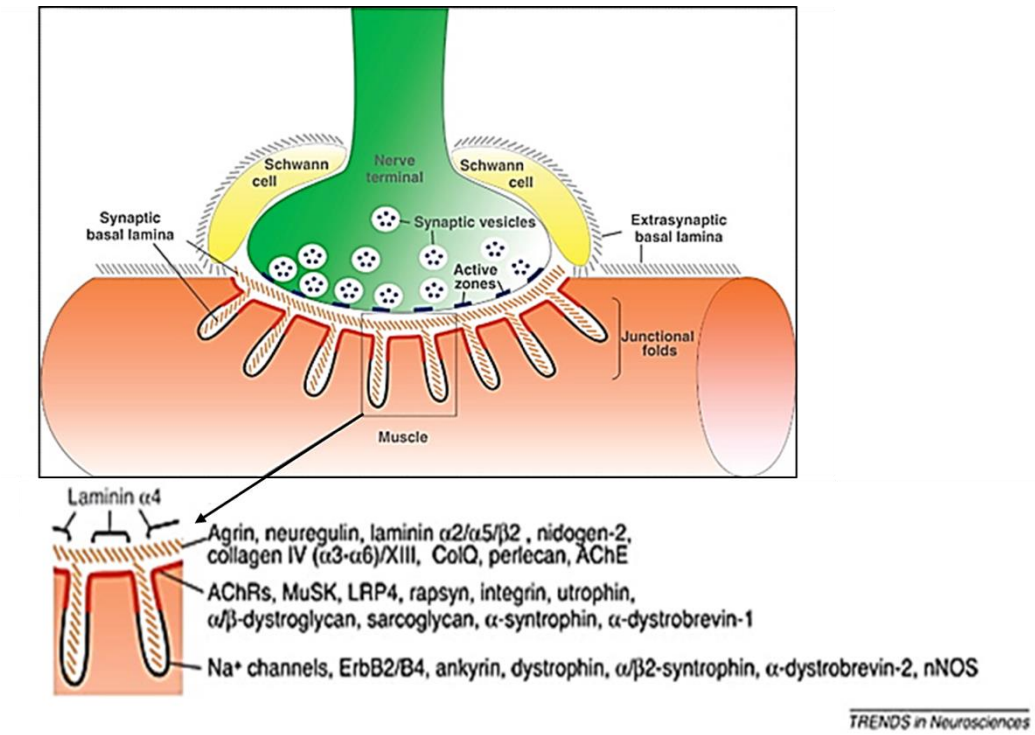

Figure 1.4. Schematic illustration of spacial organization of channels, receptors and key molecules at the post-synaptic terminal of NMJ (image adopted from Shi, Lei, Amy KY Fu, and Nancy Y. Ip, *Trends in neurosciences*, 2012).

1.2.2. Neuromuscular signal transmission

1.2.2.1. Cholinergic signal transmission

The nerve-muscle signal transmission is a multistep process starting with the depolarization of the pre-synaptic membrane that travels down the axons and reaches the motor nerve terminal. The depolarization of the pre-synaptic membrane causes a local Ca^{2+} influx which stimulates the fusion of synaptic vesicles at the active zone, and subsequently release of the acetylcholine neurotransmitter into the synaptic cleft. The ACh molecules enclosed in a single vesicles is termed quantum, and depending on the species, is estimated that one nerve impulse releases of about 20–200 quanta[59]. The ACh neurotransmitter is exocytosed, diffuses through the cleft and rapidly binds to acetylcholine receptors at the post-synaptic terminal[60]. Upon ACh binding, the AChR channels gets opened causing a local Na^{+} ions influx, which activates the voltage-gated Na^{+} channels positioned at the post-synaptic folds depths, and this gives rise to a local depolarization called endplate potential (EPP). The Na^{+} ions current generated by the EPP, propagates down-stream depolarizing the sarcolemma, and this fires the AP. To trigger an AP in muscle, a change of potential from -70 to -50 mV is required, however the high condensation of $Na1.4^{+}$ channels at NMJ, which is estimated to outnumber 10 folds the concentration at extra-junctional sarcolemma, reduces the firing threshold[49]. The duration of cholinergic signal is regulated by AChE, which is responsible to terminate the signal through the hydrolysis of the ACh into Choline and molecules of acetic acid (AA). The choline can be then recycled back to form new neurotransmitter.

1.2.2.2. Excitation-contraction coupling

The excitation-contraction coupling (ECC) is the process by which muscle electrical excitation generates muscle contraction. The AP travels along the sarcolemma and depolarizes the membrane of the transverse-tubules (T-tubules). The T-tubules are invaginations of the sarcolemma inserted between the myofibrils, flanked in both sides by sarcoplasmic reticulum (SR) terminal cisterns, to which they are closely associated, forming the so-called ”triad-junction”. The triad-junction forms a system that plays a central role in muscle contraction as it enables the myocyte to respond to the membrane depolarization with intracellular $Ca2^{+}$ increase, released from the SR, and this signaling molecule is critical to sarcomere contraction[61]. Embedded in the membrane at the T-tubules, the dihydropyridine receptors (DHPR) are tetrameric voltage-gated Ca^{2+} channels , which detects the depolarization and communicates to its partner ryanodine Receptor (RyR1) localized at the SR membrane so that RyR opens and the Ca^{2+} from the reticulum is released into the myoplasm[61,62]. Studies from the past decade identified the

participation of a novel protein named STAC3, within the communication between the DHPR and RyR, thus this highlights that the ECC mechanism is complex and many details are still to be uncovered (**Figure 1.5**)[62].

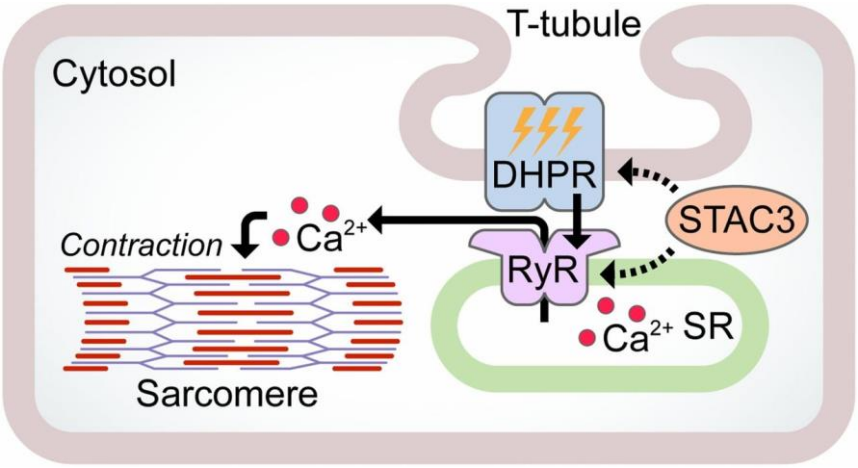

Figure 1.5. Excitation-coupling contraction scheme (adopted from Nelson, Benjamin R. et al., *PNAS*, 2013).

1.2.2.3. Sarcomere contraction

Published in 1954, the "Sliding filament theory" proposed for the first time the molecular basis of contraction, illustrating that sarcomere contraction results from the sliding of "thin" and "thick" filaments parallelly upon each other, thus generating mechanical force (see details in **Figure 1.6**). Thick filaments attach the thin filaments, pull these toward the center of sarcomere and, finally, de-attached in cyclic sequence. The filaments' sliding is achieved due to the property of myosin heads to interact with specific actin's myosin-binding site, thus allowing the formation of cross-bridge, and this binding is Ca^{2+}-dependent. Upon Ca^{2+} signaling, the Tropomyosin (Tm) can regulate the accessibility to myosin-binding site of the actin, thus influencing the possibility of thin and thick filaments to cross-bridge. The Tm exists in three conformational states regulated by Ca^{2+}: blocked, closed and open state. In absence of contractile stimuli, for example during relaxation, the myoplasm [Ca^{2+}] is low: this condition promotes the blocked state of Tm, which makes unavailable the myosin-binding sites within actin thin filaments, thus preventing thin and thick filaments interaction. Upon contractile stimuli, the myoplasm Ca^{2+} concentration increases, and Tm binds Ca^{2+}, thus this causes an azimuthal shift of Tm towards the inner domain of the thin filament which partially exposes the actin sites for myosin-binding. In this state, Myosin globular heads can

only weakly-bind the thin filaments. Subsequently, Tm further shifts and fully uncovers the actin myosin-binding sites, thus this strengthen the thin and thick filaments interactions as additional bonds can be forms. The cross-bridge is an energy-dependent mechanism that relies on the ATPase property of myosin. The phosphorylation of the Myosin the regulatory light-chain (RLC) site induces structural changes of the native form, which regulates the myosin binding capacity. The ATP bound to the myosin RLC is hydrolyzed into ADP +Pi, thus this enables the globular head of myosin to form an interaction with the myosin-binding site of actin-thin filament. Subsequently, the actin-myosin attachment promotes the release of the Pi first and then ADP, which transiently strengthen the actin-myosin interaction. Finally, RCL can bind a new ATP molecule and this binding promotes the detachment of myosin heads from the this filaments and allow this cycle to start again[63].

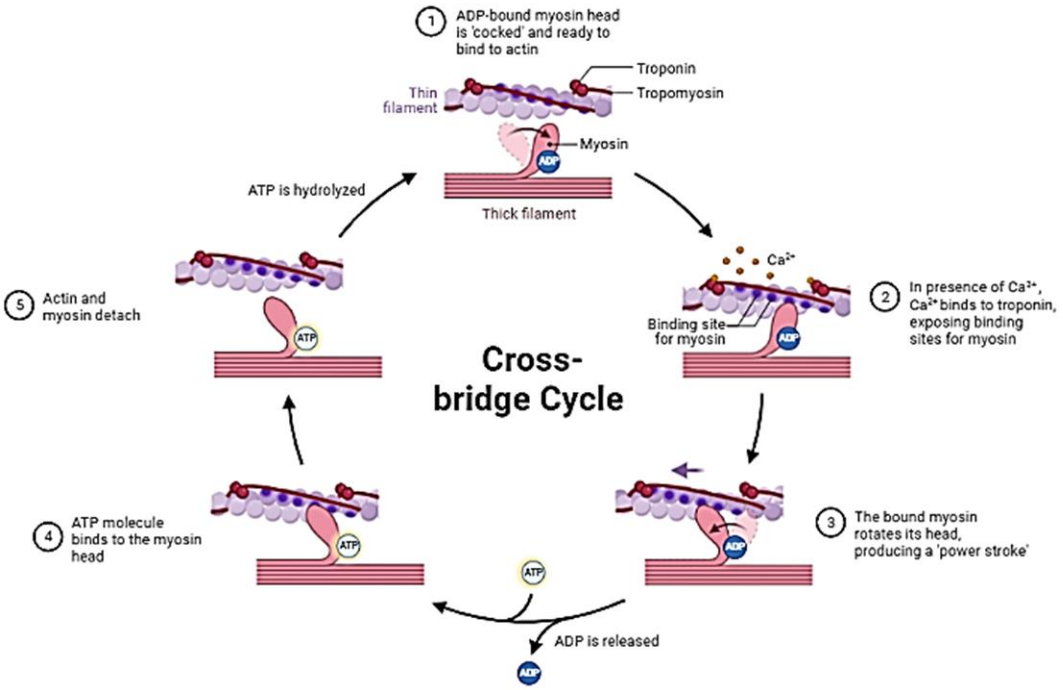

Figure 1.6. Scheme of "The sliding filaments theory" by Lymn and Taylor (image imported from Biorender).

1.2.3. NMJ development

The NMJ is a highly plastic structure which undergoes profound morphological changes across its lifespan from its formation, in the development, in response to injury, and aging[64]. The NMJ development requires the intervention of the pre-synaptic motoneuron and post-synaptic muscle and consists of a multistage process that starts at the embryonal stage and spans the early adulthood. Although the NMJ's morphology in humans are widely different compared to rodents, studies in mice have enabled to understand fundamental mechanisms of NMJ maturation common in both systems[44].

1.2.3.1. Embryonic development

Myogenesis is the differentiation process of skeletal muscle tissue. In mouse, it consists of two waves: primary myogenesis takes place at embryonic days (E) 10.5–12.5 and secondary myogenesis occurring at fetal stage (E14.5–17.5). At around embryonic day 11 (E11), the myoblasts differentiate and fuse to form multinucleated fibers called primary myotubes[65,66].

The high concentration of AChR at the post-synaptic endplate is a complex process to which two mechanisms concur: one is the mechanism that clusters AChR, and the second is the activation of synaptic nuclei which express the AChR subunits, and this counteract the repression of extra synaptic nuclei by action of electrical impulses[67]. By E12.5, primary myotubes start to express AChR which are initially dispersed on myofibers' surface and subsequently spontaneously aggregate into small clusters. The assembly of primitive aneural AChR clusters occurs in a motoneuron-independent manner as it happens prior to innervation. This phenomenon is called "prepatterning" and indicates that myotubes have intrinsic ability to form AChR clusters independently from nerve contribution[68]. Muscle fibers are the long-distance target of motoneurons, whose axons migrate to the periphery to establish synaptic connection[69]. Between day E13.5 and E14.5, the projections of nerve approach the middle region of muscle fibers and innervate some AChR clusters while others remain aneural. By day E18.5 only innervated AChR clusters persist and will develop post-synaptic machinery of NMJs, while those which fail to be innervated are dispersed and the AChR are quickly endocytosed[68,70,71]. Once innervation has occurred, the anterograde and retrograde molecular communication between presynaptic motor terminals and postsynaptic muscle fiber membrane governs different aspects of NMJ further development. Neuron starts to secrete two factors with opposing role on the postsynaptic machinery. The first one is glycoprotein agrin which promotes clustering of AChR (**Figure 1.7**). This protein is also produced by Schwann cells and muscle fibers, but neurons produce a specifically spliced isoform of agrin that is much more potent in promoting postsynaptic organization[72]. Agrin travels through the synaptic cleft to

the postsynaptic part. It is not known how this highly glycosylated protein of 250kDa up to 600kDa finds its way through the 60 nm cleft that is densely packed with ECM, but when it riches the muscle fiber surface where it binds to its major receptor Low-density lipoprotein receptor-Related Protein4 (LRP4)[73]. The binding of Agrin triggers dimerization of LRP4 and its co-receptor Muscle Specific Kinase (MuSK). MuSK dimerizes and rapidly auto-phosphorylates. This phospho-modification increases MuSK's catalytic activity and also provides substrate for the recruitment of binding-partners. The activation of MuSK is a critical step as this initiates a chain of downstream events culminating with the formation of AChR clusters. Rapsyn and Dok7 are direct partner of MuSK, and act downstream to organize the AChR clusters[74,75]. Upon MuSK activation, Rapsyn responds by linking the AChR to cortical actin-cytoskeleton, thus this stabilizes the receptors at the post-synaptic-terminal, while DOK7 is an intracellular activator of MuSK via dimerization which controls and the responsiveness of MuSK to Agrin in AChR clustering[76,77,78,79,80]. The second important postsynaptic organizer released by motor neuron axons is neurotransmitter ACh. On one hand it binds to AChR causing the receptors to open, which initiates action potential and muscle contraction, but on the other hand it triggers AChR endocytosis and removal from the postsynaptic membrane. Therefore, agrin and ACh have opposing roles on the organization of the postsynaptic domain, triggering its formation and disassembly, respectively.

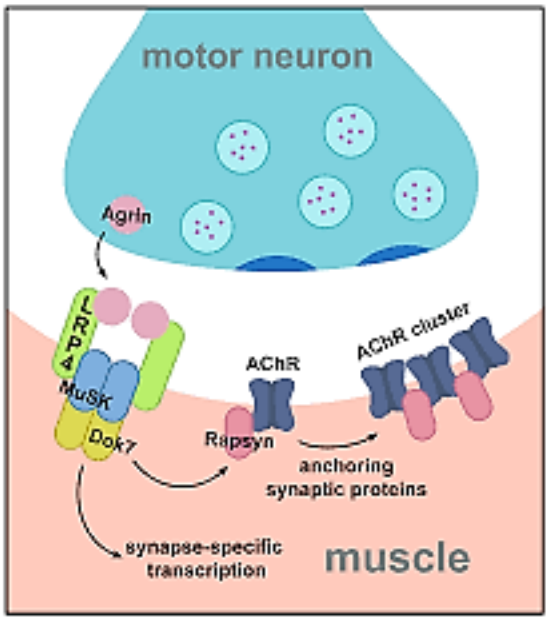

Figure 1.7. Scheme of the agrin-dependent AChR clustering. The neuron-secreted agrin, binds LRP4, coreceptor of MuSK. This stimulates rapid phosphorylation of MuSK which recruits the downstream effectors Dok7 and Rapsyn. Dok7 via Rapsyn interaction, cluster and anchor the AChR at the post-synaptic site. Dok7 also is involved in gene expression of perisynaptic myonuclei (adopted from DePew, A.T. and Mosca, T.J., *Journal of Developmental Biology, 2021*).

1.2.3.2. Post-natal development

1.2.3.2.1. Synaptic elimination

The pre- and post-synaptic endplates are tightly linked and, eventually, reciprocally coordinate with anterograde and retrograde signaling. Therefore, changes orchestrated on the one side of the junction trigger the reorganization on the other. At early post-natal age, the NMJ is poly-innervated by multiple motor axons terminating at the same post-synaptic site. Later during the development, the redundant and immature connections are pruned by a mechanism of competition between nerves called "synaptic elimination". At the end of this process around postnatal day (P)15, only a single "winner" motor axon will occupy the postsynaptic endplate; thus the mature NMJ is monoinnervated[81]. The axon terminals compete to occupy the territory on the postsynaptic machinery and get access to the retrograde signals from muscle, such as the one mediated by β-catenin, thus this consolidates the connectivity with the post-synaptic terminal, leading the axon to prevail in the competition[82]. Furthermore, such consolidation seems to be activity-dependent and recently, the PSCs are emerging to be regulators of this process. Indeed, the PSC express neurotransmitter receptors, and respond to the synaptic stimuli with intracellular Ca^{2+} increase. PSC express muscarinic AChR (mAChR) and purinergic receptors (P2Y1R) which enables these cells to respond respectively to the ACh and ATP molecules released into the cleft by effect of motoneuron activity; the increase of intracellular level of Ca^{2+} levels, stimulates PSCs to the release of ATP in the synaptic cleft, where it is hydrolyzed to ADP, thus this results in the overall increase of the adenosine levels in the synaptic cleft. Motor axons possess different classes of purinergic receptors whose activation is dependent on adenosine levels: low adenosine concentration activates the "inhibitory" A1 purinergic receptors (A1ARs) leading to neuronal depression. However, when the adenosine level is high, a second class of "facilitatory" purinergic receptors (A2ARs) are activated, whose involvement potentiates motor-axon connectivity[83]. The PSCs also regulate synaptic elimination via Neuregulin1 (NRG1)[84].

1.2.3.2.2. Fetal to adult AChR maturation

In mice the process that eliminates the excess of motoneurons coincides with the maturation of AChR: at early-postnatal stage the embryonic γ-subunit is replaced by the ε-subunit within the AChR, and this exchange increases calcium conductance of the channel. The mRNA expression of γ (fetal) and ε (adult) subunits is influenced by signals deriving from the nerve, and it has been found that perisynaptic and extra synaptic nuclei respond differentially to the pre-synaptic signals[85]. The expression of fetal γ-subunit drops postnatally at different time-points according to the muscle fiber type. Indeed, in fast-twitching fibers, the γ-subunit is

no more detectable at P17, while its expression persists longer, up to P50, in slow-twitching fibers[85]. By contrast, the expression of AChR ε-subunit is upregulated by nerve signals, and this event occurs at E17-19, after innervation[86]. The AChRs turnover internalizes the AChRs and directs the receptors to the endocytosis pathway for degradation, so that the fetal version of AChRs are replaced during the development by the mature ones[87].

1.2.3.2.3. Plaque-to-pretzel transition

Furthermore, in rodents, the NMJ undergoes a sequence of structural rearrangements that increase its structural complexity across the development, known as "plaque-to-pretzel" transition. At birth, the NMJ's post-synaptic machinery is simple and oval-shaped; within a few days, the oval structure grows in size and the first perforations start to appear (P10 in **Figure 1.8**). Over the next 2 weeks after birth, the number of perforations increases and the openings fuse together. Full maturation of the NMJ is achieved at early adulthood when post-synaptic machinery exhibits highly branched morphology, often referred to as "pretzel"[88]. Although details of the mechanism involved in the development of elaborated NMJ structure are still not fully-elucidated, it is evident that the remodeling of actin-cytoskeleton is the principal mechanisms underlying the rearrangements of post-synaptic machinery[89]. The NMJ contains an intricate subsynaptic network made of actin and the remodeling of this structure sustains the morphological changes occurring during the development and synaptic plasticity. The F-actin enriched at the post-synaptic apparatus is rearranged in response to the semantogenic signals. For example, the Agrin-activated MuSK induces cortical actin polymerization and this produces propelling force that drives the gathering of AChR into clusters; also, the inhibition of actin polymerization impedes the AChR aggregation[89,90].

1.2.3.2.4. Formation of synaptic folds

The topological rearrangements lead the post-synaptic membrane to form invaginations[91,92]. Comparative studies have shown that NMJs in mammals are different among species, and these differences include neurotransmitter quantal content, size, and ultrastructure[59]. In human adults the NMJs are much smaller and fragmented, this structure is often referred as "en-grape" shape by some authors. Human NMJs also exhibit the largest folds in contrast to rodents or frogs, thus suggesting that the NMJ invaginations might represent a crucial biological advantage within evolution and the ultrastructure maintenance is essential for optimal NMJ functionality[49]. Simplified and reduced folds of NMJ have been observed for autoimmune myasthenic syndromes, and these structural defects are also accompanied by muscle weakness and waste[93]. It is not clear how synaptic

folds form, however some models have been recently reviewed[91]. Additionally, most of the studies on human NMJs comes from amputated limbs from diabetic patients or victims of accidents, cases that do not guarantee that the NMJs are in their original innate state. The post-synaptic invaginations are characterized by channels and proteins specifically localized in such district. The hallmarks of this NMJ folds depths are $Na_{1.4}$ channels, Ank, β-spectrin, dystrophin and dystrobrevin. It is known that during the post-synaptic endplate development, the AChR clustering precedes the Na1.4 channels clustering at the folds depths as this occurs only between 1-2 post-natal weeks[56,57]. At NMJ the muscle-specific variant AnkG270 promotes the Na1.4 channels clustering. In contrast to neurons where AnkG is the sole responsible for Na^+ channels at AIS, at NMJ it has been found that the loss of AnkG can be compensated by AnkB and AnkR variants, and only the concomitant ablation of all the three variants impair the Na^+ channels clustering *in vivo*. Interestingly, a recent finding has shown that although the ankyrins' loss leads to failure of Na^+ channels clustering at NMJs, no structural sign of muscle atrophy has been observed *in vivo*[57]. Furthermore, in the same study, only a higher susceptibility in the context of prolonged locomotion and fatigue through time has been reported. All together, these recent findings have raised a controversial question concerning the significance of Na^+ channels in the motor-neuron communication and the biological significance of membrane folds organization is being recently questioned[57].

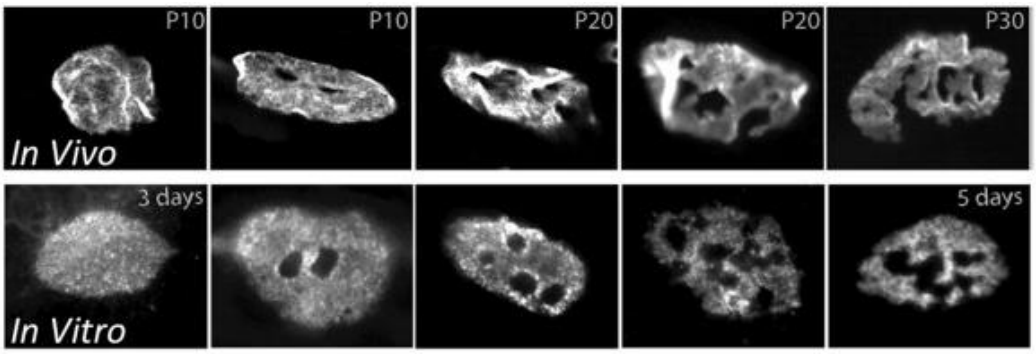

Figure 1.8. Stages of postsynaptic machinery development *in vivo* (top) and in laminin-cultured myotubes (bottom) known as "plaque-to-pretzel" transition (adopted from Bernadzki et al., *European journal of cell biology*, 2014).

1.2.4. The dystrophin-glycoprotein complex

The dystrophin–associated glycoprotein complex (DGC) is a large macromolecular complex spanning the sarcolemma, linking the extracellular matrix to the cortical intracellular actin cytoskeleton (**Figure 1.9**)[58,94]. The DGC plays a vital role for skeletal muscle integrity and has received increasing interest over the past decades as dysfunctions in its components are often associated to muscular dystrophies[94]. At the NMJ, the DGC is involved in many steps of synaptogenesis and NMJ stabilization and maintenance. At the post-synaptic site, the DGC acts extracellularly as a receptor for the axon-secreted Agrin or laminins, and this produces a downstream effect leading to the AChR clustering, while intracellularly, the DGC acts as a scaffold for the recruitment of signaling and cytoskeleton regulating molecules, thus it is central for signal-transduction mechanisms that promote the maturation of the NMJ[58,94]. The complex consists of two classes of components: the core components and the satellite components[58]. Dystrophin, utrophin, dystroglycans, sarcoglycans, sarcospan, syntrophin, and dystrobrevins represent the core components of the DGC, while molecules such as nNOS, GRB2, catulin, and liprin belong to the class of satellite peripheral components[58,95].

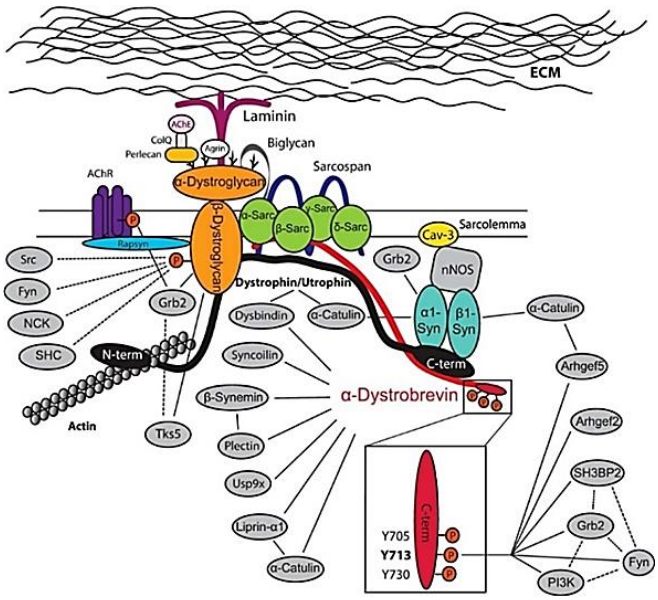

Figure 1.9. Scheme of the dystrophin glycoprotein complex (DGC). The DGC is a transmembrane macromolecular complex connecting the extracellular matrix to the intracellular actin cytoskeleton. DGC stabilizes the AChR at the postsynaptic endplate and offers a recruiting platform for signaling molecules crucial for AChR clustering, post-synaptic maturation and NMJ's maintenance. SGs: Sarcoglycans; α-/β-DG: α-/β-Dystroglycans; α-DB1: α-Dystrobrevin1 (adopted from Gawor et al., *Annals of the New York Academy of Sciences*, 2018).

Dystrophin. Dystrophin is the central component of this complex and in the past century received great interest as the dystrophin gene was the first identified cause of Duchene muscular disease (DMD). In 1990, the dystrophin was isolated for the first time from the sarcolemma along with its interactors and further intensive study revealed that DGC components are also essential for integrity of muscle fibers, and that their dysfunctions were also associated to dystrophies[58,94]. The dystrophin is a 427 kDa cytoplasmic protein uniformly present at the sarcolemma and enriched at the post-synaptic specialization. At the NMJ, the dystrophin functions is to mediate the recruitment of key signaling molecules [58,94].

Dystroglicans. Within the DGC, β-Dystroglycan (β-DG) is a direct dystrophin interactor. The DG is the core component of the complex with both structural and signaling functions. Synthesized as a precursor peptide, the DG is post-translationally cleaved into two subunits: the β-DG, spanning the sarcolemma and covalently bound to the α-DG, which is localized extracellularly[96]. α-DG is a key receptor of laminins α4 α5, and this interaction is essential for DG enrichment at the post-synaptic site; furthermore α-DG binds agrin and MuSK via biglycan, and through this interaction it directs the AChR clustering and promotes NMJ maturation[34,97,98]. The DG is target for post-translational modifications and hypoglicosilation seems to be leading cause for a group of muscular disease named ”dystroglicanopaties”[99].

Utrophin. Utrophin, is a dystrophin-homolog which present at early development in the whole skeletal muscle fiber. Later during development, utrophin is replaced by dystrophin in the muscle fiber, and remains exclusively localized at the NMJ, specifically at crests of the junction folds where it interacts with AChR and stabilizes the receptors[58].While the expression of utrophin in dystrophic mice with X-chromosome-linked muscular dystrophy (mdx) seems to compensate for lack of dystrophin therefore, this representing a valuable potential for therapy of dystrophies, on the other hand, the NMJs of utrophin-deficient mice seem to be only subtly affected in the structure with no consequence for its functioning. Furthermore, the localization of Utrophin’s interactors at the NMJ appears unaltered[99,100]. Utrophin has been recently found to be linking Rapsyn to α-dystrobrevin[100].

Sarcoglycans. Sarcoglycan complex consists of four transmembrane glycoproteins (α, β, γ, and δ) and is an additional key core component of the DGC. The sarcoglycan complex is interactor of β-DG and also the α-sarcoglycan has been recently involved in age-dependent mechanisms that stabilize synaptic-machinery vis its interaction with the receptor for agrin LRP4[101,102,103].

α-Dystrobrevins. α-Dystrobrevin1 (αDB1) is another key intracellular component of the DGC. The α- corresponding gene (αdbn) encodes multiple splicing variants producing proteins of different size. In skeletal muscle, αDB1 (84 kDa) and its C-

terminal truncated version αDB2 (65 kDa) exhibit different localization pattern: while αDB1 is enriched at the post-synaptic terminal, αDB2 instead exhibit extra synaptic localization, suggesting a specific role[104]. At the DGC, the αDB1 is direct interactor of dystrophin, utrophin and syntrophins. In mouse model, the depletion of α-DB1 causes mild muscular dystrophy and the murine NMJ's structure displays a number of defects including ragged edges with spicules, decreased AChR density and aberrant junctional folds (**Figure 1.9**). The defects of NMJ in αDB-deficient mice are believed to be consequence of reduced levels and instability of ACh[105]. All together, these abnormalities suggest the involvement of αDB1 in mechanisms of maintenance and stabilization of the post-synaptic machinery[106].

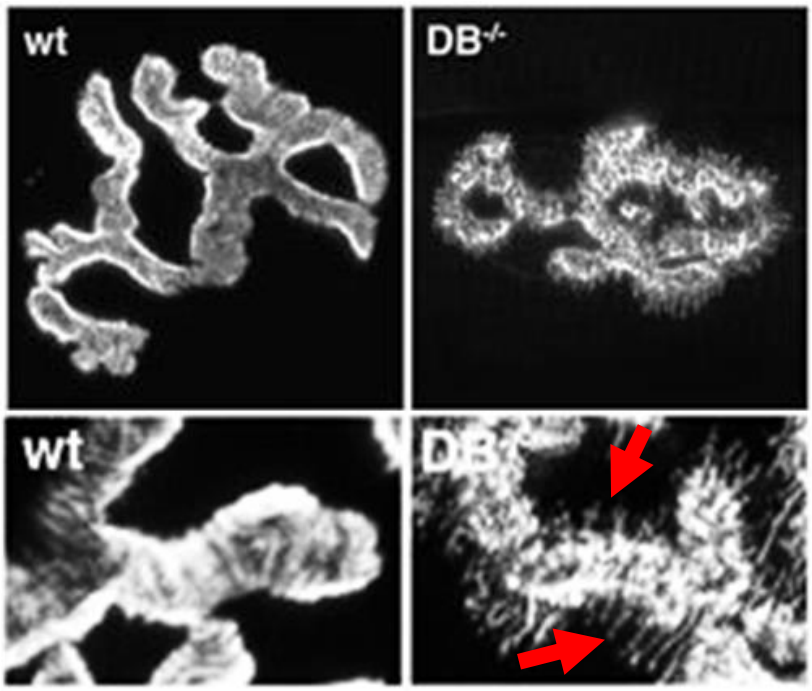

Figure 1.10. NMJ structure is destabilized in aDB1-deficient mice. Spicules visible at the NMJs of aDB1KO NMJs (red arrows) (adopted from Grady, R. Mark, et al., *The Journal of cell biology*, 2003).

1.2.5. Cultured myotubes as a model to study post-synaptic machinery

NMJ is a complex synapse, where different components are linked and can compensate for deficits of certain functions. The molecular mechanisms governing the NMJ development are still poorly understood due to the intervention to this process of various cell types, including muscle cells, PSCs and motoneurons. In this respect, culturing *in vitro* myotube turned out to be a valuable approach to dissect

the muscle-intrinsic mechanisms involved in the formation and development of neuromuscular machinery. To date, it has been observed that the laminin-cultured myotubes form AChR plaques which undergo structural rearrangements, similarly to the development of post-synaptic machinery *in vivo* (**Figure 1.8**). Thanks to in-vitro studies, it has emerged that muscle cells initiate post-synaptic differentiation forming AChR-rich plaques, thus this has led to review the dogma based on hierarchical predominance of the motoneuron over the muscle[106]. Furthermore, *in vitro* cultures have also facilitated the study of the molecular mechanisms responsible in the plaque formation and reshaping. To date, three methods are adopted to induce AChR clusters in myotubes in-vitro: the first is based on stimulation of differentiated C2C12 myotubes with soluble recombinant agrin, which forms AChR agglomerates at the apical and lateral surface of myotubes; the second method is based on differentiation of C2C12 on precoated surface with agrin and provokes myotubes to form simple oval-shaped clusters; the third approach consists of precoating the culturing surface with laminins, and in contrast to the methods based on agrin, laminins induce the formation of more complex clusters with perforations, similar to those observed *in vivo (*recapitulation in **Figure 1.11***)*[107]. Thus, laminins seem to be crucial for the formation of complex AChR clusters, although the mechanisms is still not known. In cultured-myotubes, the AChR-rich hot-spots have been found to rich of actin and actin-regulators[88]. Our laboratory has discovered the presence of a special organelle, called "synaptic podosome", at the site of perforation within forming AChR clusters[87,108]. Similarly to podosomes described in other cells, the synaptic podosomes are rich in actin and actin-regulators; these organelles are organized in one internal core, where actin, Arp2/3 complex, cortactin are found, and this is surrounded by an external cortex, where paxillin, src kinase, integrin β1 localize[87]. Furthermore, other studies identified the presence of components of the DGC, such as dystroglycans and utrophin, at the podosomes in myoblasts, and this finding is interesting because the dystroglycans are receptors of laminins[109]. Synaptic podosomes seems to be multifunctional in the process that reshapes AChR clusters and links exist between the role of synaptic podosomes and the appearance of perforation within AChR plaques. These adhesive organelles have been proposed to mediate the attachment of AChR sites to the substrate. Furthermore, synaptic podosomes seem to localize with sites of proteases exocytosis, leading to local degradation of laminins at the ECM[110]. Therefore, this destabilizes the AChRs at the membrane which are internalized. Synaptic podosomes have been found at the sites of intense endocytic activity, and this is believed to result into perforations, that is the AChR-empty spots within the plaques. Interestingly, despite the structural differences between human and murine NMJ, synaptic podosomes are also found in cultured human myoblasts, suggesting a similar initial developmental mechanism[107]. However, the presence of this organelle has not been confirmed in-vivo.

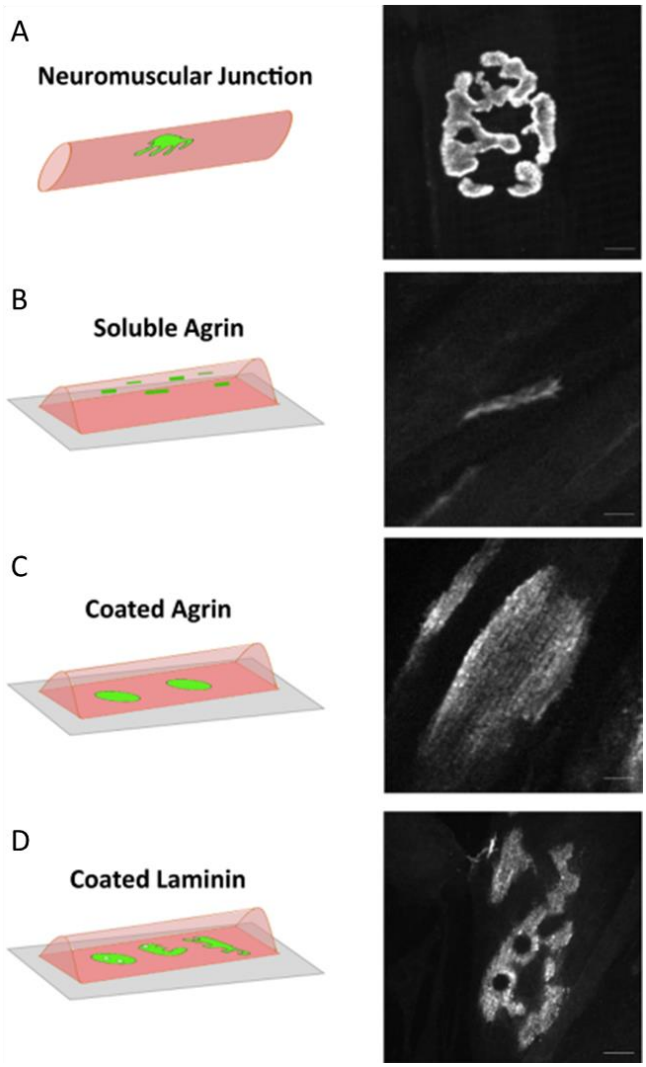

Figure 1.11. *In vivo* and *in vitro* models for post-synaptic machinery studies. *In vitro* AChR cluster exhibit different complexity accorded to the culturing method (image adopted from Pęziński, M. et al. *Scientific reports*, 2020).

1.3. Cytoskeleton

The cytoskeleton is a complex meshwork of interconnected filaments with associated proteins, consisting of three filamentous polymer's types: microtubules (MTs), intermediate filaments, and microfilaments. The role of cytoskeleton is to sustain cell morphology, compartmentalize the inner space and supports biochemical processes by providing the binaries for vesicle trafficking, endocytosis and exocytosis. However, the cytoskeletal network is more than a static structure as it rapidly and constantly reshapes to sustain principal biological events such as cell migration and morphological changes during development[111]. What is more, the remodeling of cytoskeleton is involved in signaling mechanisms.

1.3.1. Microtubules (MTs)

The microtubules (MTs) are robust filaments consisting of α- and β-tubulin heterodimers. These subunits form linear protofilaments and then laterally associate to form ~25nm diameter hollowed cylinders. Both α- and β-tubulin monomers can bind GTP nucleotide, but only the latter is able to hydrolyze. GTP hydrolysis promotes the incorporation of the heterodimer in the growing microtubule. MTs are characterized by "dynamic instability" which enables the rapid rearrangement of the filaments[112].

1.3.2. Intermediate filaments (IF)

The intermediate filaments (IF) are the second class of cytoskeleton filaments with a 10 nm diameter. In contrast to MTs and microfilaments, which are polarized filaments composed of globular subunits, the IF proteins form non-polarized filaments made of fibrous units. Also, IFs lack of enzymatic activity and self-assembling, and this represents a further difference in contrast to MTs and microfilaments[113]. IF proteins are classified in five groups based on structure: group I and II include acidic and basic heteropolymers; Keratins, the first IF proteins studied, belong to group I. Group III is characterized by homopolymers of Vimentin and Desmin. Neurofilaments, present in axons and dendrites, belong to Group IV and Lamins that form a network in the inner side of the nucleus belong to GroupV[114].

1.3.3. Actin

Actin is the most abundant protein on earth and decades of studies revealed its atomic structure, described its dynamics and uncovered the plethora of cellular mechanisms in which it is involved[115]. In prokaryotic and eukaryotic cells, actin

can be either found as a monomer (G-actin) or polymerized into double helical polarized filaments (F-actin). F-actin is a structure which exhibits peculiar kinetic properties at its extremities: the "barbed-end" of F-actin is the site where actin monomers are incorporated within the filaments, whereas the "pointed-end" is the side of F-actin from which the monomers are detached from the filament. The balance between G- and F-actin is maintained by a constant polymerization/depolymerization cycle, known as treadmilling, and the vast majority of actin biological functions depend on this dynamics[113]. In mammals, α-, β- and γ- actin types exist and this classification is based on their molecular charge, with α-actin exhibiting the most negative charged/acidic, followed by β-actin and then γ-actin positively charged/basic[114,115]. Furthermore, six isoforms are counted: α- skeletal, α-cardiac, α-smooth, γ-smooth, β- cytoplasmic, and γ-cytoplasmic[115]. This second classification type reflects tissue expression and localization of these isoforms, thus α- skeletal, α-cardiac, α-smooth are present in respectively skeletal, cardiac and smooth muscles respectively. Furthermore, in smooth muscles also γ-smooth isoform is present. Last, β- and γ-cytoplasmic isoforms are also known and are ubiquitously expressed. The skeletal muscle provides an effective example of how the different actin isoforms can be differentially localized within the cell. Within the myofiber, α- skeletal actin is found to be mainly present at the contractile apparatus; by contrast, γ-cytoplasmic initially appeared localized at the sarcolemma, and only subsequent accumulating studies reported that γ-cytoplasmic is also present at the sarcomere z-disks[116,117,118,119,120,121,122,123]. Notably, the six actin isoforms are encoded by different genes and the small isotypes differences are believed to be key determinants for their localization and biological role. Moreover, it is hypothesized that actin isoforms exhibit distinct subcellular localization as a result of differential actin-binding interactors.

1.3.3.1. The sarcomere components and structure

The sarcomere is the site where neuron-stimulated increase in intracellular Ca^{2+} becomes translated into the mechanical force underlying the contractile capacity of the striated muscle, thus it is considered as the basic contractile unit[124,125]. Structurally, the sarcomere is a repetitive unit made of "thin" filaments, consisting of f-actin, troponin (Tn) and tropomyosin (Tm), and "thick" filaments made of myosin. Within the sarcomere, the thin and thick filaments run in a parallel fashion and partially overlapping. Named Z-disks, the extremities of the sarcomere are sites that link adjacent sarcomeres via α-actinin, and site of attachment for f-actin barbed-ends of thin filaments. Also, through the Z-disks the sarcomere is tethered to the sarcolemma. Moving towards the center of the sarcomere, the I-band is the zone exclusively occupied by the thin filaments which extend to the center of the sarcomere, overlapping the thick filaments at the A-band. The thick filaments of myosin occupy for their entire length the A-band, in the middle of which the so-

called " M-band" is the portion where the thin filaments are missing (**Figure 1.12**)[124,125].

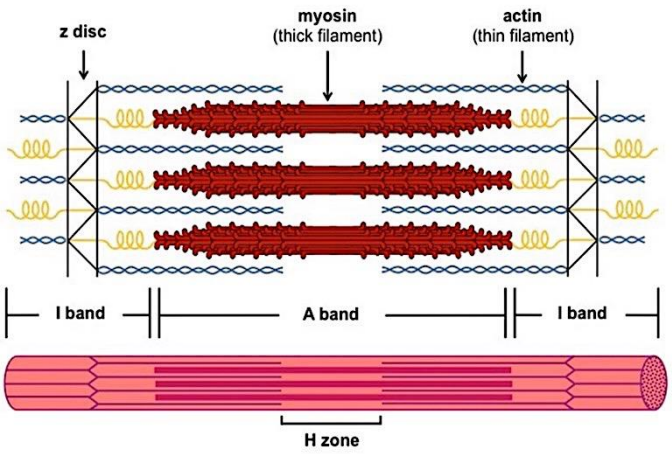

Figure 1.12. Scheme of the Sarcomere (image adopted from ib.bioninja.com).

Thin filaments

Tropomyosin. Tropomyosin (Tm) forms two-chained α-helical coiled-coils, which polymerize in a head-tail fashion through the entire length of the thin filaments, and this tm fiber interacts with actin filaments in such a way that each tm dimer spans seven actin monomers. Tm exerts a structural role at the sarcomere as it influences actin by increasing the stiffness of actin filaments and prevents f-actin depolymerization[126]. Furthermore, Tm is implicated in the contractile function of sarcomere by regulating the thin-thick filaments interaction[127].

Troponin complex. Troponin complex encompasses three subunits: troponin C (TnC) that carries a Ca^{2+}-binding site, Troponin T (TnT) that bind s to Tm, and Troponin I (TnI) that inhibit the acto-myosin interaction mechanism[128,129].

Thick filaments

Myosins. The majority of proteins of the myosins family are involved in motility with myosin II being the isoform present at the striated muscle. Structurally, sarcomeric Myosin is a hexamer consisting of two "heavy" coiled-coiled α–helical chains (MyHC), subdivided into "neck" and "tail". In adult mammalian skeletal muscle, four main heavy chain isoforms (I, IIa, IIb, and IIX) exist and in skeletal muscles the MyHC different expression pattern leads to different muscular contractile properties. Each MyHC monomers carries a globular head consisting of an essential light chain (ELC) and a regulatory (RLC), which exhibits an ATPase

catalytic function thus this confers critical importance to the Myosin being the enzymatically active component of sarcomere[125].

1.3.4. The Actin binding proteins (ABPs)

Actin-binding proteins (ABPs) represents an enlarged group of proteins that promote the actin polymerization and are emerging as central regulators of actin functions during the development[114]. The actin polymerization can occur in length, with Formins being the best-characterized protein family involved in mechanisms of actin elongation; alternatively, actin can be organized to form branched structure and the actin-related protein (Arp)-2/3 complex is the most studied factor for his function of branching-actin[130]. The Arp2/3 complex promotes the synthesis of new daughter actin-filaments from a pre-existing mother actin-filament, branching a 70° angle from it, thus this action increases the complexity of the actin-based network (**Figure 1.13**). Nucleation promoting factors (NPFs) synergize and sustain the actin-remodeling function of the Arp2/3 complex and are classified in two main groups based on the mechanism of Arp2/3 activation and their impact on actin-branching. Type I NPFs are characterized by a C-terminal VCA (or WCA) domain that binds ATP -actin monomers and present these to the Arp2/3 complex. Therefore the function of type I NPFs is to prime the actin-nucleation reaction of Arp2/3 complex and the VCA domain plays a central role in the catalysis of this reaction[131,132]. Type II NPFs possess an Arp2/3 complex-binding domain, lack of G-actin binding domain and exhibit a F-actin-binding domain. Type II NPFs are not primary activator of Arp2/3/ complex in the actin-branching mechanism but are believed to be important in promote the of the y-branched actin[132,133].

1.3.5. Cortactin

Discovered in the early ’90 as substrate of Src kinase’s, Cortactin (Cttn) is a ~63-65kDa adaptor protein and actin-cytoskeleton organizer of the cellular cortex, hence its name[134]. Cttn is a Type II NPFs and participates to dynamics of actin-cytoskeleton supporting the function of Arp-2/3 complex. Furthermore, Cttn responds to the activation of Src kinase. Structurally, Cttn is exhibits a N-terminal acidic domain (NTA) responsible for the interaction with the Arp2/3 complex, followed by 6.5 37-amino acid tandem repeats that mediate the binding of actin; a central prolin-rich domain with serine, threonine and tyrosine residues which represent the site of regulation by Src kinases, and a Src-homology 3 (SH3) domain harbored at the C-terminal and that mediates the interaction with other cytoskeleton regulators such as the Wiskott- Aldrich Syndrome protein1 (WASp) protein superfamily (**Figure 1.14**)[134,135]. It is known that Cttn activates the Arp2/3 complex, which is an obligatory regulator that orchestrate the branching of actin-based structures. Furthermore, Cttn synergizes with WASp1 and drastically potentiate

actin-polymerization action of Arp2/3 complex[135]. Cttn is involved in several cellular actin-based events such as cell adhesion, endocytosis. Furthermore, Cttn is localized at the leading edge of migrant cells, and recent studies have linked the function of Cttn to form invadopodia to tumor aggressiveness and metastasis, thus suggesting that Cttn could be a clinically relevant protein and represent a potential target for cancer therapy[136,137]. The studies on the role of Cttn in invadopodia formation in cancer have shed light on intriguing aspects of Cttn's regulation, according to which the cellular location and actin-remodeling activity of Cttn seems to be modulated by the histone-deacetylase6 (HDAC6)[138,139]. Interestingly, HDAC6 has been recently found to be involved in mechanisms of AChRs clustering in myotubes through the regulation of α-tubulin of MT, thus it might be speculated that Cttn is modulated by HDAC to participate to the same mechanism occurring at the forming NMJ[140].

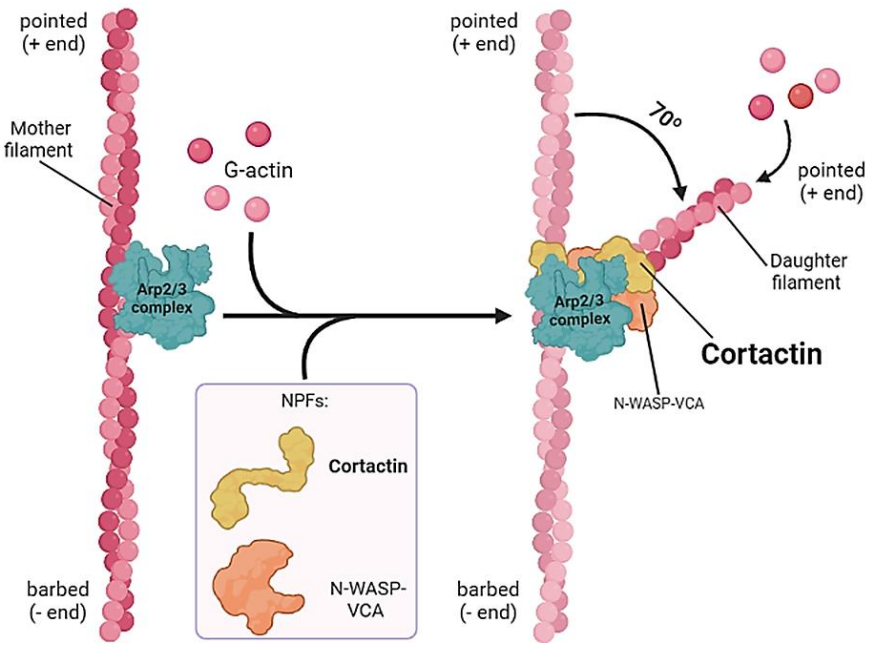

Figure 1.13. Mechanism of actin branching. The Arp2/3 complex nucleates new daughter F-actin from the mother F-actin increasing the complexity of actin network. Cttn is a synergistic activator of actin branching along with other nucleating promotion factors such as N-WASP. Abbreviations: NPF = nucleating promotion factor (image created in Biorender).

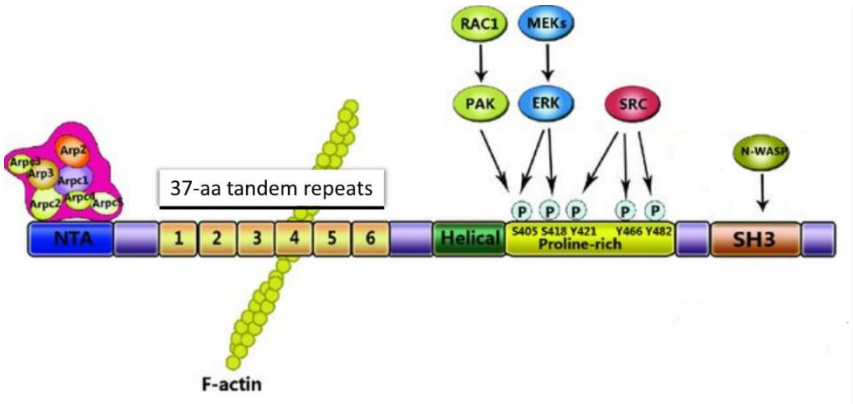

Figure 1.14. Cortactin structural domains and motifs. N-terminal acidic domain (NTA), 6 tandem repeats consisting of 37 amino acids (aa), central helical and proline-rich domain with Ser and Tyr phospho-regulated residues, Src-homology3 domain (adopted from Yin, M. et al., *Oncotarget*, 2017).

1.3.6. The Cyclase-associated proteins (CAPs)

1.3.6.1. The Structure of CAPs

Cyclase-associated proteins (CAPs) are multifunctional proteins that in yeast consist of 526 aa. In vertebrates and also in mouse two isoforms are known: CAP1 made of 474 aa and CAP2 which is 476 aa[141]. CAPs exhibit several domains and motifs with specific functions: a coiled-coiled domain at the N-terminal mediates CAPs's oligomerization (OD, oligomerization domain). Furthermore, this domain is responsible to bind the adenylyl-cyclase in yeast. The helical folded domain (HFD) follows: this domain binds the ADF/cofilin- G-actin complex and also interacts with ADF/cofilin-bound actin and is in charge of F-actin severing and is a unique structure among other ABPs. The central region of CAPs is characterized by two proline-rich domains (P1 and P2), that mediate the actin. What is more, P1 and P2 are spaced by a Wh2 domain, which binds G-actin and is believed to be responsible for the ADP- to ATP-nucleotide exchange function. Finally, the C-terminal portion of CAPs exhibits a CAPR domain which can bind actin independently from the central region (**Figure 1.15**)[141].

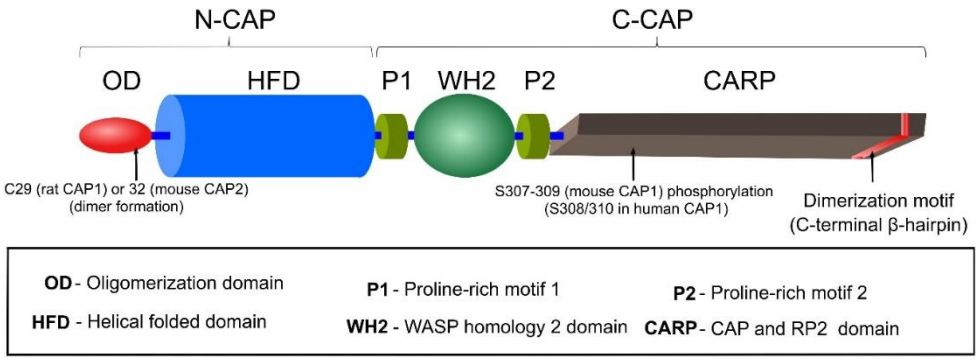

Figure 1.15. Structural domains and motifs of CAPs (adopted from Rust, M.B. et al., *Frontiers in Cell and Developmental Biology*, 2020).

1.3.6.2. The origin of the name "CAP"

Svr2 were discovered three decades ago in *Saccharomyces cerevisiae* and are the homologous of mammal CAPs[142]. Identified for the first times in yeast as an adenylyl-cyclase-complex's interactor, the first role ascribed to Svr2/CAPs was connected to the Ras-cAMP signaling pathway and to cell growth mechanisms. However, this features remains exclusively limited to yeasts, while it is believed to be lost in mammals[142]. Consistent number of studies have discovered a conserved function of CAPs connected the organization of the cytoskeleton due to their properties of binding actin. Therefore, CAPs are believed to be central in many cellular activities including cell migration, morphogenesis and endocytosis and also believed to underlie many diseases caused by actin structure and dynamics defects. Although intensive studies strived to unravel the mechanisms through which CAPs remodels actin-structures, still little is known and sometimes controversial. Studies *Saccharomyces cerevisiae* revealed that CAPs can sequester globular (G-)actin and make actin monomers unavailable to be incorporated within filaments[143,144]. However latest research revealed that CAPs can influence the actin state in different multiple ways and this reflects the multifunctional nature of this protein family.

1.3.6.3. Function of CAPs in actin dynamics

CAPs can promote the disassembly of F-actin and exert this function either alone or in concert with molecular partners[145]. For example, a known function of CAPs is to participate with ADF/cofilin to the disassembly of F-actin participating to the actin "treadmilling"[146]. Actin filaments decorated with ADF/cofilin are severed and this amplifies the number of the depolymerizing "pointed-ends". In this mechanism, CAPs accompanies this process as an enhancer. Additionally, CAP proteins facilitate the displacement of ADF/cofilin from actin monomers which are newly released from the filaments in their uncharged form which binds ADP. Moreover, CAPs can indirectly influence mechanisms of filaments elongation promoting

ADP-for-ATP nucleotide exchange. This mechanism recharges the newly-released actin monomers which can be incorporated again within the actin filaments (scheme in **Figure 1.16**)[147,148].

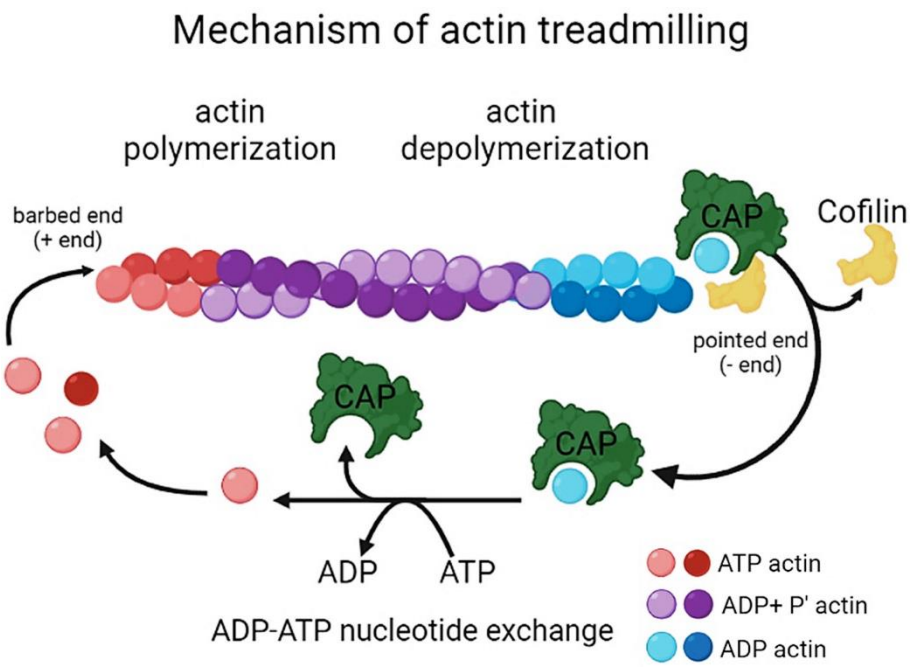

Figure 1.16. Illustration of the role of CAPs in the actin "treadmilling". ATP-charged actin monomers are incorporated at the barbed-end of the filamentous actin by ATP-hydrolysis. The central portion of F-actin is decorated with ADP+ P'- actin treadmilling towards the pointed end. Inactive ADP-actin monomers are removed from the pointed end by the concerted action of Cofilin and CAPs. CAPs recharge the actin monomers with ATP by ADP-ATP nucleotide exchange, recharging actin and feeding the actin treadmilling (image created in Biorender).

1.3.6.4. CAP2

In mammals, two forms of CAPs exists, with roughly 64% of identity and different expression pattern. During the embryonic development of mammals, CAP1 is expressed in almost all tissues except for skeletal muscle. Instead, CAP2 expression is mainly restricted to the heart, skeletal muscle and some regions of the brain, suggesting that CAP2 may play a specific role in these districts[149].

1.3.6.5. CAP2 is a multitask protein

In murine cardiomyocytes, CAP2 localizes at the M-line of sarcomeres in correspondence of the pointed ends of the thin filaments[150]. Also, in fast skeletal

muscles of CAP2-deficient mice exhibit abnormal arrangement of the sarcomere that forms actin rings instead of longitudinal disposal along the fiber, and this is feature of myopathies (**Figure 1.16**); all together, these findings indicate that CAP2 might have a crucial role in the sarcomere organization. The actin-rings are known to be hallmark for several myopathies, some of which are still of unknown etiology[151]. CAP2 is implicated in the post-natal myofibril differentiation, which includes the replacement of smooth muscle (α-SMA) and cardiac muscle (α-CAA) α-actin) actin isoforms into the skeletal muscle (α-SKA) α-actin isoform. CAP2 action facilitates the release of immature α-actins from the myofibrils by F-actin severing, and this allows the subsequent incorporation of mature α-actins within the filaments[150,151]. Further studies identified a function of CAP2 as a actin-state sensor which can regulate gene transcription, and this novel physiological role seems to be potentially relevant in the field of cardiomyopathies [152,153,154].

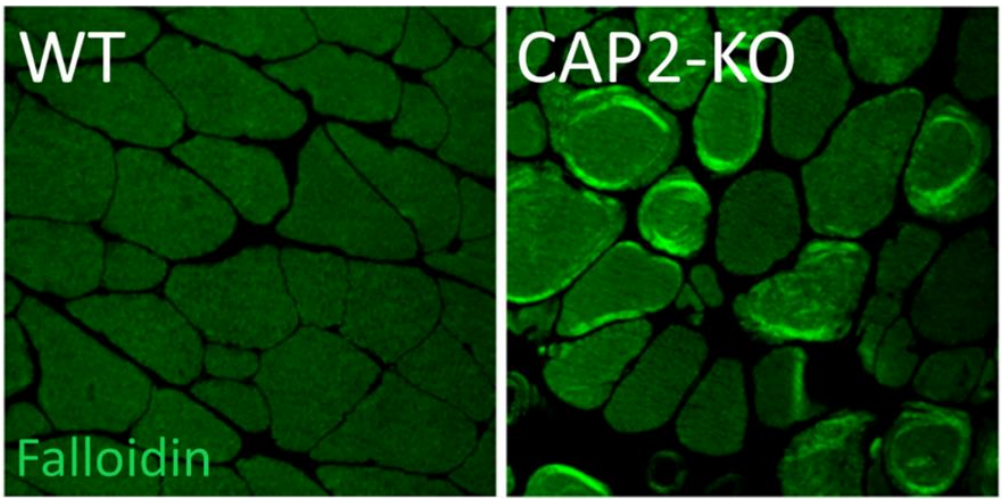

Figure 1.17. Abnormal disposition of the sarcomere forms Actin Rings in fast-twitching fibers (Quad). Within muscle transversal cross-sections, the circular formations of higher fluorescent intensity termed "actin rings" can be observed (image source: Kepser, Lara-Jane, et al., *PNAS*, 2019).

2. Hypothesis

Actin cytoskeleton plays important role in the organization of cortical protein assembly machinery at the CNS and NMJ. Therefore, I hypothesized that the novel actin-organizing proteins could regulate NMJ. My studies are focused on CAP2 and Cttn and their role at the NMJ.

2.1. CAP2 is a key NMJ organizer

CAP2 is an actin-remodeling factor and in mammals is specifically expressed brain, muscle and heart, thus suggesting specific functions in these districts. Recently, novel roles of CAP2 are emerging in cardiac disease, indicating that CAP2 is a potential target to delay diseases like dilated cardiomyopathy[152,153]. Furthermore, recent studies in skeletal muscles strengthen the link of CAP2 with myopathies[151]. Moreover, CAP2 has been implicated in in mechanisms of synaptic plasticity at CNS, however its role at NMJ has never been investigated[155]. Thus, I hypothesized that CAP2 might have a unique function at NMJ and the aim of this study is to provide a comprehensive characterization of the CAP2 phenotype at the neuromuscular synapses and dissect the mechanism of CAP2 as NMJ organizer.

2.2. Cttn is recruited at the NMJ via αDB1

αDB1 recruits peripheral partners to the post-synaptic terminal to organize the AChR, promote post-natal NMJ maturation and preserve the integrity of the DGC itself[156]. Cortactin (Cttn) was identified as a phospho-Y730-dependent interactor of αDB1 from a Mass-spectrometry based screening performed from the laboratory I am affiliated (**Table** in **Figure 2.1**), therefore I hypothesized that Cttn could be a novel peripheral effector of the DGC, recruited at the NMJ by αDB1. Moreover, Cttn is an actin-remodeling factor, thus I hypothesized that Cttn might be involved in mechanisms of actin remodeling for the organization, stabilization and maintenance of AChR at the post-synaptic at NMJ through the remodeling of the cortical actin. In support of this hypothesis, *in vitro* studies reported that the absence of Cttn impairs the mechanisms of AChR clustering in myotubes, suggesting a role in these processes (**Figure 2.2**)[157]. Thus, the aim of this study is to provide full characterization of the role of Cttn at NMJ.

Actin-regulators and interactors of α-DB1 Y730				
Protein	ID	kDa	unphospho-Y730	phospho-Y730
Arp2/3 complex (subunit 2)	sp|Q9CVB6|ARPC2_MOUSE	34 kDa	2	0
Arp2/3 complex (subunit 1B)	sp|Q9WV32|ARC1B_MOUSE	41 kDa	4	2
CAP1	sp|P40124|CAP1_MOUSE	52 kDa	5	0
TKS5	sp|O89032|SPD2A_MOUSE	124 kDa	8	0
F-actin-capping protein (subunit alpha)	sp|P47753|CAZA1_MOUSE	33 kDa	0	5
Alpha-actinin-2	sp|Q9JI91|ACTN2_MOUSE	104 kDa	0	10
Src substrate cortactin	**sp|Q60598|SRC8_MOUSE**	**61 kDa**	**0**	**2**

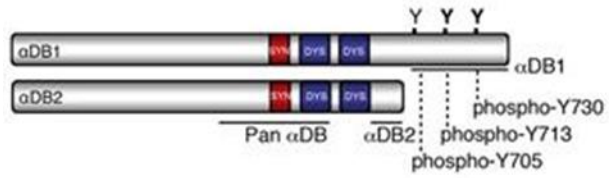

Figure 2.1. Cttn is potential interactor of αDB1 via phospho-730-tyrosine residue in mass-spectrometry analysis. Table) Results for interactors of phosphorylated and unphosphorylated αDB1 peptide 730 performed in the lab. **Lower image**) Illustration of αDB isoforms adopted from Gingras, Jacinthe, et al., *Journal of cell science,* 2016.

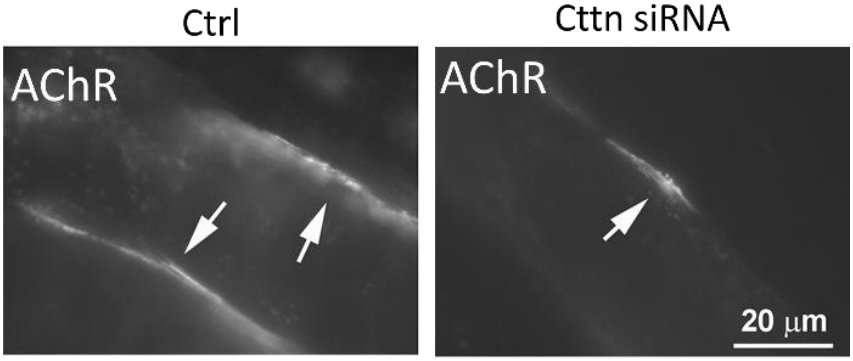

Figure 2.2. In-vitro Cttn knock-down in C2 myotubes is associated to reduced AChR cluster formation. The white arrows indicate AChR clusters on myotubes (image adopted from Madhavan, Raghavan, et al., *PLoS One*, 2009).

3. Materials and Methods

3.1. Materials

Table 3.1. Buffers and media

Buffer	Composition	Application
Blocking buffer	2% BSA, 2%NGS, 0.5% Triton, 0.02% NaN_3) in PBS	Immunostaining
Co-immunoprecipitation (Co-IP) lysis buffer	50 mM Tris-HCl, 150 mM NaCl, 50 mM NaH_2PO_4, 10 mM imidazole, 0,1% NP-40, 10% glycerol, adjusted to pH 8.0, store at 4ºC.	Co-immunoprecipitation
DMEM Cell culture media	DMEM, 10% FBS, 100 IU/ml penicillin, 100 µg/ml streptomycin and fungizone	HEK293T growth medium
Phosphate buffered saline (PBS)	80g NaCl, 2g KCl, 14,4g Na_2HPO_4, 2,4 gr KH_2PO_4 in 1L H_2O [10X]	washes
10X Running (1L)	30gr Tris base, 144g glycine, 10g SDS	SDS-acrylamide gel electrophoresis
50X TAE	242g Tris-base, 18,61g disodium EDTA, 57,1 mL Glacial acetic acid	Agarose gel electrophoresis
10X Tris-buffered saline (TBS)	87.7g NaCl, 100mL 1M Tris-Cl, pH 7.5 in 1L H_2O [10X]	Preparation of TBST buffer
Tris-buffered saline with Tween	0.1%Tween-20 in 1XTBS	Membrane washes/ preparation antibody for WB
5XTURBO	112g glycine, 182g Tris-Base, 5g SDS in 1L H_2O	Protein transfer buffer preparation; diluted before use 1:3:1 (5 x transfer buffer: H2O : ethanol)

Table 3.2. Commercial kits

Commercial kits	Supplier
Clarity and Clarity Max ECL Western Blotting Substrates	Cat#: 1705061, Bio-Rad
Dynabeads™ Antibody Coupling Kit	Cat#14311D, ThermoFisher
GenElute ™ Plasmid Maxiprep Kit	Cat#: PLX15-1KT, Sigma
KAPA HotStart Mouse Genotyping Kit	Cat#: KK7352, Roche
NEBuilder® HiFi DNA Assembly Cloning Kit	Cat#E5520S, BioLabs
Plasmid Miniprep DNA Purification Kit	Cat#: E3500, Eurx
PCR Master Mix (2X)	Cat#: K0171, ThermoFisher
SuperSignal™ West Femto Maximum Sensitivity Substrate	Cat#: 34094 ThermoFisher

Table 3.3. Antibodies and fluorescent toxins

Primary antibody	Supplier	Dilution/use
Synaptophysin 1	Cat#: 101004, Sysy	1:500 for IF
Neurofilament	Cat#AB1991, Millipore	1:200/500 for IF
anti-GFP (N-term) [E385]	Cat#: ab32146, Abcam	1:3000 for WB
anti-FLAG (1) [M2]	Cat#: F3165, Sigma	1:1000 for WB

anti-FLAG (DYDDDDK tag) (2) [D6W5B]	Cat#: 14793, Cell Signaling	1:1000 for WB
anti-CAP2	Gift by Marco Rust	1:2000 for WB
Secondary antibody	Supplier	Dilution/use
Goat anti-Guinea Pig IgG (H+L), Alexa Fluor™	Cat#: A21450, ThermoFisher	1: 1000 for IF
Goat anti-Rabbit IgG (H+L), Alexa Fluor™	Cat#: A32731, ThermoFisher	1:1000 for IF
Anti-rabbit-HRP	Cat#: 7074S, Cell Signaling	1:2000-1:10'000 for WB
Anti-mouse-HRP	Cat#: 7076S, Cell Signaling	1:2000-1:10'000 for WB
Fluorescent toxins	Supplier	Dilution/use
α-Bungarotoxin	Cat#: B35451, ThermoFisher	1:500 for IF
Fasciculin F225 + FITC	Cat#: F-225, Alomone Labs	3.5 µg/µL for IF
Phalloidin	Cat# A34055, ThermoFisher	1:500 for IF
DAPI	Cat#A4099,0005 BUJNO Chemicals	1:1000 for IF

3.2. Animal models

The experimental procedures were performed in mice of C57BL/6 genetic background. Animals were bred in a specific pathogen free (SPF) animal facility at the Nencki Institute of Experimental Biology and PORT-Łukasiewicz Research Network under the supervision of veterinarian and technical staff. All the animals were housed in cages supplemented with food and water *ad libitum* and in 12/12 light/dark cycle. All the experimental procedures were approved by the Local Ethical Committee for Animal Experimentations located in Warsaw and in Wrocław. CAP2 mutant mice were a generous gift of Professor Dr. Marco Rust (University of Marburg, Germany) and obtained from the European Conditional Mouse Mutagenesis Program (EUCOMM). Cttn mutant and Cttn floxed mice lines were generous gift from Professor Dr. Klemens Rottner (Technische Universität Braunschweig , Germany). Muscle-specific Cttn mutant mice were generated in our laboratory by crossing Cttn fl/fl mice with Myf5-CRE mouse line. Myf5-CRE mouse line was provided by from Professor Dr. Marcus Ruegg, (University of Basel, Switzerland). Myf5 is a muscle-specific transcription factor that regulates myogenesis during skeletal muscle development, while ACTA1 encodes for skeletal alpha-actin, the most representative and tissue-specific of skeletal muscle (see **Figure 3.1**)[158]. The genotyping protocols were executed according to the instructions provided by the provider of the mouse line.

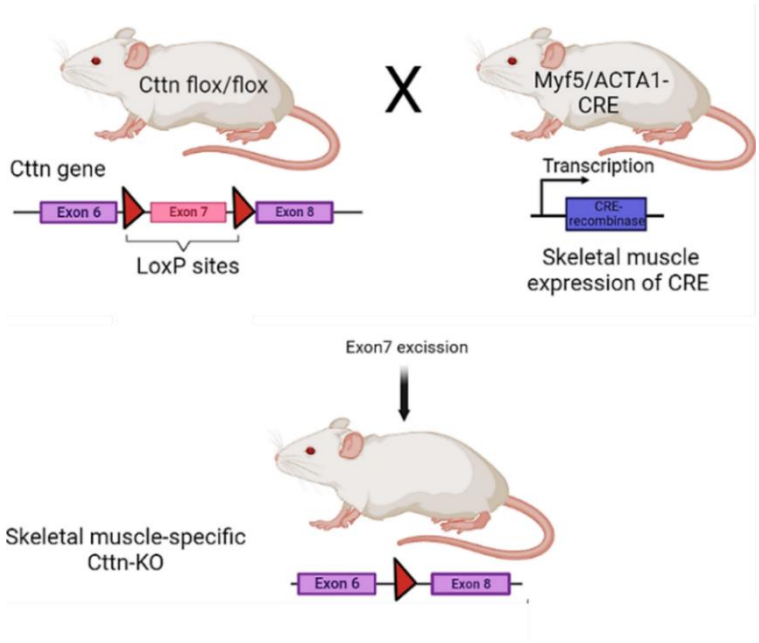

Figure 3.1. Muscle-specific KO mice generation. Exon 7 of Cttn gene is flanked by LoxP sites in Cttn flox/flox mice. These are crossed with Cre mice expressing the Cre-recombinase regulated by the promoter Myf5 or ACTA1 genes, expressed specifically in muscle at embryonal and postnatal developmental stage. The generation of skeletal muscle-specific Cttn-KO mice line is mediated by LoxP sites by the excision of exon 7(image generated in Biorender)**.**

3.2.1. Genotyping of Cap2 mutant mice

The CAP2 line was routinely genotyped by the use of the commercial KAPA Mouse Genotyping Kit (details in **Table 3.2)** according to manufacturer instructions. Genomic DNA was isolated from the mouse biopsies in a reaction assembled as described in **Table 3.4**. The extraction reaction was set up at 75°C for 10 min with 1000 rpm on a thermos-shaker, then the enzyme was inactivated at 95°C for 5min. The samples were vortexed for 2-3 seconds and centrifuged at maximum speed for 2 min. Finally, the supernatant is collected and used for PCR reaction as template in a reaction set up as described in **Table 3.6** and amplified as described **in Table 3.7.** The details of primers used for the PCR reaction are in **Table 3.5**.

Table 3.4. "KAPA Kit DNA Extraction" reaction set-up

Reagents	Volume
10X KAPA Express Extract Buffer	10 µL
1 U/µl KAPA Express Extract Enzyme	2 µL
Mouse tissue	2-3 mm
ddH2O	88 µL
Total	100 µL

Table 3.5. Primers used for CAP2 mouse line genotyping

Primer	5'→3' Sequence	Direction	Bands
566_Cap2-5'arm	TACCTGGAAGAGCTACAGAGG	Forward	WT: 561 bp KO: 617 bp Het: both
567_Cap2-3'arm	GTTCACAGGGACTTTGGTTGG	Reverse	
568_LAR3	CAACGGGTTCTTCTGTTAGTCC	Reverse	

Table 3.6. "KAPA HotStart Mouse Genotyping Kit" set-up

PCR reagents	Volume
2X KAPA Fast HotStart Genotyping Mix with dye	6.25µL
Primer 1 (566_Cap2-5'arm; 10 µM)	1.11µL
Primer 2 (567_Cap2-3'arm; 10 µM)	1.225µL
Primer 3 (568_LAR3; 10 µM)	0.5µL
ddH2O	2.165µL
Tissue lysate	1
Total	12.25µL

Table 3.7. PCR cycling conditions

Step	Temperature	Time	N° cycles
Initialization	95°C	3 min	
Denaturation	95°C	15 sec	
Annealing	65°C	30 sec	X35
Extension	72°C	30 sec	
Final Extension	72°C	10 min	
	4°C	+∞	

3.2.2. Genotyping of Cortactin mutant mice

Genomic DNA was isolated from the mouse tail using Chelex 100 [Catalog #: C7901, Sigma]. A small piece of tail tissue was added into 200 µl of 10% Chelex solution and incubated at 95°C for 20 min, and subsequently centrifuged at 12 000 g at RT for 10 min. The supernatant was collected and used for the PCR reactions as a template. To genotype the Cttn-KO line, primer 1 and 2 were added to the PCR mix. A second PCR reaction was performed in parallel with a different set of primers (primer 4 and 5) to confirm the presence of the WT allele. Furthermore, for the genotyping of the muscle-specific Cttn-KO lines, the presence of Cttn fl/fl and CRE alleles were confirmed by the use of allele-specific primers. The details of primers are described in as in **Table 3.8**. All PCR reactions for Cttn line were performed using PCR Master Mix (2X) (**Table3.2**) is a reaction assembled as in **Table 3.9** and with PCR cycling conditions described in **Table 3.10**.

Table 3.8. Primers used for Cttn lines genotyping

Primer	N°	5'→3'Sequence	Direction	Genotype	Bands
Cttn fwd1	1	AGGGTCTGACCATCATGTCC	Forward	CttnKO	WT: 900 bp KO: 400 bp
CttnR2	2	GTGCTGTTCATCCACAATGC	Reverse		
CttnwtFwd4	4	CCTGGAATAAGTCAGCCAAGC	Forward	CttnWT	WT: 328 bp
CttnwtRev5	5	CGGAGAGCTAGGCTGTTAGC	Reverse		
Cttn fwd1	1	AGGGTCTGACCATCATGTCC	Forward	Cttn-Flox	WT: 150 bp Cttnfl/fl: 250bp
CttRevFlox3	3	GACTTATTCCAGGCACAGCA	Reverse		
CRE1	-	GCCTGCATTACCGGTCGATGCAACGA	Forward	CRE	700bp
CRE2	-	GTCGCAGATGGCGCGGCAACACCATT	Reverse		

Table 3.9. "2X Master Mix" reaction

PCR reagents	Volume (µl)
Master Mix	12.5µL
primer F	0.5µL
primer R	0.5µL
H2O	9µL
DNA	2.5µL
Total	25µL

Table 3.10. PCR cycling conditions

Step	Temp.	Time	N°
Initialization	95°C	2 min	
Denaturation	95°C	20	
Annealing	58°C	30	X35
Extension	72°C	45	
Final	72°C	3min	
	4°C	+∞	

3.2.3. Electrophoresis

The PCR-amplified DNA products were resolved on agarose gel prepared with 1-1.5% Low Melting Agarose -Molecular Biology Grade (Catalog# E0303, EurX) dissolved in TAE buffer (**Table 3.1)** with the addition of Midori Green Advance DNA Stain (Catalog#: MG04, Abo). PCR samples were prepared for the electrophoresis by addition of 1X DNA Gel Loading Dye (Catalog# R0611, ThermoFisher). 90-120 V voltage current was used to resolve the DNA products during the electrophoresis run. Perfect 100-1000 bp DNA Ladder (Catalog#: E3141-01, Eurx) was used as a reference DNA ladder. The products were visualized by ChemiDoc XRS+ Gel Imaging System and visualized by Image Lab™ Software (Catalog#: 1708265, Bio-rad).

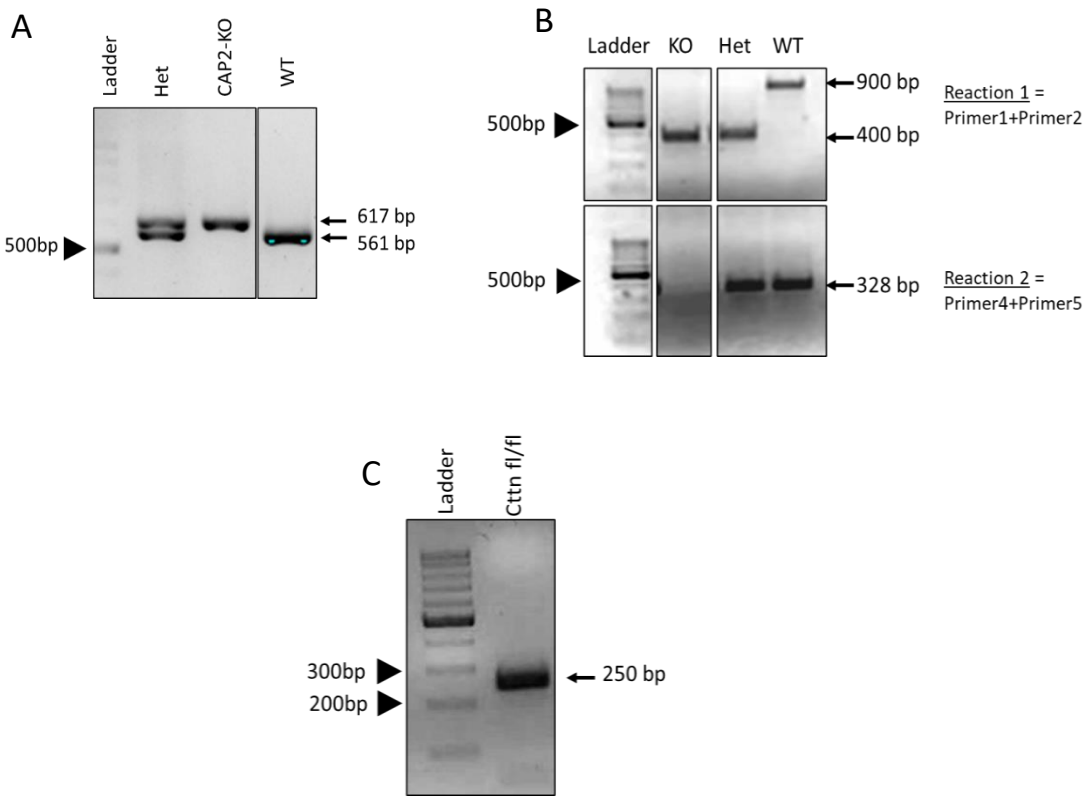

Figure 3.2. Expected DNA products from the mice genotyping. A) Genotyping of CAP2 mice **B**) Genotyping of Cttn-KO mice **C**) Genotyping of Cttn-flox/flox mice.

3.3. Immunofluorescence

3.3.1. Tissue preparation

Animals were intracardially perfused with 4% paraformaldehyde (PFA) to fix tissues. Then, the muscles of interest were dissected with surgical tools from 4% PFA perfused mice. Alternatively, animals were euthanized in compliance with the regulations of the animal facility where the procedure was performed. After excision of the entire leg and removal of the skin and connective fascia that envelops the muscles, the whole leg was incubated in a 4% PFA solution per 45 minutes at room temperature. The skeletal muscles frequently dissected from the hindlimbs more are Tibialis anterior (TA), Soleus (Sol), Quadricep (Quad). The muscles of interest were identified according to position (ventral/dorsal) and morphology, (see **Figure 3.3**). Whole length fibers were delicately isolated from the fixed whole muscle with surgical. A stereoscope and surgical tools were used to magnify the whole muscle and isolate fibers from it. Once dissected, the fibers were treated by incubation in blocking buffer (see **Table 3.1**) per 1 h at room temperature on slow shaker.

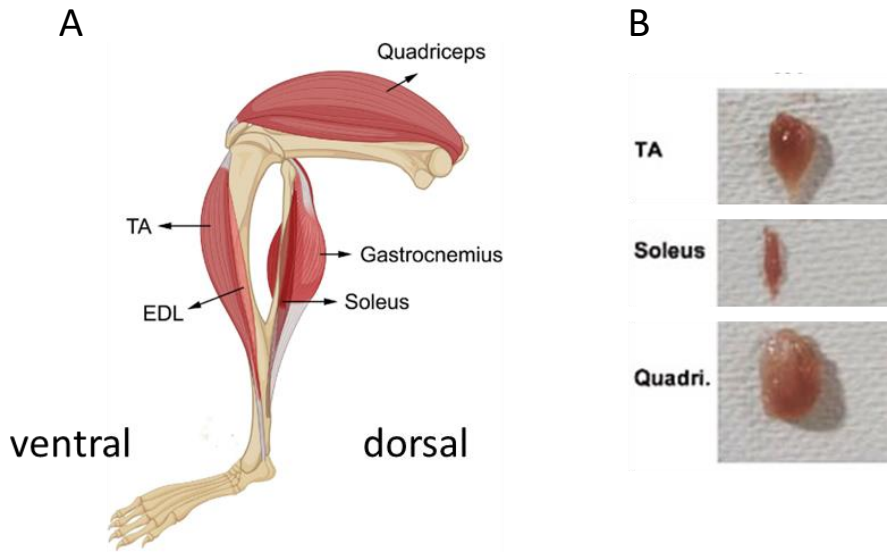

Figure 3.3. A) Schematic illustration of murine hindlimbs muscles. (image adopted from Mytidou, C. et al., *Frontiers in physiology*, 2021). **B**) Morphology of dissected muscle from mouse hindlimbs (adopted from Miura, S. et al., *Journal of Biological Chemistry, 2003).* Abbreviations: TA = Tibialis anterior, EDL = Extensor digitorum longus, Quadri. = Quadriceps.

3.3.2. Muscle cross-sections

For the cross-section of muscles, the muscles of interest were dissected, the excess of moisture was delicately removed from the tissue., Then, the whole muscle was embedded in OCT, and snap-frozen by immersion in isopentane cooled down in liquid nitrogen and then stored at −80°C until use. Transverse 20 µm-thick sections were obtained by using Sakura CRYO 3 cryostat, collected on super frost slides, dried at room temperature for 1 h, and stored at −20°C until use. Before immunostaining, sections were fixed with 4% PFA for 10 min at room temperature and then permeabilized with blocking buffer (see **Table 3.1**) for 1 h.

3.3.3. Immunostaining

Permeabilized fibers were incubated with primary antibody solution, prepared as indicated in **Table 3.3** on a shaker at 4°C overnight. Then, the primary antibody solution was removed, the residuals were eliminated by washing the fibers 3 times per 5 minutes with PBS buffer (see **Table 3.1**) on a moving shaker at room temperature. Subsequently, the fibers were incubated with secondary antibodies in dark conditions (see **Table 3.3)** on a moving shaker per 2 h at room temperature. Toxins conjugated to fluorescent dyes were used to label compartments of NMJ: Fasciculin, is a toxin that targets Acetylcholinesterase (AChE), the major marker of synaptic clef of NMJ. For that, the fibers were incubated with a fasciculin solution prepared as described in **Table 3.3** in blocking buffer on a moving saker per 30 minutes at room temperature. Fluorescently-labelled bungarotoxins (BTX) bind AChRs and enabled to visualize the post-synaptic terminal of NMJ. The fibers were incubated in BTX solution prepared in PBS buffer as described in **Table 3.3**, and on a moving shaker at room temperature. Fibers subjected to a final wash in PBS at room temperature and then mounted on slides with Fluoromount Aqueous Mounting Medium [Catalog#: F4680-25ML, Sigma]. The fluorescent toxin Phalloidin that binds F-actin, was used to obtain contrast of the muscle cross-sections. The cross-sections on the slides were incubated at room temperature and in dark conditions with fluorescent phalloidin, prepared in blocking buffer (see **Table 3.1)** as in **Table 3.3**. Also, the myonuclei were visualized by DAPI staining (see **Table 3.3)**, prepared in PBS buffer. Cross-sections on slides were incubated with the DAPI solution at room temperature and in dark conditions. The slides were subjected to final wash in PBS solution and closed by Fluoromount Aqueous Mounting Medium [Catalog#: F4680-25ML, Sigma].

3.4. Bimolecular Fluorescence Complementation (BiFC)

3.4.1. Cloning Strategy: NEBuilder HiFi DNA Assembly

The plasmids used for the BiFC experiment were cloned by NEBuilder® HiFi DNA Assembly Cloning Kit (see **Table 3.2**) according to the manufacturer instructions. This method is based on one-step reaction where multiple inserts generated by PCR amplification with 15-25 bp ends overlapping with the linear vector are assembled. The reaction includes 3 different enzymes that work in sequence together in the same buffer: the 5'- Exonuclease creates single-stranded 3′ overhangs. This allows the annealing with inserts that share complementarity at one end (the overlapping region). These fragments are produced by PCR amplification. Then, the polymerase fills in gaps within each annealed fragment. Finally, the DNA ligase seals nicks in the assembled DNA. The reaction is assembled according to the manufacturer instruction, incubated at 50°C per 1 hour and then used to transform NEB 5-alpha Competent *E. coli* (provided with the cloning kit). The primers used in the PCR reaction to generate fragments with overlapping ends were designed by NEBuilder Assembly Tool v2.2.3 and the details are in **Table 3.11**.

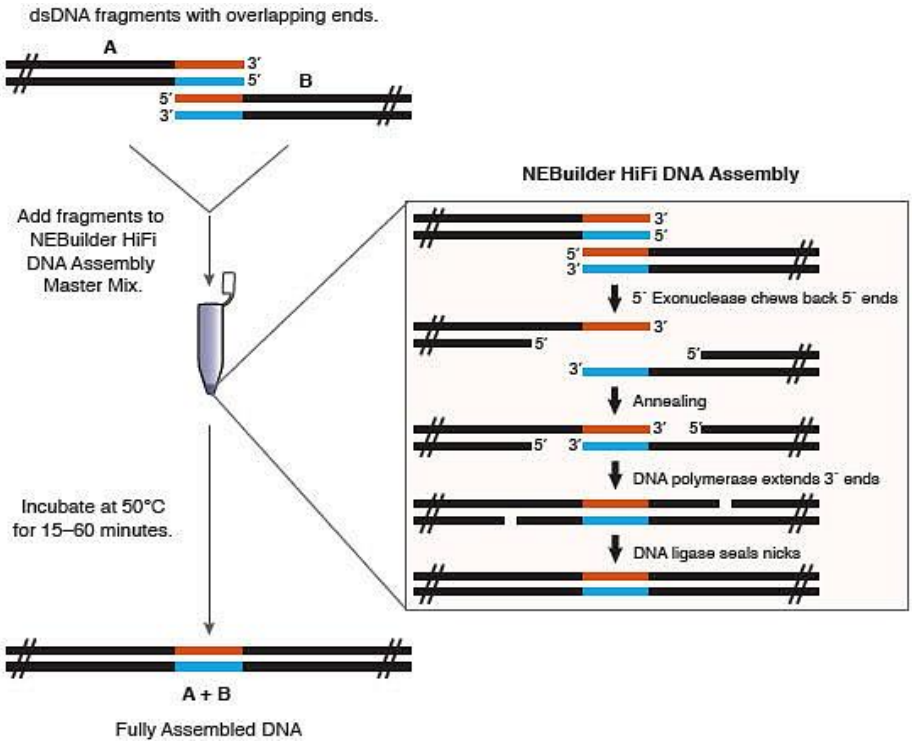

Figure 3.4. Schematic illustration of the Cloning strategy based on NEBuilder HiFi DNA Assembly Method (image adopted from www.neb-online.de).

3.4.2. αDB1VN173 construct for BiFC

pcDNA3.1(+)-aDB1VN173 construct was generated by inserting aDB1nucleotide sequence fused with Venus173 into a pcDNA3.1(+)backbone. The pCDNA3.1_LRP4(mouse)_VN173 plasmid in our possession was digested with FastDigest NheI and FastDigest XhoI (see **Table 3.12**) in a reaction assembled according to the manufactured instructions. This way, I obtained empty and linearized pcDNA3.1(+)backbone. In parallel, the aDB-VN173 fragment was amplified by PCR from the template pBiFC-aDB-VN173, a plasmid provided by Professor Mohammed Akaaboune. aDB1-VN173 fragments were inserted within the empty pcDNA3.1(+) backbone by HiFi assembly strategy.

3.4.3. Cttn-VC155 constructs for BiFC

Empty pBiFC-VN173 commercial plasmid [Plasmid#: 22010, Addgene] was digested with FastDigest BamHI and FastDigest EcoRI (see **Table 3.12**) to generate the linear vector used as a backbone and to excise the VN173 sequence. GFP-cortactin and pBiFC-VC155 (RD validated) (see **Table 3.13)** were used as template to obtain the fragments of Cttn and VC155 by PCR amplification. In the "HiFi assembly strategy", the insertion fragments within backbones is based on PCR amplification, thus two sets of 4 primers were designed and used to generate Cttn in frame with N- and C-terminal VC155. All the intermediate steps of purification from agarose gel and PCR clean-up were performed with GeneMATRIX Basic DNA Purification Kit (see **Table 3.2**) according to the manufacturer protocol. A representative map example of plasmids engendered for BiFC is in **Figure 3.5**.

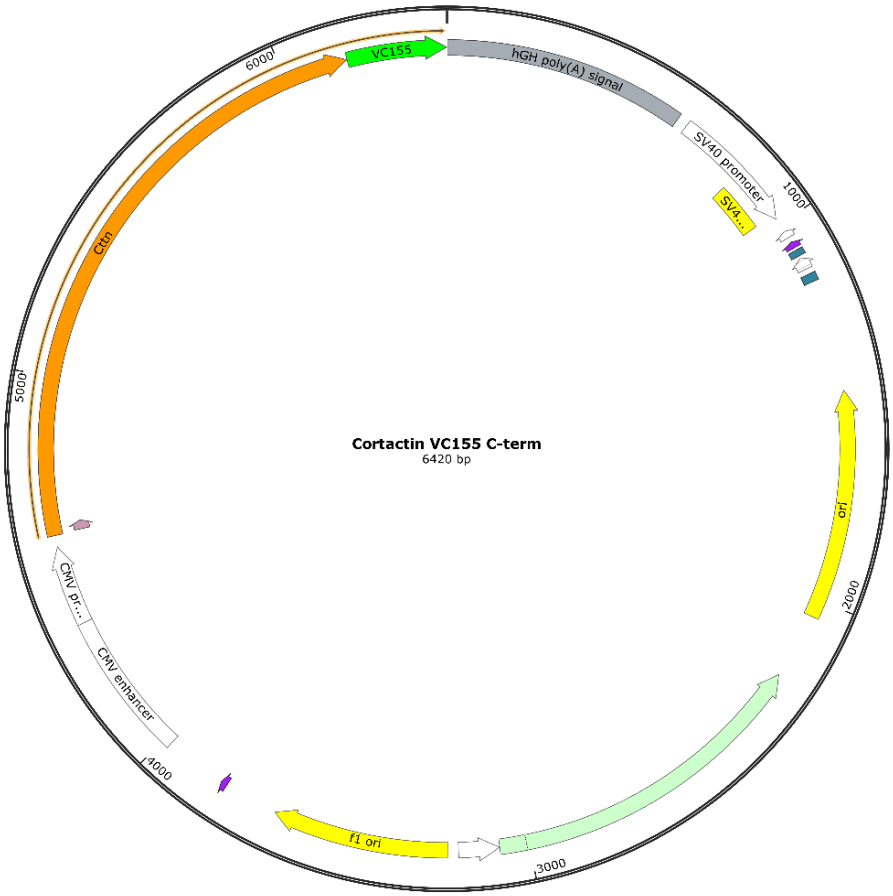

Figure 3.5. Representative map of pBiFC-Cortactin-VC155 plasmid. The Cttn coding sequence is in flame with Venus fragment sequence (VC155), so that the corresponding Cttn protein is fused with VC155 at its C-terminal (image produced by SnapGene).

Table 3.11. Primers designed for Hifi assembly cloning strategy

Primer	5'→3'nucleotide sequence	Plasmid product
ADBVN173_Fwd	TATAGGGAGACCCAAGCTGGATGATTGAAGATAGTGGAAAAAGAG	pcDNA3.1(+)-aDB1VN173
ADBVN173_Rev	TTTAAACGGGCCCTCTAGACCTACTCGATGTTGTGGCG	pcDNA3.1(+)-aDB1VN173
5VC155_Fwd	ACGACAAGCTTGCGGCCGCGGCCACCATGGACAAGCAGAAGAACGGC	pBiFC-VC155-Cortactin
6VC155_Rev	CTTTCCACATCTTGTACAGCTCGTCCATG	pBiFC-VC155-Cortactin
7Cortactin_Fwd	GCTGTACAAGATGTGGAAAGCCTCTGCAG	pBiFC-VC155-Cortactin
8Cortactin_Rev	GTCACAGGGATGCCACCCGGCTACTGCCGCAGCTCCAC	pBiFC-VC155-Cortactin
9Cortactin_Fwd	ACGACAAGCTTGCGGCCGCGGCCACCATGTGGAAAGCCTCTGCAG	pBiFC-Cortactin-VC155
10Cortactin_Rev	TCTGCTTGTCCTGCCGCAGCTCCACATAG	pBiFC-Cortactin-VC155
11VC155_Fwd	GCTGCGGCAGGACAAGCAGAAGAACGGC	pBiFC-Cortactin-VC155
12VC155_Rev	GTCACAGGGATGCCACCCGGTTACTTGTACAGCTCGTCC	pBiFC-Cortactin-VC155

Table 3.12. Restriction enzymes used for cloning strategy

Enzyme	Cat#/Supplier	Purpose
FastDigest NheI	FD0974, Thermofisher	Cloning pcDNA3.1(+)-aDB1VN173
FastDigest XhoI	FD0694, Thermofisher	Cloning pcDNA3.1(+)-aDB1VN173
FastDigest BamHI	FD0055, Thermofisher	Cloning pBiFC-VC155-Cortactin/pBiFC-Cortactin-VC155
FastDigest EcoRI	FD0274, Thermofisher	Cloning pBiFC-VC155-Cortactin/pBiFC-Cortactin-VC155
FastDigest BglII	FD0083, Thermofisher	Colony Screening
FastDigest NotI	FD0593, Thermofisher	Colony Screening

3.4.4. Competent bacteria transformation

Competent bacterial cells (commercial for BiFC experiment, lab-made for standard plasmid amplification) were gently thawed on ice per 10 minutes, then plasmid DNA or, as for HiFi cloning, the chilled assembled product was added. The whole mixture was incubated on ice for 30 min. Subsequently, tubes were put at 42°C in a thermoblock for 45 sec (heat shock), then cooled down on ice for 2 mins and incubated with vigorous shaking after adding 900 µL of LB (see **Table 3.1**) or SOC in 37°C for 45-60 min. After incubation cells were spread on LB agar plates containing a proper antibiotic and incubated overnight at 37°C.

3.4.5. Cloning verification

The bacteria colonies were randomly picked from the plate (standard technique of picking up with pipette tip), inoculated in 2mL LB and grown per ~8h at 37°C under shaking conditions. The amplification of plasmid was purified from each colony by the commercial Plasmid Miniprep DNA Purification Kit (see **Table 3.2**) according to the manifacturer instructions. The plasmid was eluted from the column of the kit with UltraPure™ DNase/RNase-Free Distilled Water [Catalog# 10977049, ThermoFisher]. The concentration and purity of plasmids were assessed by Nanodrop. Each purified plasmid was digested with a suitable combination of restriction enzymes (see **Table 3.12**) to assess and the bands resolved by electrophoresis performed on agarose gel. After electrophoresis run, the band were

visualized on a UV transilluminator available in our lab. Furthermore, the authenticity of the cloned plasmids was confirmed by Sequencing outsourced from external facility. Once the sequencing results confirmed the correct sequence, home-made competent *E. coli* competent cells were transformed with the generated plasmids and high volume culture were set in 200 mL LB medium with the addition of suitable antibiotic. The plasmid was purified by GenElute ™ Plasmid Maxiprep Kit (see **Table 3.2**). The concentration and purity of the eluted plasmid was assessed by Nanodrop.

3.5. Animal procedures

3.5.1. Mice anesthesia

General anesthesia in mice was performed with ketamine/xylazine anesthetic mix prepared as follows: 90mg/kg of ketamine and 5mg/kg xylazine prepared in sterile PBS and administered intraperitoneally. Alternatively, the anesthesia was induced with the use of rodent anesthesia machine based of isoflurane vaporization.

3.5.2. Plasmid electroporation of TA

After 10 min from anesthesia induction, leg was shaved using hair removal cream (Isania). 25 µL of ~1 µg/µL solution of DNA were injected into the tibialis anterior (TA) muscle with a Hamilton syringe followed by electroporation of the whole leg 10 x with 20 ms pulses of 1 s each (1 Hz) by electroporator BTX ECM 830. Electrodes were wetted with PBS to enable ion flow and the voltage was set at ~70-90 V (~4-5 mm thickness of the leg). After electroporation painkillers were administered by subcutaneous injection of 1-5 mg/kg of butorphanol and by putting on the skin a lignocaine gel (lignocainum, Jelfa) containing 2% lidocaine. 7 days after the procedure, the mouse was sacrificed to extract the electroporated tissue. The details of plasmid used for electroporation experiment can be found in **Table 3.13**.

Table 3.13. Plasmids for electroporation

Plasmid	Source	Description
GFP-cortactin	Cat#26722, Addgene	Full-leght Cttn fused with N-terminal GFP
pcDNA3.1(+)-aDB1VN173	self-generated	Full-length aDB1 fused with VN173 fragment (1-172 aa) at N-terminal
pBiFC-VC155-Cortactin	self- generated	Full-length Cttn fused with Venus fragment (VC155 155-238 aa) at N-terminal
pBiFC-Cortactin-VC155	self- generated	Full-length Cttn fused with Venus fragment (VC155 155-238 aa) at C-terminal
pBiFC-Rapsyn-VC155	provided by Prof. Mohammed Akaaboune	Full-length Rapsyn fused with Venus fragment (VC155 155-238 aa) at C-terminal
CAP2-GFP	provided by Prof. Marco Rust	Full-length Cttn fused with GFP
Cttn-flag	Cat#74476, Addgene	Full-length Cttn fused with N-terminal flag
aDB1-GFP	provided by Prof. J. Sanes	Full-length αDB1 with N-term GFP
aDB2-VN173	(outsource) Gene Universal	aDB2 fused with VN1731 Venus fragment (1-172aa) at C-terminal

3.5.3. Denervation

One day beforehand surgery, mice were administered with dose of 2 mg/kg dose of non-steroidal anti-inflammatory drug Meloxicam by intraperitoneal injection. On the next day, 1 hour before surgery, mice were administered with 0.1 mg/kg dose of Buprenorfin by intraperitoneal injection. The anesthesia was induced with the use of rodent anesthesia machine based of isoflurane vaporization. The leg was carefully shaved and skin was cleansed with surgical swabs. Then, the skin was incised posterior, 1 cm sided from the vertebral column posterior and perpendicularly to the femur. The biceps femoris were bluntly separated and the sciatic nerve exposed. Once exposed, the sciatic nerve was compressed by the use of flat-tip tweezers per 30 seconds and repositioned in the hindlimb. The wound was sewed by nylon sutures. Lidocaine was applied to the leg after surgery. After the procedure, 2 mg/kg dose of Meloxicam was administered to the mice per 2 consecutive days. The animals were sacrificed at different time points after nerve damage. The procedure was approved beforehand by the Ethical Committee (LKE #008/2021).

3.5.4. New-born mice AAV injection

The anesthesia in newborn CAP2-KO pups (P0) was induced in-ice. Then, the animals were placed in ice per 3-5 minutes while gently wrapped in towel paper to prevent skin burn due to the direct contact of the nude skin with ice. 3.5 μL of the AAV2/9 CAP2-GFP virus (see **Table 3.14**) were injected in one leg, while the other leg was injected with Control- AAV9-GFP. Each new-born mouse was processed singularly. At P21, the mice were sacrificed and tissues extracted and processed for NMJ analysis.

Table 3.14. Virus used for rescue experiment in newborn CAP2-KO pups

Virus	Source
AAV2/9 CAP2-GFP	Nencki Facility
Control- AAV9-GFP	Cat#: SL100840, SignaGen

3.6. Cell culture

The commercially available human embryonic kidney (HEK) 293T cell line, purchased from ATCC [Catalog# CRL3216] was cultured in Dulbecco's Modified Eagle's Medium (DMEM), with 4.5 g/L Glucose, without *L*-Glutamine, supplemented with 10% Fetal bovine serum, 1% Penicillin-Streptomycin (5,000 U/mL) [Catalog#: 15070063, Thermofisher], and 0.1% Amphotericin B, [Catalog #: 15290018, Thermofisher]. Once reached 90% confluency, the cultured cells are washed with 37°C sterile and warmed-up commercial Phosphate buffered saline (PBS) 1X [Catalog #: E504-500ML, VWR] and dissociated by incubation at 37°C with Trypsin-EDTA (0.25%), phenol red [Catalog #: 25200056, Thermofisher]. The dissociated cells were pelleted at 200G per 3 minutes, and 1/10 seeded on a new petri-dish and cultured in the incubator. HEK293T cells were incubated at 37°C and 5% CO2.

3.6.1. Cell transfection

The transfection of the HEK 293Tcells with TransIT®-LT1 Transfection Reagent [Catalog #: 2300, Mirus Bio] was performed in accordance with the indications of the manufacturer. Therefore, 2.5 µL of 1µg/µL concentrated plasmid was diluted in 250 µL Opti-MEM [Catalog #: 11058021, ThermoFisher]. Subsequently 7.5 µL of TransIT®-LT1 Transfection Reagent was added to the diluted plasmid and incubated at room temperature for 30 minutes. Finally, the mixture was dropwise added to the 70-80% confluent cells seeded in 6-well plate.

3.6.2. Cells Lysis

After 48 hours in ice, the cells were washed with Phosphate buffered saline (PBS) and were mechanically removed from the dish with the addition of 500 µL co-ip lysis buffer (see **Table 3.1**) supplemented with cOmplete™, EDTA-free Protease Inhibitor Cocktail (Catalog# 4693116001, Roche) per well. After incubation on a rotor at 4 °C for 30 minutes, the samples are centrifuged at 14000 rpm in 4 °C per 30 minutes and the supernatant is collected.

3.7. Co-Immunoprecipitation

3.7.1. Protein isolation from cells

Cells were placed on ice and the culturing media was removed. Afterwards, the cells were washed with fresh PBS and lysed in lysis buffer (**Table 3.1**). The cells

were scraped off the dish, incubated at 4°C on a rotor per 30 minutes centrifuged at 14000 rpm for 30 min, at 4°C.The supernatant was separated from the pellet and frozen at -20°C until use.

3.7.2. Protein isolation from tissue

Muscles were stripped of connective tissues, cut into smaller pieces using razorblade and sonicated in lysis buffer. Performed in ice, sonication consists of multiple pulses of 10s at 20% amplitude intensity until the muscle mass is entirely lysed and the solution starts to create foam. Afterwards, the sample is centrifuged at 4°C for 10 minutes at 10'000G and supernatant is collected and used or frozen at -20°C until use.

3.7.3. Magnetic beads preparation

Magnetic beads [Dynabeads™ M-270 Epoxy, Catalog#: 14301, Thermofisher] were resuspended in PBS supplemented with 0,1% NP40, and aliquoted in new tubes (0.2 mg in 25 µl per sample).

3.7.4. Antibody binding

1µg of antibody (see **Table 3.3**) per sample was bound to Dynabeads™ M-270 Epoxy beads by the use of the Dynabeads™ Antibody Coupling Kit (see **Table 3.2**) according to the manufacturer instructions.

3.7.5. Co-immunoprecipitation

200µL of protein samples were added to the antibody coupled Dynabeads™ M-270 Epoxy beads and incubated at 4°C overnight on a rotor shaker. After the incubation, the tubes were put on a magnetic rack and the supernatant was collected. The beads-Ab-Ag complexes were washed 3-4 times in 200 µL PBS + 0,1% NP40 (per sample).

3.7.6. Target protein complex elution

After removal of the supernatant from the last wash was, 30 µL (per sample) of 2XLaemmli Sample Buffer [Catalog #: 161-0747 , Bio-Rad], supplemented with 50 mM DTT, was added. After heat denaturation for 10 min at 95°C the elution was loaded onto a gel or stored at -20°C until use.

3.7.7. SDS-PAGE

Each protein sample was prepared by the addition of 4XLaemmli Sample Buffer [Catalog#: 161-0747, Bio-Rad] and supplemented with 50mM 1,4-Dithiothreitol DTT [Catalog #: 6908.1, Carl Roth]. The mix was boiled at 95°C for 10 min, fast centrifuged at room temperature and loaded on the gel. SDS-PAGE (Sodium dodecyl sulfate polyacrylamide gel electrophoresis) was performed using the PowerPac Basic system (BIO-RAD) in electrophoresis buffer (see **Table 3.1)** under 80-100 Voltage conditions. Standard preparation for acrylamide gels was used. For protein size reference, commercial protein markers were used: Color Prestained Protein Standard, Broad Range [Catalog#: P7712S, NEB].

3.7.8. Western blot

After SDS-PAGE, the proteins were transferred from the acrylamide gel onto a 0.2 µm pore size nitrocellulose membrane [Catalog#: 1620112, Bio-rad]. The apparatus used to the transfer was Trans-Blot® Turbo™ Transfer System [Catalog#: 1704150EDU, Bio-rad] and transfer was performed according to 7-min-long default protocol (1.3A, 25V current). The membrane was incubated in 10% non-fat milk blocking TBST buffer on a shaker at room temperature. The membrane was incubated overnight with primary antibody solution (**Table 3.3**) prepared in 5% non-fat milk TBST (see **Table 3.1**). The next day, primary antibody solution was removed and the residual antibody was removed by washing the membrane 3 times with TBST buffer at room temperature per 5 minutes. The membrane was then incubated with a solution of secondary antibody (see **Table 3.3**) prepared in in 5% non-fat milk TBST (see **Table 3.3** for used dilutions) per 2h at room temperature. The excess of antibody was eliminated by TBST buffer. Finally, immunolabelled proteins were detected with the chemiluminescent SuperSignal West Femto Maximum Sensitivity Substrate or Clarity Western ECL Substrate (see **Table 3.2**) by incubation for 1 minute at room temperature. Membranes were developed for visualization either in a dark room with Kodak® BioMax® MS films (Carestream, Rochester, NY, USA, cat. #771468) and a film processor (Fujifilm, Tokyo, Japan, cat. #FPM 800A) or with ChemiDoc XRS+ Gel Imaging System and visualized by Image Lab™ Software (Catalog#: 1708265 Bio-rad).

3.8. Behavioral experiments

In total 16 mice (n = 8 WT and 8 Cttn-KO) aged 12-24 weeks were used in the behavioral experiment. To minimize the sex-related variability, the experiments were performed on female animals only. To habituate the animals to the experimenter and reduce the stress, the mice were handled per 5 consecutive days

beforehand behavioral tests. All the behavioral tests were performed blind of the animals genotype.

3.8.1. The "grip strength" test

The device utilized consists of an electronic strength device (Grip Strength Meter by Ugo Basile, Catalog#47200) that electronically records the peak-pull force. The force gouge of the apparatus is connected to a grid bar. The grid bar I choose enabled the animal to hold the bar by all limbs, thus allowing the measurement of the force from both forelimbs and hindlimbs. The animal was placed on the grid bar and, when pulled backward by the tail, the mouse was firmly grasping the grid bar to contrast the involuntary backward movement, the pulling force overcomes the grip strength, and the bar is released by the animal. The peak-pull force is automatically recorded by the device. Each measurement was repeated 10 times per animal with an interval break of 60 sec between each measurement.

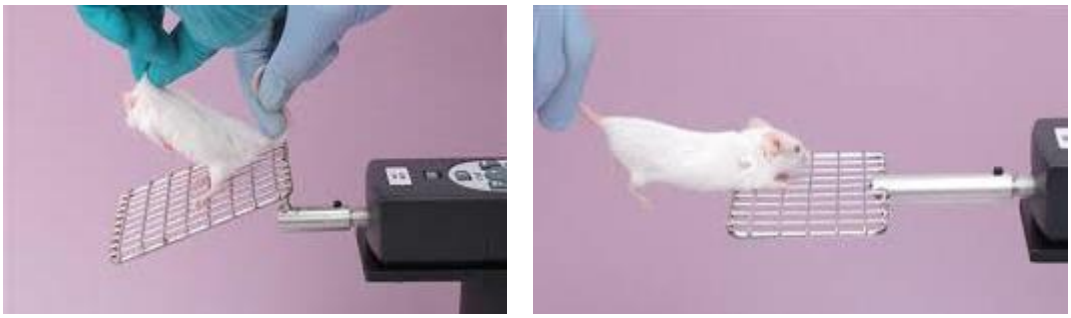

Figure 3.6. Illustration of a grip strength experiment. The rodent was delicately placed on a grid bar that allowed all limbs grasp. The black arrow indicates the direction of the pulling force (adopted from the Internet).

3.8.2. The "voluntary wheel" test

The locomotor activity of the animals was tested using the Running Wheels for rodents' motor activity measurement, by the use of an apparatus similar as in **Figure 3.7** (Catalog# 1800-1850, Ugo Basile). Each apparatus consists of a cage completed with a wheel connected to a magnetic counter that records the wheel's revolutions. The animals were placed singularly in the apparatus and had free access to the wheel, thus this type of exercise is performed upon will of the animal. The magnet measurements were tracked and recorded by ANY-maze Software during the rodents' active period from 18-6 day time. Each apparatus was supplied with food and water *ad libitum*.

Figure 3.7. Voluntary wheel apparatus (image adopted from https://www.bioseb.com).

3.8.3. The “exhaustion” test

The exhaustion test evaluates the endurance of mice to exhausting exercise and was assessed by a motorized treadmill (Catalog# 57630, Ugo Basile). In this test, animals were forced to run at gradually increasing speed to exhaustion over a conveyor belt modulated according to the protocol. Each lane of the treadmill was provided with air-puffs activated by the mouse standing on the sensor grid at one extremity of each running lane. The air-puff were employed as a noxious stimulus that forced the animals to run on the treadmill against their natural behavior. The mice familiarized with the instrument beforehand by running at 10m/min speed, 0% slope per 5 minutes per 5 consecutive days on this treadmill. After the habituation period, the animals were subjected to 5 minutes of warm-up at 10m/min speed and 10% slope, then the treadmill was automatically and progressively accelerated by 1m/min, 10% slope. The exhaustion was considered reached when the animal was subjected to a minimum of 15 seconds of consecutive air-puff stimulation and unable to run distant from the air puff grid. Once fatigued was reached, the air-puff was manually inactivated to allow the animal to rest.

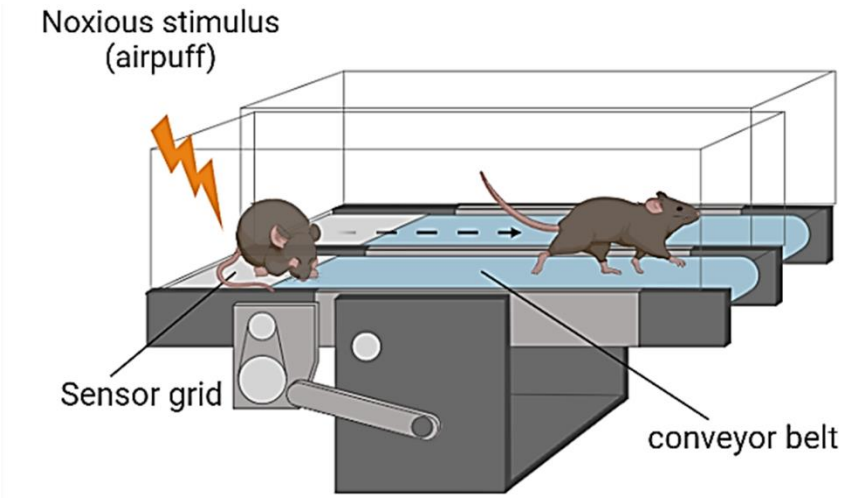

Figure 3.8. Schematic illustration for endurance test on treadmill for rodents (image created with Biorender).

3.9. Microscopy

Immunofluorescence microscopy was performed using a spinning disk confocal microscope (Zeiss) from the facilities of Nencki Institute of Experimental biology and Bioimaging Laboratory of PORT-Łukasiewicz Research Network. The images were acquired in z-stack including the volume of all analyzed structure. Orthogonal projections of the collected images were performed by Fuji ImageJ Software. The automated analysis of NMJ was performed by the ImageJ plug in of NMJ-morph.

3.10. Statistics

The statistical analysis was performed in GraphPad Prism 6 (GraphPad Software Inc., San Diego, CA, USA) and Microsoft Excel the results are shown as mean ± SD/ ± SEM. The raw data collected were analyzed by unpaired Student's t-test or Chi-square test. The statistical tests which revealed a p-value < 0.05 were considered statistically significant.

4. Results

4.1. CAP2 project

We have previously demonstrated in collaboration with prof. Marco Rust Laboratory (University of Marburg, Germany) that Cap2-KO mice have abnormal contractile machinery in skeletal muscles and shortly after birth exhibit motor coordination deficits. It is not clear, however, if Cap2 is anyhow involved in NMJ organization and regulation of synaptic transmission. Therefore, I decided to perform detailed analysis of NMJ morphology in Cap2-KO mice.

4.1.1. Adult CAP2-KO NMJs are abnormal in size

I visualized the NMJs of Tibialis anterior (TA) by labelling the pre-, post-synaptic machinery with anti-Synaptophysin antibody and Bungarotoxin conjugated with Alexa dye. Additionally, I stained tissues with fluorescently labeled fasciculin toxin, which binds to synaptic cleft marker AChE. I discovered evident structural abnormalities in the NMJs of these mice line. Cap2-KO mice have normal alignment of the presynaptic marker, postsynaptic AChR, and synaptic cleft protein AChE that were comparable to control (WT) mice. It demonstrated that synapses were formed. CAP2-KO mice have, however, apparent population of NMJs with abnormally small size, which I called “Small NMJ” (**Figure 4.1**). At the same time, I observed that Cap2-KO mice have also a population of NMJs that was much larger than those in control animals, which I called “Large” NMJs. To quantify abnormal NMJs I decided to categorize them to three groups based on the largest synaptic diameter. Small synapses were defined as < 35 μm, medium size group constituted synapses 35-65 μm and the Large NMJs were of size exceeding 65 μm (**Figure 4.1 A-C**).

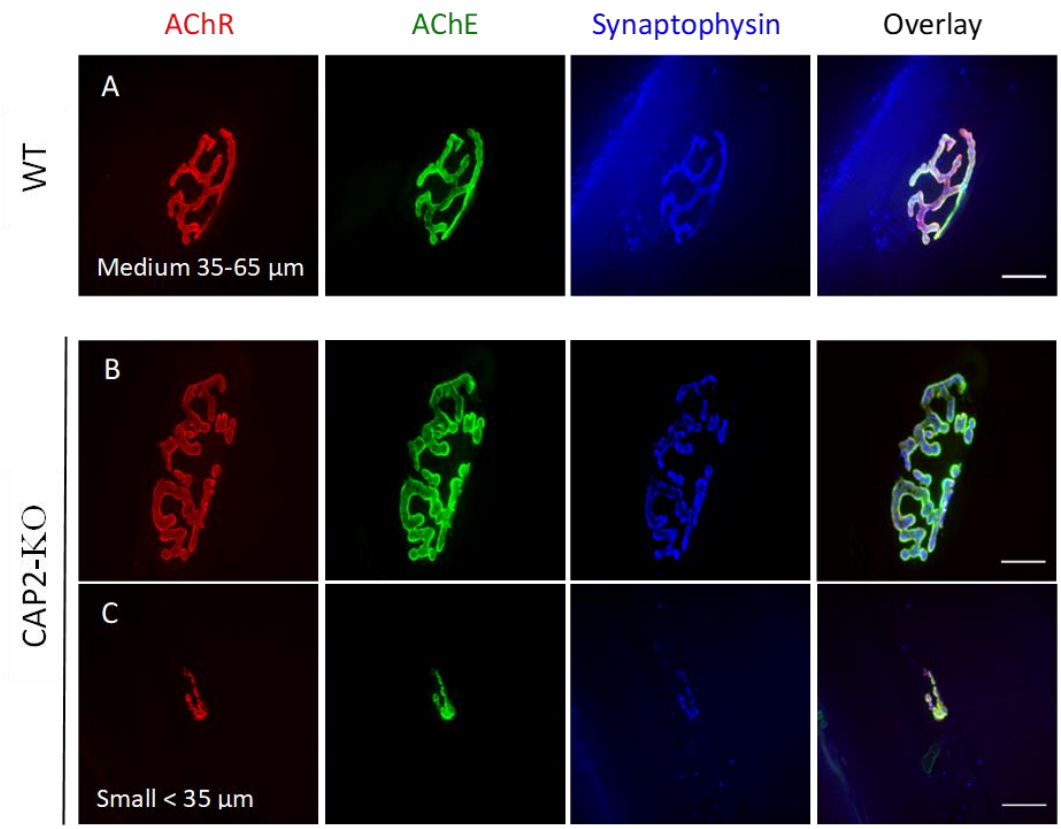

Figure 4.1. Abnormal NMJ size in CAP2-KO. A) Upper panel's line: example of healthy NMJ of normal size (size range 35-65 µm) . **B, C**) Lower panel: example of enlarged size (size range > 65 µm) and diminished size (size range < 35µm), scale bar = 20µm).

Quantitative analysis demonstrated that Cap2-KO mice have decreased percent of medium size NMJs and strongly increased percentage of Small and Large NMJs in TA muscle (**Figure 4.2 A**). To determine whether NMJs in different muscle types are also affected by CAP2 deletion, I analyzed NMJs in the slow-twitching Soleus muscle and the fast-twitching Quad muscle. Quantification of NMJ size confirmed that the number of enlarged NMJs is statistically increased in CAP2-KO mice in both fast and slow-twitching muscles (**Figure 4.2 A, B, C**). Whereas the number of Small NMJs is increased in TA and Soleus muscles but not to Quad muscle. It is interesting observation, because TA and Quad muscles have similar contractile and metabolic properties. These results seem to indicate certain phenotype variability for Small NMJs. Furthermore, I wondered whether any relationship existed between NMJ size and muscle fiber size, therefore I performed such correlation analysis and I observed that small NMJ were predominantly formed by thinner fibers and large NMJs are present on fibers of medium and large diameters in CAP2-KO (**Figure 4.2 D, E**). Lack of correlation was confirmed by statistical analysis (Pearson's correlation, r: 0.575, p-value< 0.000). At the same time I have

not detected substantial differences in fiber diameter between WT and Cap2-KO mice (**Figure 4.2 F**).

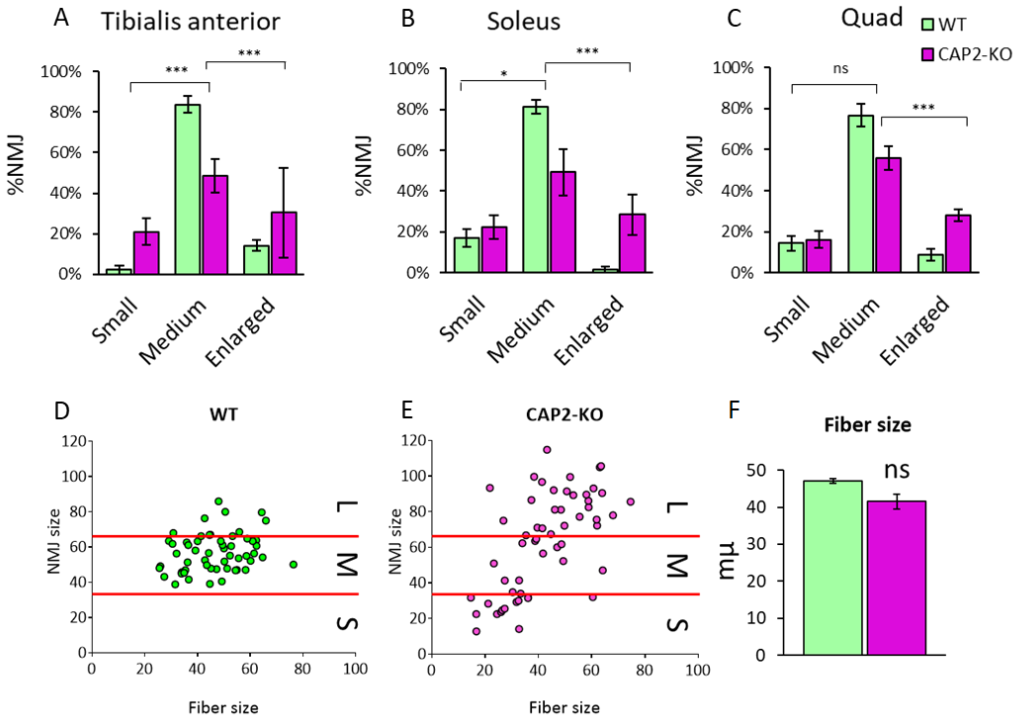

Figure 4.2. Quantification of NMJ phenotype *in vivo*. A-C) NMJ size quantification in TA, Sol, and Quad muscles (n animals per genotype = 3; n NMJs in TA ≥ 59, Sol ≥ 43, Quad ≥ 62; for statistical analysis X2 test was used; bars = means, error bars - SEM). **D-E**) Correlation plot of fiber size and NMJ size. **D**) WT (correlation(r): 0.287, p-value: 0.069). **E**) CAP2-KO (correlation(r): 0.575, p-value< 0.000). S=small, M=medium, L=large. **F**) Fiber size quantification in WT and CAP2-KO (statistics: t-Test, p-value= 0,1018, bars = means, error bars = SEM).

4.1.2. NMJ fragmentation in CAP2-KO

The NMJs of CAP2-KO mice appeared to be more fragmented compared to those in WT animals, with some NMJs consisting of up to 21 fragments (**Figure 4.3**). To quantify this observation, I classified the NMJs according to the number of contiguous AChR-labelled units. Class I constitute synapses that contain from 1 to 3 fragments, Class II contained junctions with 4-5 fragments, and Class III represents the most fragmented NMJs with more than 5 fragments (**Figure 4.3 A**). Quantification analysis revealed that Cap2-KO mice have increased NMJ fragmentation in fast-twitching TA and Quad muscles as well as in slow-twitching Soleus muscle (**Figure 4.3 B**). Altogether, these findings show that the lack of CAP2 affects the integrity of the neuromuscular synapses. I can speculate that the CAP2-dependant mechanism underpinning the NMJ's organization is independent of the one previously reported (Kepser et al., PNAS, 2019) governing sarcomere organization, which has been observed only in fast-twitching but not in slow-twitching fibers, as these defects have been ascribed exclusively to fast-twitching muscle.

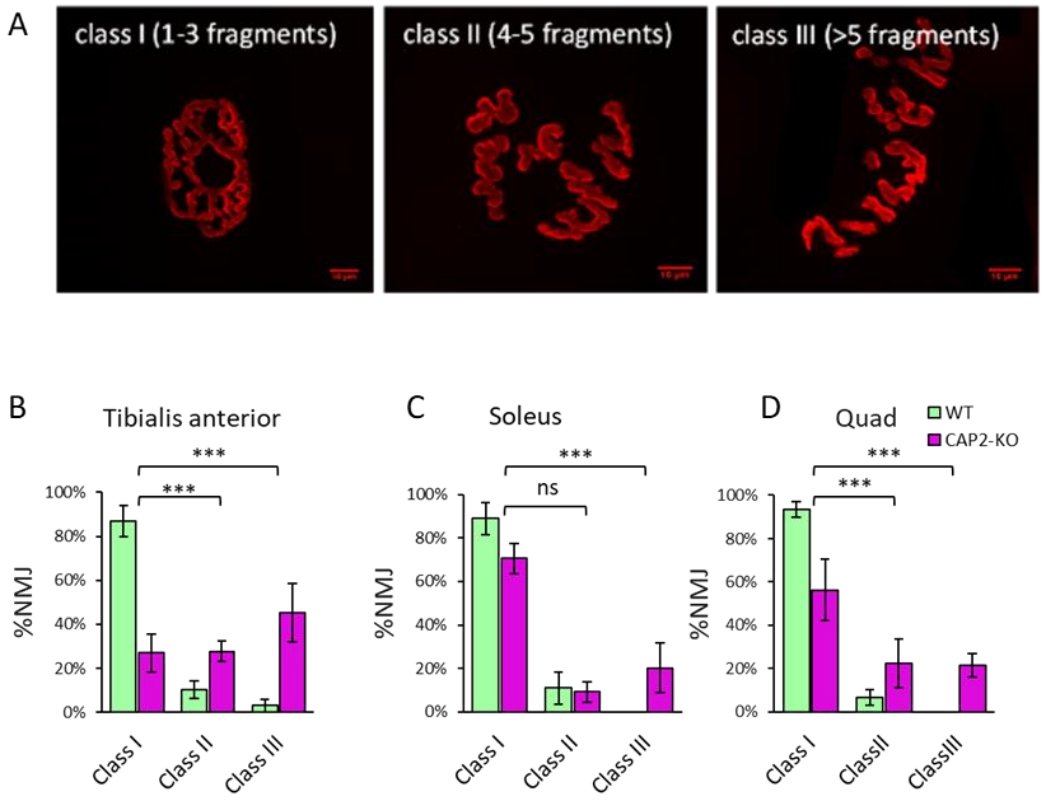

Figure 4.3. Increased NMJ fragmentation in CAP2-KO mice. A) Classification of NMJ based on class of fragmentation, scale bar = 10µm. **B-D**) Quantification of fragmentation in different muscle type (n animals per genotype = 3; n NMJs in TA ≥ 59, Sol ≥ 43, Quad ≥ 66; statistics: X2; error bars = SEM).

4.1.3. Developmental study of CAP2-KO NMJs

To identify at which developmental stage the CAP2 phenotype starts, I analyzed the NMJs from mice aged 20 days and I confirmed a tendency similar to P30, with significant abnormal NMJ size and higher fragmentation associated with CAP2-KO in TA (**Figure 4.4 A, B**) Subsequently, I visualized the NMJs of CAP2-KO mice aged P7 (**Figure 4.4 C**). At P7 the NMJs exhibit simplified and unbranched structure in both CAP2-KO as WTs, however quantification of NMJs' size showed a small but significant increase in the NMJ size (**Figure 4.4 D**).

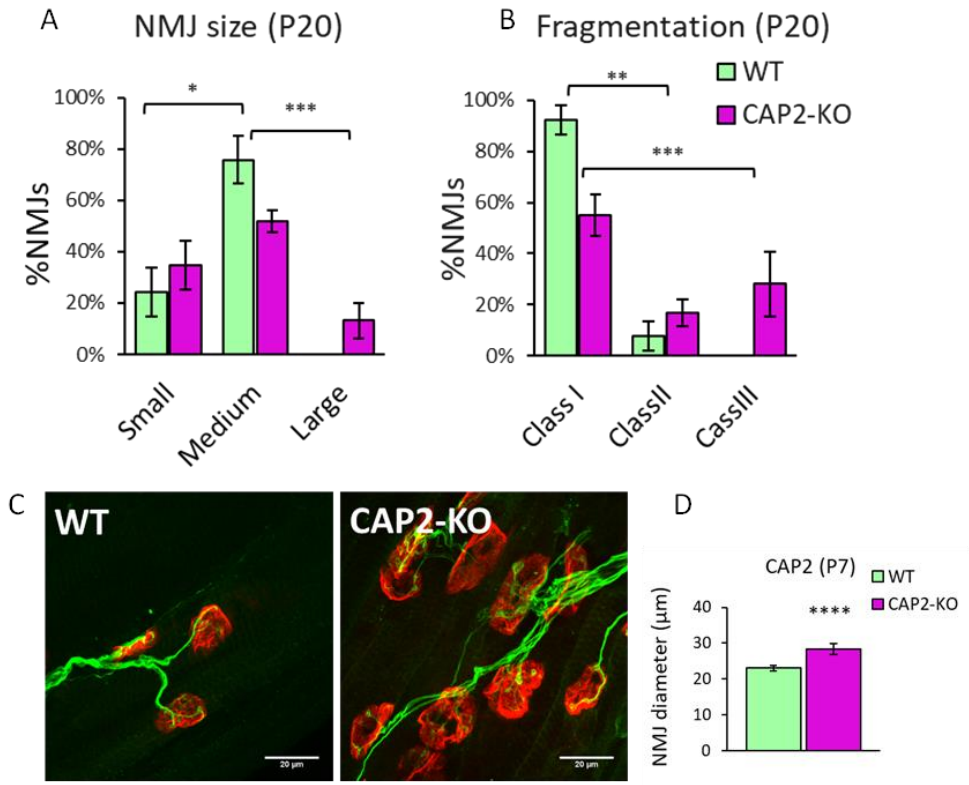

Figure 4.4. Abnormalities during postnatal synaptic development in CAP2-KO mice. A) NMJ abnormal size in CAP-KO P20 mice. n NMJs = 81 for WT and 98 for CAP2KO. **B**) NMJ fragmentation in CAP2-KO P20 mice. n animals per genotype = 3; n NMJs = 53 for WT and 47 for CAP2KO; statistical test = X^2; error bar + SEM. C. NMJs in P7 animals. Scale bar = 10µm. **D**) Increased NMJ size in P7 CAP2-KO mice; n animals per genotype = 3; n NMJs = >160; statistics: unpaired t-test, bars = means, error bars - SEM, p-value = < 0.0001.

4.1.4. The “small” NMJ lay on single fibers

In response to lack of presynaptic signals, muscle fibers often form additional, ectopic postsynaptic machineries that could be innervated by the nerve after injury. To rule out the possibility that the Small NMJs might be ectopic junctions form additionally to the normal synapses formed in other regions of the fibers, I isolated and analyzed single fibers from WT and Cap2-KO TA muscles and study the localization and the number of the postsynaptic machinery visualized with bungarotoxin. Firstly, I observed that small NMJs are the only synapses present on a single fiber (**Figure 4.5. A**), and secondly that enlarged NMJ are alone and no other AChR agglomerates are formed on the same fiber (**Figure 4.5. B**). Altogether, these observations indicate that the small NMJs are indeed independent synapses, and also it is possible to hypothesize that small NMJs are impeded to fully maturate during the postnatal development (after P7).

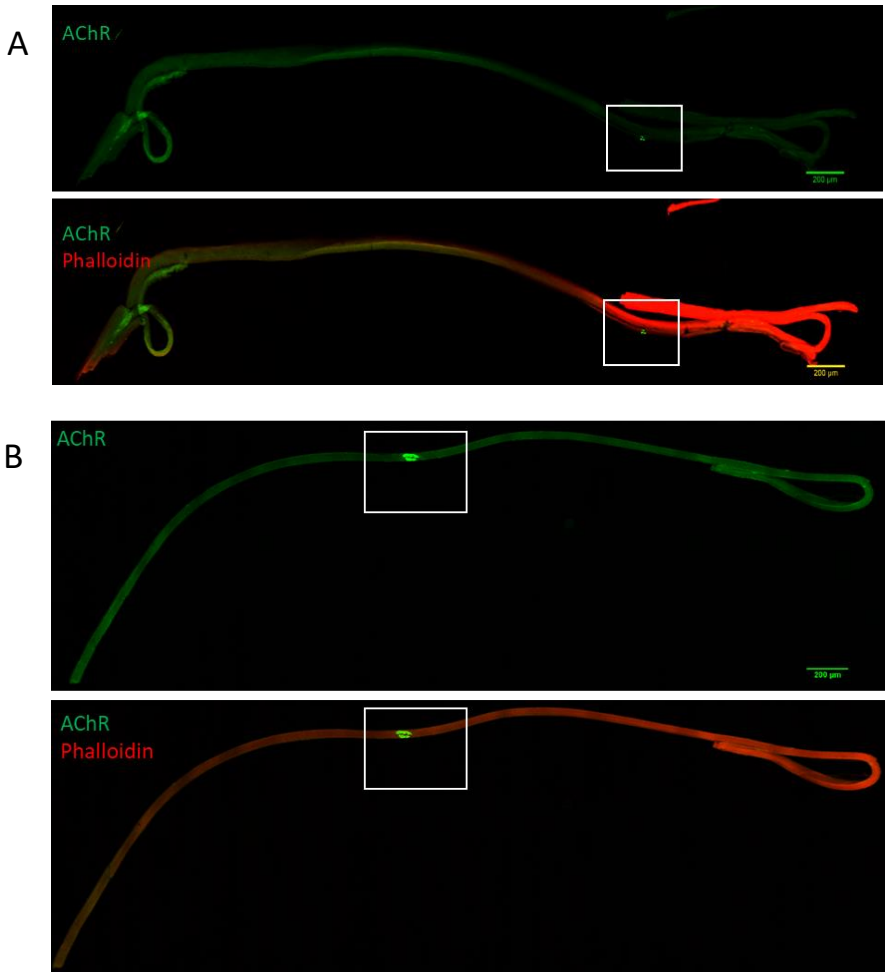

Figure 4.5. A) Example of dissected entire muscle fibers with single small NMJ on it. NMJ size = 31,7µm. **B)** Example of single large NMJ on a single isolated fiber. NMJ size = 78,312 µm. Scale bar = 200µm.

4.1.5. Localization of CAP2 at NMJ

In literature, CAP2 has been shown to be present at the pointed end of the actin filaments within cardiomyocytes. To assess the localization of CAP2 in skeletal muscles, I electroporated the GFP-CAP2 encoding construct in WT TA muscle and I observed the presence green fluorescence (**Figure 4.6 C, C'**) concentrated at the NMJ in a pattern that overlaps AChR (**Figure 4.6 B, B'**). However, GFP-CAP2 plasmid electroporation also led the formation of fluorescent agglomerates with weak capacity to diffuse along the muscle fibers, and this made the experiment difficult to replicate because electroporation often led to expression limited to small region of the fiber away from NMJs. Thus, due to this technical limitation, the results hinting that CAP2 localizes at NMJ should be considered with caution and require further consolidation.

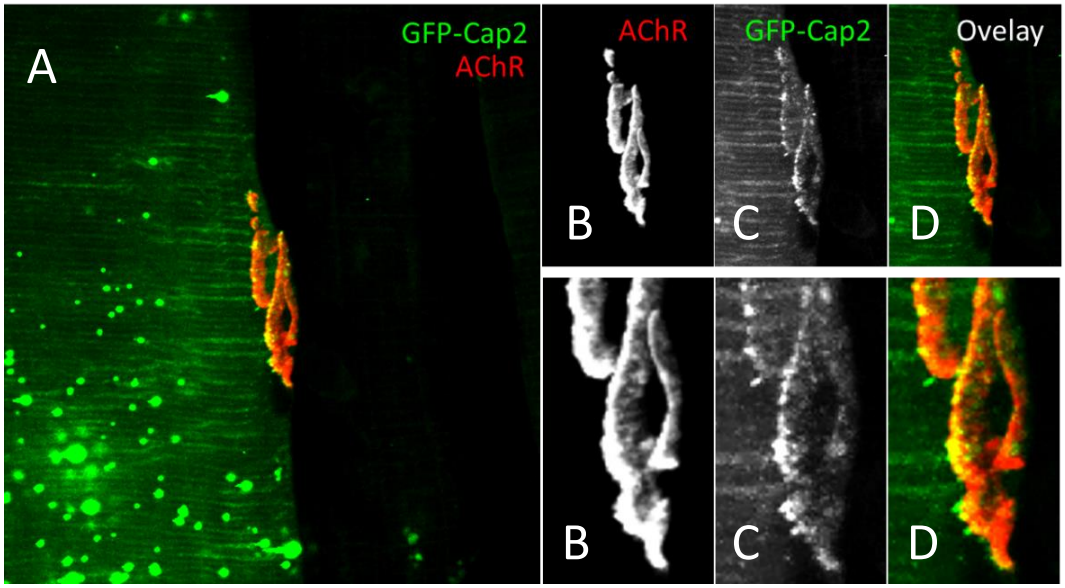

Figure 4.6. GFP-CAP2 concentrates at the NMJ in WT TA muscle electroporated with plasmid.

4.1.6. Re-expression of CAP2 in muscle fails to rescue the NMJ phenotype

To assess whether the defects in the NMJ structure depends on lack of CAP2 in skeletal muscles, I reintroduced CAP2-GFP by AAV2/9 vector injection in TA of new-born Cap2-KO mice that were sacrificed at P20 (**Figure 4.7 A**). The visualization of the NMJs revealed that the reintroduction of CAP2 have not ameliorated of the synaptic architecture as I could still observe enlarged and fragmented NMJs (**Figure 4.7 B,** white arrows) and small NMJs (**Figure 4.7 B,** yellow arrows). This observation led me to question whether the leading cause of the NMJs defects might derive from the lack of CAP2 in muscle fibers. The alternative possibility is that NMJ phenotype could be a consequence from the lack of Cap2 in the nerve. Furthermore, my observations are in contrast to previous report that AAV-mediated expression of GFP-Cap2 in KO mice rescued the sarcomere defects in skeletal muscle (Kepser et al., *PNAS*, 2019). In both studies I used the same batch of GFP-Cap2 AAV serotype 2/9 and I infected animals at the same developmental time. Collectively, this strengthen the hypothesis that the NMJ phenotype in CAP2-KO mice is independent from the sarcomere abnormalities.

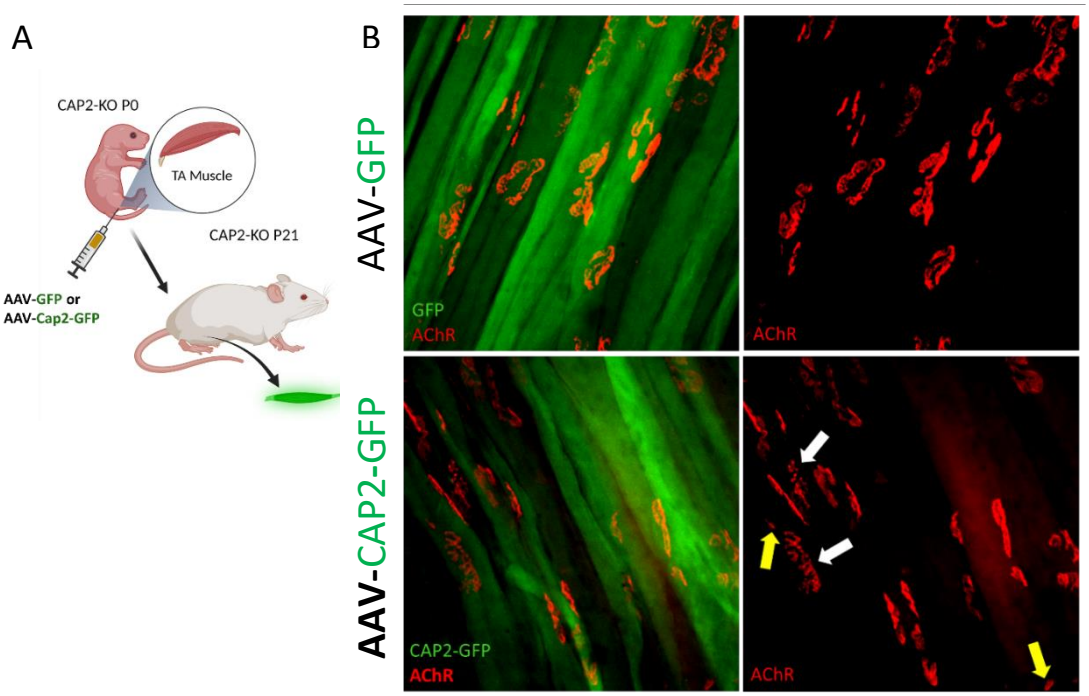

Figure 4.7. Ectopic expression of GFP-CAP2 fails to rescue NMJ phenotype. A)Scheme illustrating the experimental procedure of GFP-Cap2 expression in CAP2-KO TA muscle. **B**) The AAV2/9- mediated expression of exogenous GFP-CAP2 is unable to revert the structural NMJ abnormalities in CAP2-KO. Yellow arrows point at fragmented and enlarged NMJs; white arrows point at small NMJs.

4.1.7. Synaptic poly-innervation in CAP2-KO

Since several lines of evidence suggest that NMJs abnormalities are not due to the lack of Cap2 function at the NMJs, I performed detailed analysis of the motor neurons axons. I visualized the CAP2-KO motor axons (MN) processes by immunostaining with anti-neurofilament antibodies and I noticed that the NMJs from adult CAP2-KO mice appeared to be unusually polyinnervated, meaning that single postsynaptic site was contacted by multiple axons (**Figure 4.8 A**). The quantification of such phenotype revealed a significant 4-folds increase of poly-innervation in KO compared to WTs in both the TA and the Soleus muscles (**Figure 4.8 B, C**).

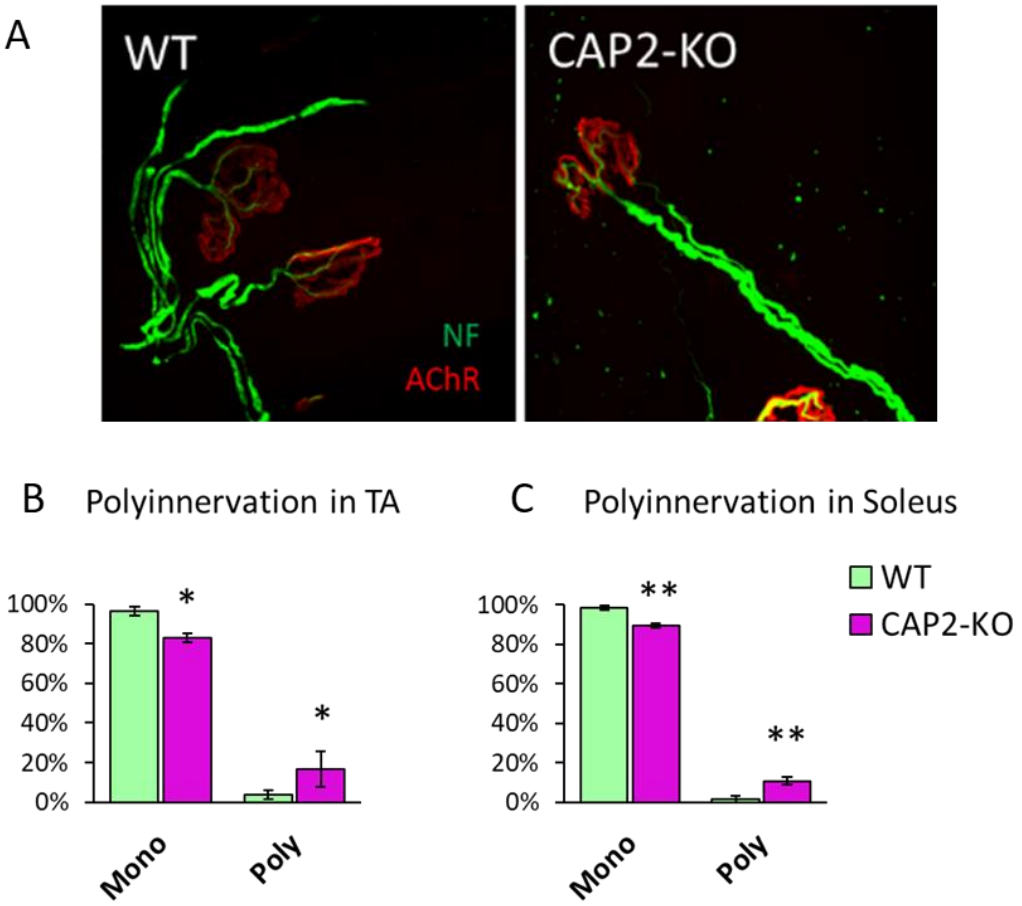

Figure 4.8. A) NMJ Polyinnervation in adult CAP2-KO mice. WT NMJs are contacted by single axon. Cap2-KO mice have increased number of NMJ innervated by multiple axons (NF - neurofilament). **B**) Quantification of polyinnervation in TA (n animals per genotype = 3; mice age: P75; n of NMJs per genotype = 151 in WT and 120 in CAP2-KO. **C**) Quantification of polyinnervation in Soleus (n mice = 5 per genotype; mice age: P75-P91, n of NMJs per genotype = 153 in WT and 160 in CAP2-KO. Statistics: One-way ANOVA with Tuckey correction; error bar = SEM).

4.1.8. Motoneuron defects in CAP2-KO

I observed that CAP2-KO axons exhibited also heterogeneous morphological abnormalities. Some axons were visibly "swollen" displaying increased diameter along the entire length (**Figure 4.9 A**) or had a short portion of the axon swollen. Some axons contain swelling close proximity with the junction which I called "bulbs" (**Figure 4.9 B**). This term I used in similarity to well-known retractory bulbs, a characteristic swelling of axons next to the junctions when the nerve terminal degenerates and retracts from the postsynaptic machinery. Such processes occurs in development during elimination of polyinnervation and after nerve injury. The retractory bulbs look exactly like bulbs in Cap2-KO, however, I have never observed retraction of the nerve terminal from the postsynaptic machinery in Cap2-KO animals (the alignment of the pre- and the postsynaptic machinery was normal). A third feature I observed concerns the highly fragmented NMJs, whose multiple AChR agglomerates are contacted by axonal branches displaying a peculiar terminal swelling (**Figure 4.9 C**) localized in the middle of each AChR fragment. Finally, one last feature emerged from the tissue analysis and consists of the presence of axons which apparently fail to target correctly any synaptic terminal. Altogether, these findings indicate that the depletion of CAP2 leads to multiple structural presynaptic alterations. In the light of the property of CAP2 to participate in counteracting mechanisms of actin-remodeling, it is possible to speculate that the heterogeneity of CAP2 phenotype at the motor axon mirrors the multitasking nature of CAP2.

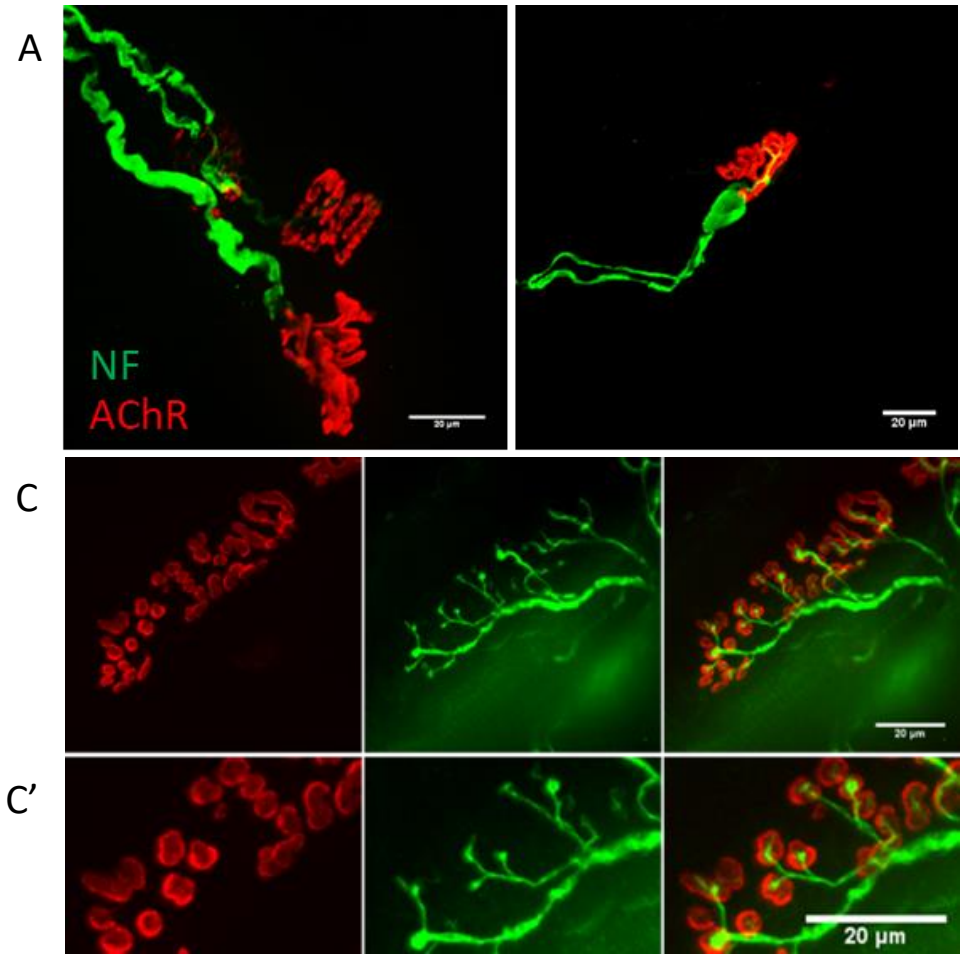

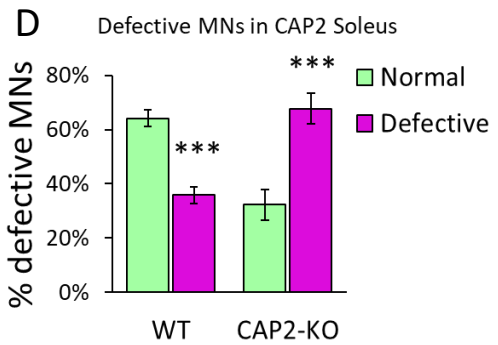

Figure 4.9. Defects of MN in CAP2-KO. A) Swollen axon innervating NMJs in CAP2-KO. B) Axon with bulbs. **C**) Terminal swelling of axon innervating highly fragmented NMJs in CAP2-KO (NF - neurofilament). C'. Magnification of selected area from image in C. **D**) Quantification of MN defects in Soleus expressed in percentage (n animals per genotype = 5, mice age = P75-P91, n NMJs per genotype = 151 in WT and 143 in CAP2-KO, statistics: One-way ANOVA test with Tukey's multiple comparisons correction, error bar = SEM).

4.1.9. Axon regeneration after nerve crush

The rapid actin rearrangements facilitates mechanisms such as axon navigation during development and also axon regeneration after injury. Thus, it's possible that axonal actin dynamics disturbed upon lack of CAP2 with consequences for the NMJ stability. Furthermore, bulbs and axon swelling are known to be signs that precedes axonal loss during the developmental process of "synaptic elimination" and also axonal shedding after nerve injury. To test the axonal regenerative capacity in CAP2-KO, I decided to perform denervation of the sciatic nerve and assess the effects for NMJ maintenance in the hind limbs' skeletal muscles. In this experiment the skin at the hind leg is cut to expose the sciatic nerve. The nerve is then squeezed by forceps for 30 seconds. This procedure leads to nerve injury and subsequent degeneration of the axon down the injury site. However squeezing does not disconnect axon, which over the next weeks regenerates and regrow back to muscles innervating the same postsynaptic machinery. Firstly, I observed the loss of axonal contacts with the NMJ postsynaptic machinery 1-week after nerve crush in WT mice, shown by the lack of axonal branches (NF) and pre-synaptic machinery (synaptophysin) at the NMJ (**Figure 4.10,** upper panel). 4-weeks after denervation the pre-synaptic structures seem to be fully restored (**Figure 4.10**, lower panel). As expected, 2-weeks post nerve-damage, I observed increased NMJ poly-innervation both in WT and CAP2-KO. However, poly-innervated NMJs in WTs display thicker axon diameter compared to CAP2-KO, where the axons appear to be thinner after injury (**Figure 4.11 A'**, white arrows). Secondly, I noticed diminished synaptophysin staining in CAP2-KO, and this might indicate reduced synaptic vesicles (**Figure 4.11 A'**, white square). Last, I observed 4- folds increase of denervated NMJs in CAP2-KO compared to WT, with 16% denervated NMJs in CAP2-KO against 3% in WT. Although this quantification confirms the existence of such tendency, this difference is not statistically significant (**Figure 4.11 B**). All together, these results represent a preliminary hint the CAP2-KO mice have weaker regenerative capacity after injury, and whether the observed decreased motor axon robustness has functional implications should be more thoroughly investigated in the future by electrophysiological studies. Furthermore, technical limitations connected to immunostaining as a technique have to be taken into consideration in this experiment. Because tissue immunostaining presents several challenges connected to the antibody performances and sample thickness, in the future, the use of transgenic mice expressing fluorescent proteins in motor axons e.g., Thy1-GFP or Hb9-GFP mice strains, could represent a suitable tool to address such questions with higher level of confidence.

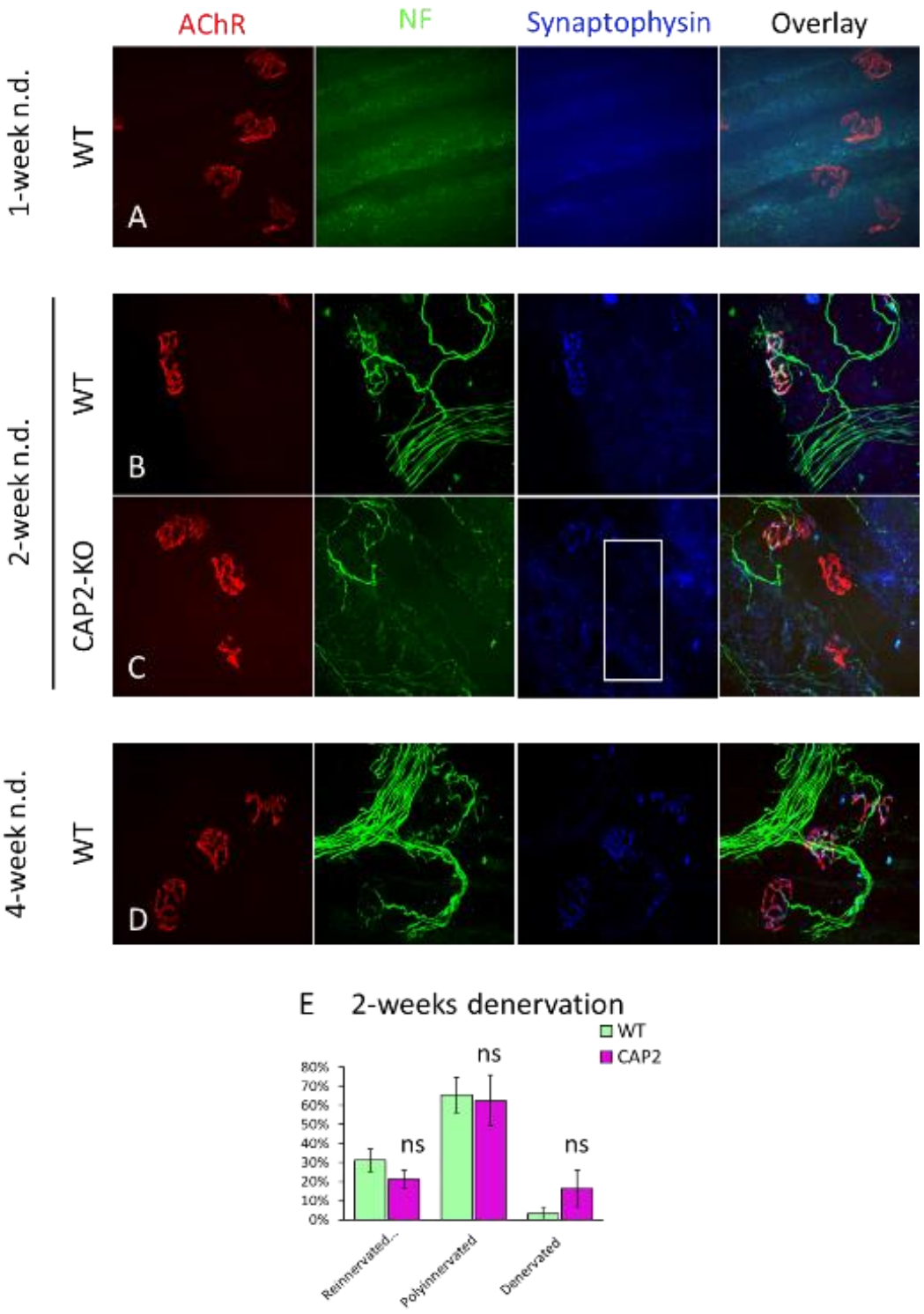

Figure 4.10. Axon regeneration after nerve damage. A) NMJ system 1 week post nerve damage (n. d.) exhibits lack of NF and Synaptophysin immunoreactivity. **B**) 2 weeks after nerve damage (n. d.) in WT, the axons takes contact to the post-synaptic terminal and enters the neuromuscular junction. **C**) Lack of axonal contacts and synaptophysin (region within the white rectangle) at NMJ 2-weeks after nerve damage in CAP2-KO. The

axons in CAP2-KO display weak NF staining. **D**) NMJ system is fully restored 4-weeks after nerve damage. **E**) Quantification of denervation at 2 weeks post nerve damage (n.d.) (n animals = 3 for WT and 4 for CAP2-KO, n NMJs ≥ 130; statistics: One-way Anova, Tuckey correction; bars = means, error bar = SEM).

4.2. Cortactin project

The second actin-organizing protein that I become interested in is Cortactin (Cttn). Previous studies in our laboratory has identified Cttn as a candidate protein interacting with the cytoplasmic component of the dystrophin-glycoprotein complex called αDystrobrevin1. Interestingly, Cttn has been shown as a critical organizer of the AChR clustering in cultured muscle cells (Raghavan, et al., PLoS One, 2009), but its localization and functions at the neuromuscular junctions in vivo have never been reported.

4.2.1. Cortactin is enriched at the NMJ in mouse

To assess the localization of Cttn in skeletal muscle, I electroporated the TA muscle of adult WT mice with the Cttn-GFP plasmid and observed green fluorescent emission that colocalizes with the AChR at NMJ, thus this results show that Cttn is enriched at NMJ in mouse (**Figure 4.12**). Fluorescent signal slightly extended beyond the area occupied by AChR visualized with bungarotoxin, which indicates that the protein is enriched at the postsynaptic machinery. The green signal at the edges of AChR is stronger because of the topology of the membrane, which at these locations extends in the Z dimension.

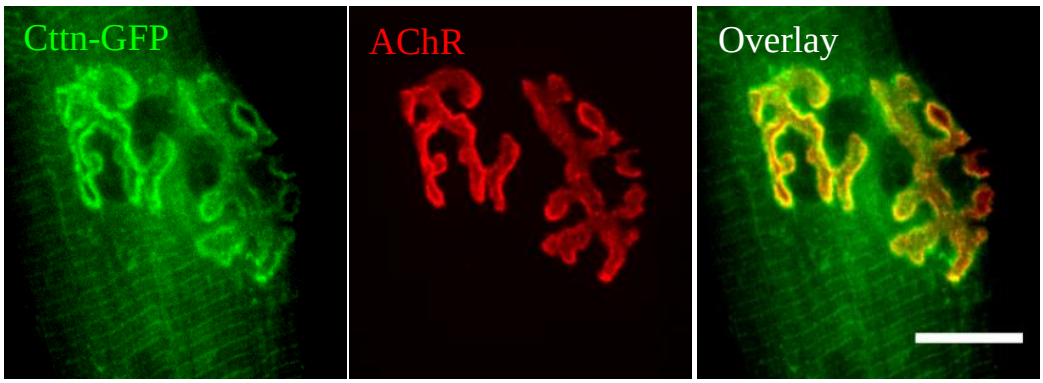

Figure 4.12. Localization of Cttn-GFP to the NMJ in TA muscle, scale bar = 20μm.

4.2.2. Cttn interacts with αDystrobrevin1

Mass spectrometry results obtained in our laboratory suggest that Cttn can interact with αDB1. To confirm this possibility, I performed co-immunoprecipitation (co-IP). For that, I coated magnetic beads with full-length aDB1-GFP (87 kDa) and used as a bait to pulldown its putative partner Cttn-flag (~61kDa). Indeed, I observed that Cttn-flag is pulled down by aDB1 (**Figure 4.13 A**, red square), thus strengthening the hypothesis that these molecules interact. I confirmed this result in several independent experiments. Furthermore, to test whether additional interactions exist between Cttn and other components of DGC, I attempted to pull-down Cttn-flag with Syntrophin (**Figure 4.13 B,** highlighted by the red rectangle). This experiment did not reveal interactions. Our mass spectrometry results suggested that Cttn may interact with phosphorylated tyrosine Y730 located in C'-terminal part of αDB1 (**Figure 2.1** in the introduction). This hypothesis comes from the observation that Cttn was precipitated specifically by phosphorylated peptide containing Y730 but not by unphosphorylated control peptide. To confirm the results coming from the mass-spectrometry and indicating that the Cttn- αDB1 interaction is mediated by the phospho-730-tyrosine of αDB1 C-terminal, I tried to pulldown Cttn-flag by the use of synthetic αDB1 peptides, available in couple of tyrosine unphospho- and phosphor-version. However, the results from these experiments were inconsistent, therefore at the moment this information remains still to be confirmed. Finally, to validate whether the C-terminal domain is the only domain involved in the Cttn-αDB1 interaction, I pulled down αDB2-VN173, a truncated isoform of αDB1 lacking the C-terminal domain with phosphorylated tyrosines (see **Figure 2.1**) with Cttn-flag. In this experiment, I used αDB2, which was expressed as a fusion protein with the split Venus tag (see next chapter) that can be detected with anti-GFP antibody. Firstly, I confirmed that αDB1-GFP is coprecipitated by Cttn-flag as a bait (**Figure 4.13 C**). Similar to αDB1, I observed that αDB2-VN173 is also pulled down by Cttn-flag as a bait (see **Figure 4.13 C'**), suggesting that multiple domains of aDB1 might be implicated in the interaction with Cttn.

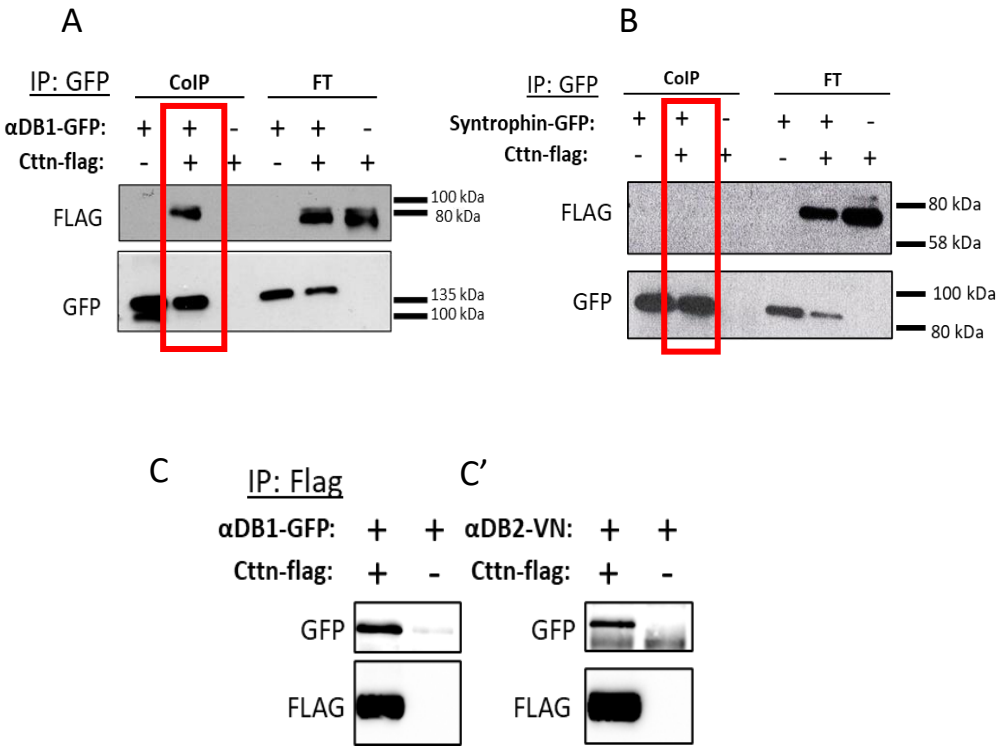

Figure 4.13. Cttn co-immunoprecipitates with αDB1 in HEK293 cells homogenates. A) Cttn co-precipitates with αDB1. **B**) Syntrophin fails to pull-down Cttn. **C, C'**) Cttn interacts with C- and N-domains of αDB1. Full-length αDB1 and its truncated version αDB2 (αDB2-VN), corresponding to its N-terminal, are both co-precipitated by Cttn-flag.

4.2.3. Cortactin interacts with αDB1 at NMJ

I performed Bimolecular Fluorescent Complementation (BiFC) assay as complementary approach to verify the site of interaction of Cttn with αDB1 in vivo. BiFC assay is based on the co-expression of two protein of interest fused with truncated C- or N-terminal green fluorescent Venus (VC155 and VN173, respectively) protein. If the two proteins of interest interact (directly or indirectly), then two halves of the VN protein are brought in close proximity and can fold emitting fluorescence. Thus, I electroporated αDB1-VN173 and Cttn-VC155 constructs in TA muscle of WT mice and observed that their co-expression generated green fluorescence signal colocalizing with the AChRs of NMJ (**Figure 4.14**). I generated and electroporated two Cttn constructs, one with the N-terminal and one with the C-terminal VC155 domain, and I obtained similar results by the electroporation of both (**Figure 4.14 C** and **D**). As a positive control, I co-expressed

the VC and VN domain-containing constructs of αBD1 and Rapsyn, which are known to interact at NMJ (**Figure 4.14 B**). Negative control were performed by another lab member and are not shown, however overexpression of a single construct does not lead to any detectable fluorescence in 488 nm channel. Thus, these results suggest that the post-synaptic NMJ is the site of interaction for αDB1 and Cttn.

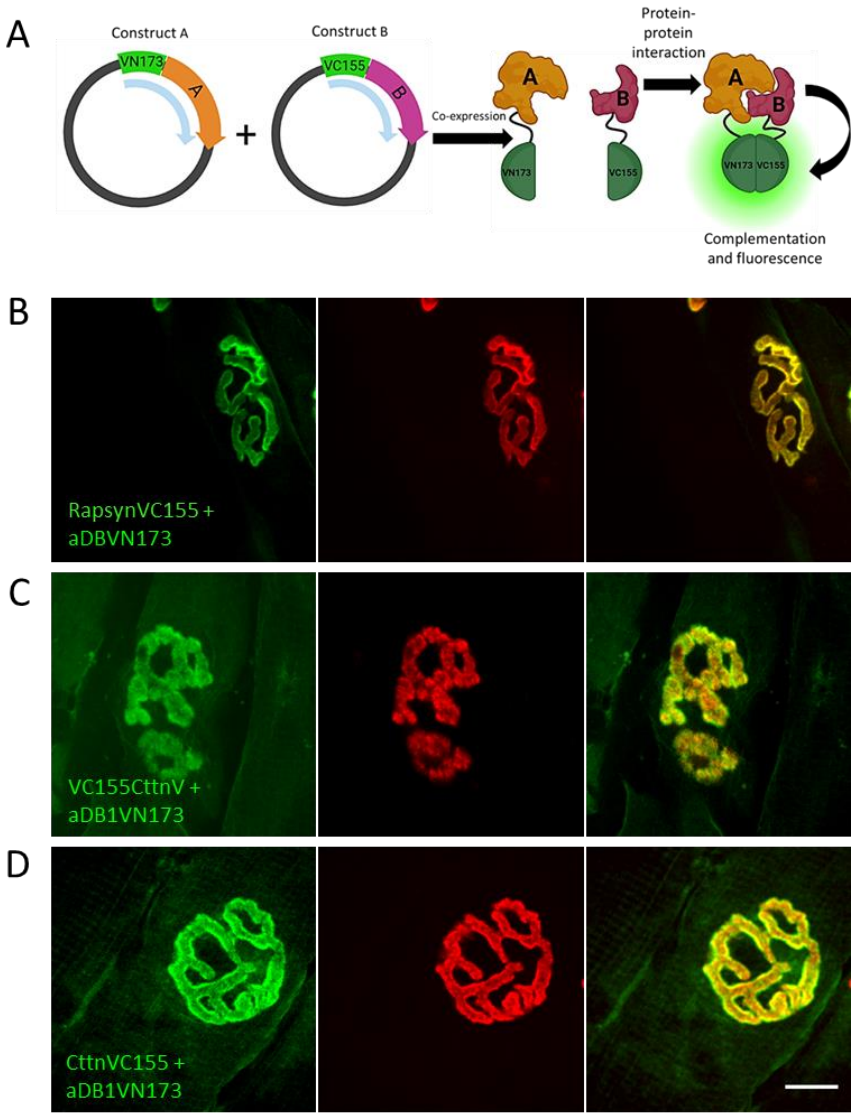

Figure 4.14. Cttn interacts with αDB1 at NMJ. A) Schematic illustration of the BiFC mechanism. **B-D**) BiFC experiment. **B**) BiFC experiment positive control: co-electroporation of Rapsyn-VC155 and αDB1-VN173. **C, D**) Co-electroporation of Cttn-VC155 or VC155-Cttn constructs and αDB1-VN173, scale bar = 15µm.

4.2.4. Cttn-KO phenotype *in vivo*

To characterize the Cttn function at the NMJ in mice, I analyzed the synaptic morphology of systemic Cttn-KO mice, which was a kind gift from prof. Klemens Rottner Technische Universität Braunschweig, Germany). For histochemical analysis, dissected muscles were fixed with 4% PFA and TA muscle fibers were teased to isolate small pieces of tissues that are easier to penetrate for antibodies. I stained the pre-, post-synaptic, and synaptic cleft components with different fluorescent markers e.i., synaptophysin, AChR, and AChE, respectively. The alignment of the three NMJ compartments in Cttn-KO mice was similar to control tissues (**Figure 4.15 A**). The general morphology of the motor axons was normal and I didn't observe any evident structural defects in Cttn-KO compared to WT, neither in fast- nor in slow-twitching muscles (**Figure 4.15 B**). Additionally, I performed unbiased automated morphological analysis of the post-synaptic terminal and assessed different structural aspects such as the post-synaptic terminal size, the area of the NMJ occupied by AChR, and the area of perforation within NMJ. Interestingly, in adult Cttn-KO mice, the NMJs of slow-twitching fibers of Soleus muscle display a significant diminished synaptic size. Also, the area occupied by AChR and perforations shrink in trend with the NMJ size (**Figure 4.15 E, D**), thus reflecting the general shrinkage of the whole synapse. By contrast, in the fast-twitching TA muscle, the NMJs exhibit a similar tendency, however the phenotype in this muscle remains non-significant (**Figure 4.16 C, D, E**). Furthermore, I quantified the fragmentation of the post-synaptic endplate, however I didn't observe any difference in fragmentation of NMJs in Cttn-KO versus WT both in TA and Soleus muscles (**Figure 4.15 G** and **4.16 F**). Altogether, these results show that the lack of Cttn has mild but significant impact at the NMJ structure of slow-twitching muscles.

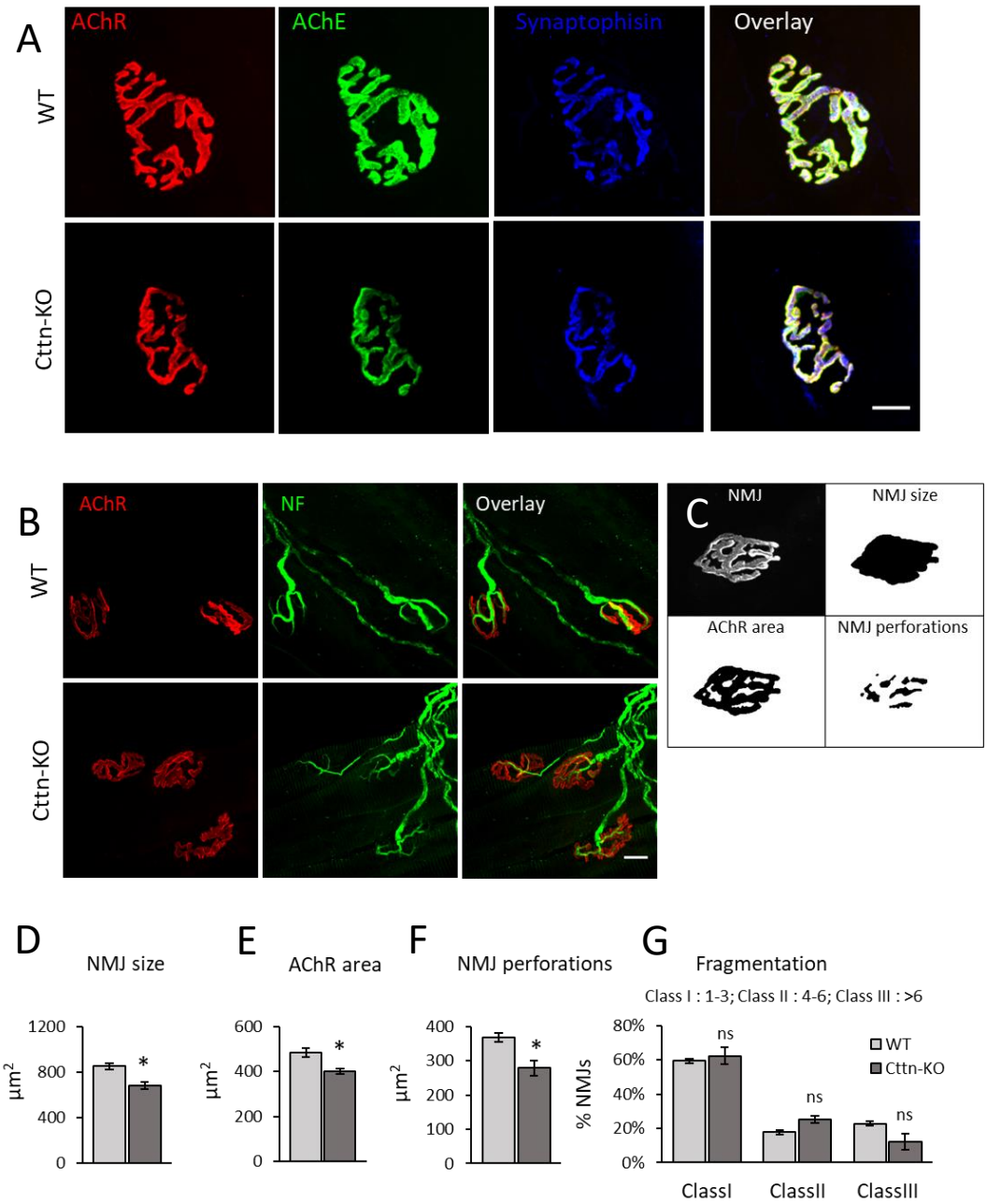

Figure 4.15. A) NMJ size is reduced in Cttn-KO Soleus muscle. Cttn-KO NMJ exhibit normal apposition of synaptic compartments in Sol. AChR was stained with bungarotoxin and AChE with fasciculin toxin. **B**) Motor neurons in Cttn-KO have normal morphology (NF-neurofilament, scale bar = 15µm). **C**) Image processing for automated NMJ analysis of size and shape by NMJ-morph, an ImageJ plug-in. **D-F**) Quantification of NMJ size (**D**), AChR area (**E**), and NMJ perforation (**F**) (P250 animals, n of animals per genotype = 3, n of NMJs per genotype = 111 in WT and 124 in Cttn-KO. Unpaired t-test; error bars = SEM). **G**) Quantification of NMJ fragmentation (One-way ANOVA with Tukey post-hoc correction, error bars = SEM).

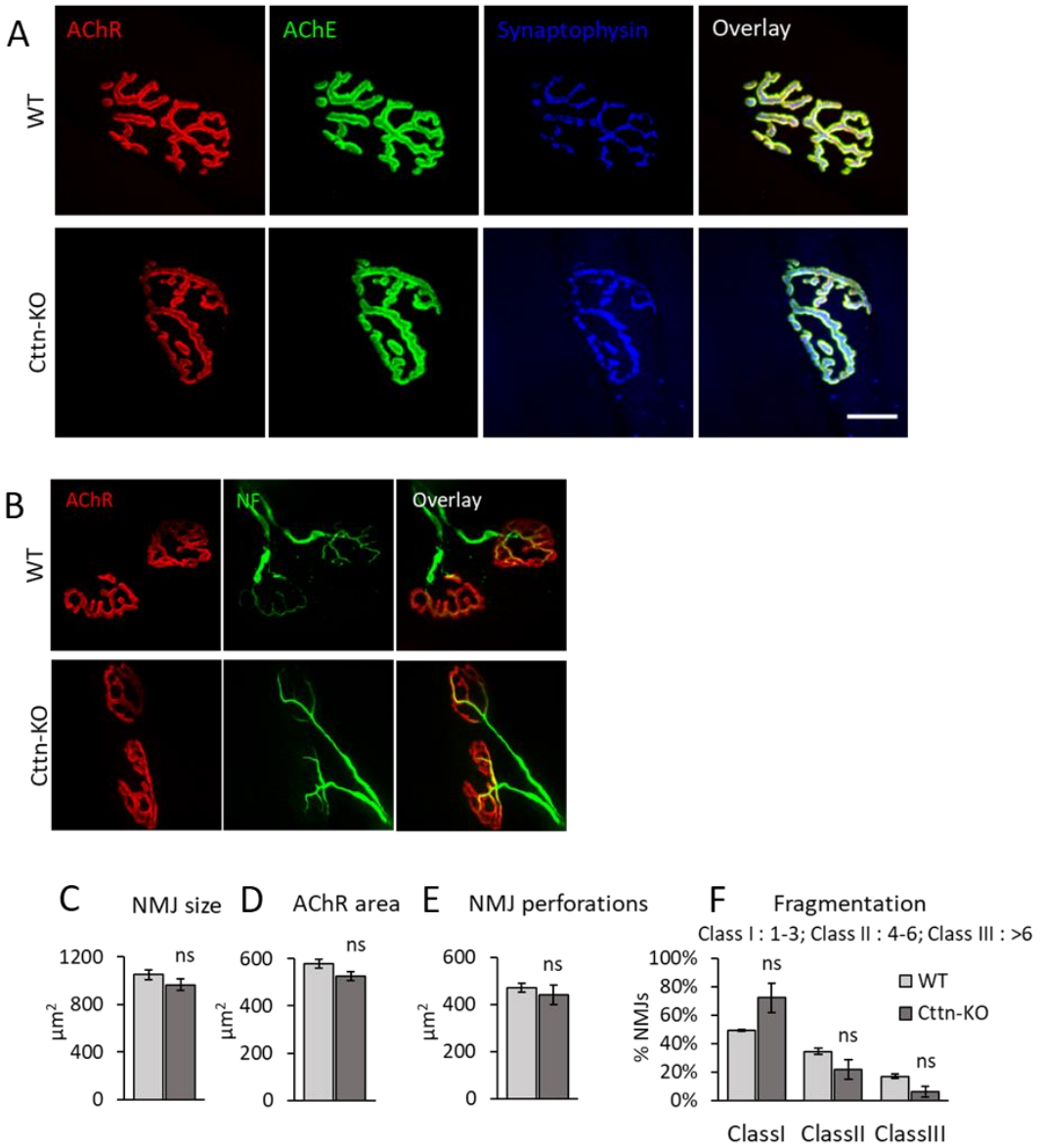

Figure 4.16. Cttn function is dispensable for NMJ in adult TA muscle. A) Cttn-KO NMJ in TA exhibit no difference in size and normal apposition of the synaptic compartments, scale bar = 15µm. **B**) Motor neurons in TA Cttn-KO appear to be normal. NF-neurofilament). **C-E**) Quantification of NMJ size, area, perforation in Cttn-KO TA (statistics = unpaired t-test, error bars = SEM). **F**) Quantification of fragmentation in Cttn-KO TA (animals age = P250, n animals per genotype = 3, n NMJs per genotype = 96 in WT and 95 in Cttn-KO, statistics: One-way ANOVA Tukey post-hoc correction; error bars = SEM).

4.2.5. Normal NMJs in muscle-specific Cttn-KO

To obtain conditional KO mice, Cttn flox/flox animals were crossed with transgenic mice line expressing CRE recombinase under the control of either Myf5 or ACTA1 promoter (**Figure 4.17 A**). This way I obtained a valuable tool to assess the impact of Cttn deficiency specifically in skeletal muscle and during development, respectively embryonal and postnatal (Myf5 and Acta1, respectively). For this analysis, I visualized the NMJs from different muscles including TA, diaphragm (Dia) (**Figure 4.17B**), and sternomastoid (SM) of P180 mice. In all these muscles, the pre- and post-synaptic compartments and synaptic cleft seem to be normally overlapping and the NMJs look structurally normal. Furthermore, I visualized the NMJs from Cttn fl/fl Acta1CRE mouse line aged P91, and I observed that also in this line the NMJs in TA appear morphologically normal and the synaptic compartments are aligned (**Figure 4.17C**).

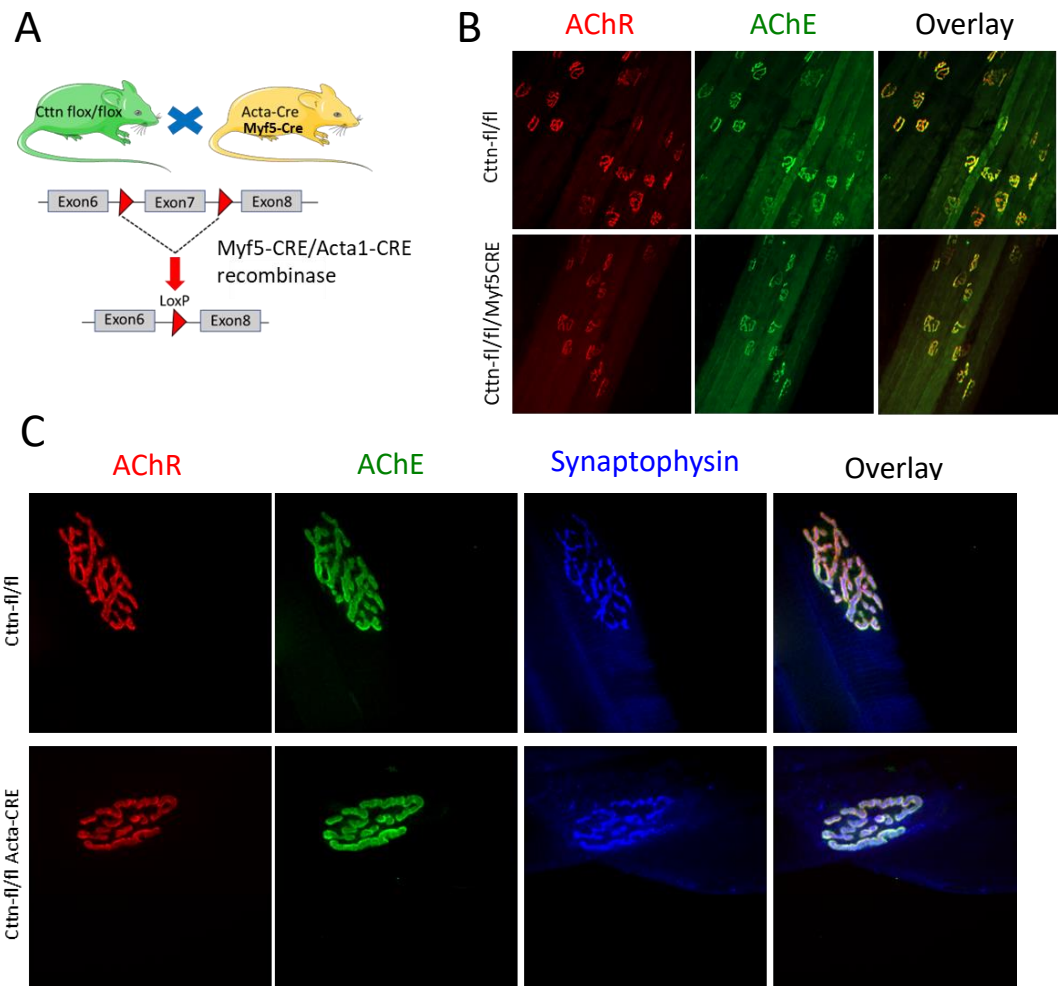

Figure 4.17. Study of muscle specific Cttn-KO mice. A) Schematic view for generation of transgenic muscle-specific KO mice line. **B**) Diaphragm from conditional Myf5-CRE/Cttn-fl/fl mice. **C**) TA from conditional Acta1-CRE/Cttn-fl/fl mice.

4.2.6. Cttn is dispensable for skeletal muscle integrity

The deficiency in DGC's components are often implicated in muscular dystrophies, an heterogeneous group of diseases characterized by muscle atrophy and weakness (**Figure 4.18 A**). Also, NMJ morphological abnormalities could be result of malfunction of synaptic programs or a consequence of general muscle fiber degeneration. To assess whether the lack of Cttn results into muscle fiber degeneration, I measured the size of muscle fibers from cross-sections of WT and Cttn-KO muscles. In TA and Sol muscle in KO animals have only a small non-significant reduction in fiber size compared to WT (**Figure 4.18 B**), indicating that the integrity of both fast- and slow-twitching fibers is preserved upon depletion of Cttn. Furthermore, the myonuclei exhibit a peculiar peripheral disposition along the fibers and their misplacement and internalization represent a common hallmark for fiber degeneration/regeneration cycles occurring in many muscular disorders. To assess if adult Cttn-KO mice exhibit this feature, I quantified the percentage of fibers with internalized nuclei. I observed no difference in fast- and slow-twitching fibers upon lack of Cttn (**Figure 4.18 C)**.

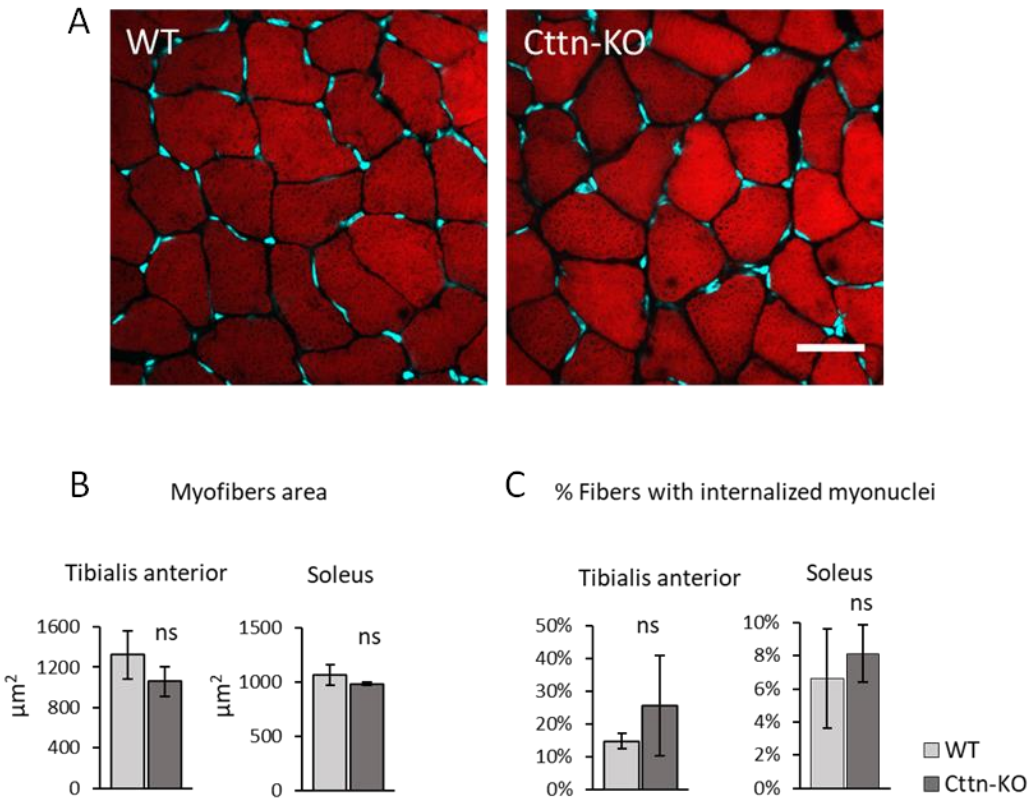

Figure 4.18 Lack of Cttn has no impact on skeletal muscle structure. A) Muscle cross-sections from Soleus. 20X image, falloidin (F-actin) in red, DAPI (nuclei) in cyan blue, scale bar = 30 µm; B/C) Fiber size quantification in TA and Sol/ quantification of fibers with internalized nuclei TA and Sol, (mice age: P42-P49, n

of animals per genotype = 3, n of images per ID >3, statistics = t-test, bars = mean, error bars = SEM).

4.2.7. Normal locomotion of Cttn-KO mice

I expanded the characterization of Cttn-KO mice to the functional level and assessed the physical performances of adult Cttn-KO mice through various behavioral tests. In the "grip strength test", I observed no difference in the peak force between Cttn-KO and WT, and this observation was recapitulated when adjusted by body weight (**Figure 4.19 A and C**). Furthermore, I assessed the will and physical capacity of Cttn-KO mice towards running in their active period in "voluntary running wheel". Although I could observe that Cttn-KO mice perform slightly worse in this test, with fewer rotations executed in overnight, the difference between the Cttn-KO and WT groups is not statistically significant (**Figure 4.19 D**). Finally, I assessed the endurance of mice subjected to progressively intense exercise on the treadmills, and I observed that both experimental groups could run similar distance in the time and reach exhaustion at similar time point (**Figure 4.19 E, F**). Altogether, these results indicate that the lack of Cttn is not impinging the muscle strength, that Cttn-KO have no significantly reduced motivation to physical activity and that they are able to sustain intensive activity similarly to WT mice.

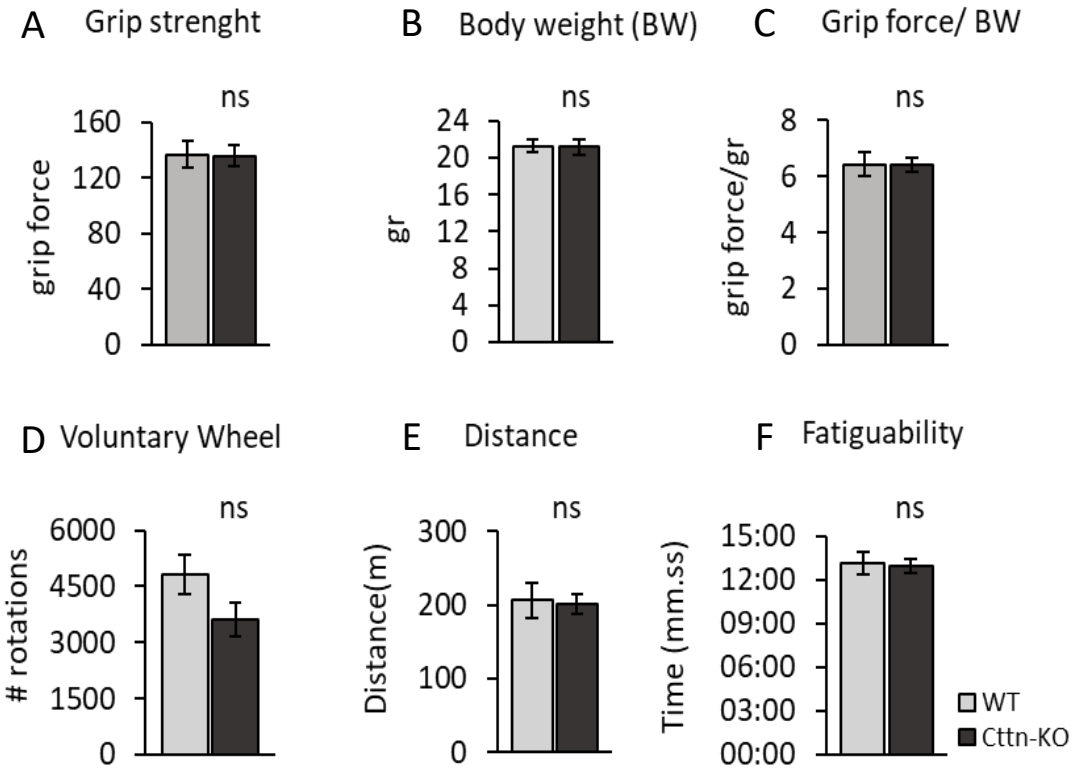

Figure 4.19. Behavioral study (Cttn-KO mice age P87-P171, n animal per group = 8, statistics = t-test, bars = mean, error bars = SEM).

5. Discussion

5.1. Summary on the molecular functions of CAP2

CAP proteins have been discovered in budding yeast three decades ago and their function is connected to the Ras-cAMP signaling pathway which controls cell-growth in these organisms[142,143]. In *S. cerevisiae, the* depletion of CAPs compromises cell-growth and increases temperature and nitrogen-deprivation sensitivity[143,144]. Furthermore, CAPs controls the morphology of these single-cell organisms, and CAPs-depleted yeast display more rounded morphology and increased cell size, suggesting that CAPs role is implicated in cytoskeletal rearrangements[145]. The original name of CAPs refers to its function in yeast, which is lost in higher Eukaryotes[142]. However, the function of CAPs as an actin organizer is maintained in higher eukaryotes and is emerging to be important in many biological mechanisms. CAPs participate to molecular dynamics that regulate the actin state and controls the mechanism of actin-remodeling termed "actin-treadmilling". CAPs participate to the ADF/Cofilin action of ADP-bound actin monomers removal from the pointed ends actin-filaments, thus controlling F-actin depolymerizations events. Furthermore, CAPs displaces ADF/Cofilin from ADP-actin monomers and sustain the events of actin polymerization by promoting ADP-ATP nucleotide exchange, a mechanism that recharges G-actin and enables the reincorporation within the filaments[141]. In vertebrates, CAP1 and CAP2 isoforms are known. CAP1 displays ad broad distribution while CAP2 is expressed specifically in brain, cardiac, and skeletal muscles[149]. Recent studies suggested that CAP2 plays a central role in the molecular mechanism of myofibril maturation during the early-post natal development[150,151]. Kepser et al., PNAS, 2019 proposed that CAP2-deficiency impinges the exchange mechanism of smooth muscle (α-SMA) and cardiac muscle (α-CAA) α-actin, present in immature myofibrils, with the skeletal muscle (α-SKA) α-actin, thus delaying myofibril maturation[151]. Therefore, loss of CAP2 stabilizes the F-actin, resulting in prolonged retention of the immature actin isoforms within the filamentous actin.

5.2. Summary of the role of CAP2 in muscles and neurons

In CNS, CAP2 participates to the remodeling of synapses and its loss affects spine density and dendritic complexity[155]. Moreover, recent study suggested that CAP2 affects the structural plasticity of excitatory synapses and found that CAP2 interaction with its binding partner Cofilin1 is compromised in patients with Alzheimer disease, thus suggesting implications in the mechanism of the disease[155,160]. Furthermore, CAPs are found enriched at the axonal growth cones of

hippocampal neurons of CNS[159]. However, of the two isoforms, CAP1 seems to play a predominant role in mechanisms of neurite differentiation and synaptic connectivity. The function of CAP2 appears to be only redundant and compensatory of the CAP1-loss[159]. Altogether, these studies indicate that the function of CAP2 is of primary importance in differentiated neurons, whereas it is dispensable in mechanism of neuronal development. In the skeletal muscle, CAP2 is implicated in mechanisms of myofibril maturation and organization of contractile apparatus. In skeletal muscle, CAP2- deficiency is found to be leading cause of abnormal sarcomere arrangement with formation of "ring-fibers", which is feature of myopathy, and re-expression of CAP2 in CAP2-deficient muscles rescues this abnormality[151]. The loss of CAP2 affects the motor functions causing increased tremor at early development stages and decreasing the muscle force during early and later stages of life in mice[151].

5.3. CAP2 in human diseases

Recent studies are shedding light on the physiological role of CAP2 and implications in dilated cardiomyopathy (DMC), a condition responsible of heart-failure and sudden cardiac death[152,153]. Mutations in the cytoskeletal proteins of the sarcomere are acknowledged causes of half DCM cases. Moreover, caused by and abnormal organization of the contractile machinery[153,152]. The serum responsive factor (SRF) is a transcription factor that controls the expression of several sarcomere proteins, including actin, and the heart defects in DCM are cause by altered expression of the genes controlled by SRF[153]. Due to its function as actin-remodeling protein, CAP2 controls SRF activation by MRTF in an actin-dependent mode and represents a potential target for the therapy of DCM[153]. Moreover, a form of human syndrome with clinical symptoms including hypotonia and developmental delay has been detected in cases of short arm chromosome 6p22 deletion in humans. The genetic locus of CAP2 is included in the chromosomic region deleted in this condition, therefore my study provides additional potential hints on how deficiency of CAP2 may contribute to the syndrome[161].

5.4. Summary of NMJ phenotype in CAP2-KO mice

Knowing the important functions of CAP2 in the organization of actin cytoskeleton, neuronal morphology and synapse formation in the central nervous system and that CAP2 deficiency leads to defects in skeletal muscle fibers organization, I decided to study its potential functions at the NMJs. The loss of CAP2 *in vivo* dramatically impacts the size of NMJs, resulting in some synapses being smaller and other abnormally enlarged. Furthermore, CAP2-deficiency disrupts the NMJs

architecture and I frequently observed highly fragmented NMJs in CAP2-KO mice. Also, I found that NMJ structural defects are apparent in both slow- (Type I) and fast-twitching (Type II) skeletal muscle fibers. Moreover, my developmental studies *in vivo* showed that at P7 the NMJs of CAP2-KO mice display small but significant increase in synaptic size compared to WT. However, at this stage the general morphology of the junction is normal and exhibit ovoidal, perforated and poorly branched shape. The lack of CAP2 seem to have no effect on the process of AChRs clustering and the plaque-to-pretzel remodeling seem to be initiated in CAP2-KO. Moreover, preliminary *in vitro* experiments seem to confirm my observations *in vivo* - siRNA-mediated CAP2 knock-down in C2C12 myotubes is not impeding cluster formation (data not shown). Altogether, these results lead me to propose that CAP2 function is mainly involved in mechanisms of NMJ maturation while it is dispensable for NMJ formation. The re-expression of CAP2 in CAP2-KO muscles failed to restore healthy NMJ structure, thus, I started to investigate the pre-synaptic terminal to understand whether the NMJ defects could derive from motor axon deficiency.

5.5. Summary of motor neuron phenotypes in CAP2-KO mice

The visualization the neurofilaments of MNs in CAP2-KO revealed various structural defects. Adult CAP2-KO mice exhibit exuberant innervation of NMJs, which can be interpreted as a feature of developmental delay. In fact, NMJ poly-innervation is characteristic of early post-natal developmental stages. In this regard, a still unanswered question is whether the phenotypical "large" NMJs might be result of exuberant stimuli to which the synapse is subjected due to multiple-axon innervation. To answer this question it would be useful to correlate poly-innervation of the postsynaptic machinery with size of NMJs. Moreover, the MNs in CAP2-KO display structural defects including swelling and presence of blebs, mostly at the perisynaptic region of MN. Less frequently, axon sprouting could be observed. Altogether, these aberrations are known in the field to be sign of premature aging[162]. Additional hallmark of premature aging are NMJ denervation and the presence of abnormally thin axons, however these features are missing in NMJs of CAP2-KO mice, which show normal presence of synaptic vesicles marker protein juxtaposing the post-synaptic machinery[162]. Thus, this raises a crucial question whether structural changes in MNs lead to the impairment of signal transmission. Behavioral study by Kepser et al., PNAS, 2019, showed that CAP2-KO mice exhibit impaired locomotor ability including tremor and reduced force, this deficit has been ascribed to the abnormalities in the contractile machinery[151]. However, it is debatable that the structural defects in the MNs observed in my study might also compromise locomotor abilities by impinging the signal transmission at NMJ. Therefore, the assessment of the functional capacity of MNs to transmit electrical stimuli could

complete our insights on the impact of CAP2 on the neuromuscular system and locomotion.

5.6. NMJ phenotypes are independent from "ring fibers"

The role of CAP2 in the skeletal muscle is recently emerging and I contributed to the study by Kepser et al., *PNAS*, 2019, confirming that the myopathy trait of actin-rings is caused by CAP2 deficits in skeletal muscles. My independent studies focus on a narrow and specialized domain of the myofiber and I report for the first time that CAP2 is a novel key NMJ organizer. The lack of CAP2 result in NMJ structural defects affecting both slow- (Type I fibers) and fast-twitching (Type II fibers) skeletal muscles. This finding is in contrast with the abnormal contractile machinery disposition in skeletal muscle of CAP2-KO reported by Kepser et al., *PNAS*, 2019, in which the "ring-fibers" were selectively affecting fast-twitching muscles of TA and Quad and were missing in slot-twitching Soleus[151]. Moreover, the re-expression of CAP2 in CAP2-deficient muscle is able to revert the contractile machinery defects of "ring fibers", whereas I showed that this fails to ameliorate the NMJ structural abnormalities. Altogether, these differences between my findings and Kepser et al., *PNAS*, 2019 lead me to postulate that CAP2 governs multiple actin-dependent processes in skeletal muscle, and that CAP2 phenotype at the contractile apparatus resulting in the "ring-fiber" formation is separate and independent from the phenotype at NMJ. Furthermore, because the rescue of CAP2 in muscles didn't restore normal NMJ architecture, I question that the NMJ defects might be the result of motor axon deficiency instead of skeletal muscle deficit of CAP2.

5.7. Elements of developmental delay

During early-postnatal developmental stages, multiple axon terminals enter the NMJ, which appears to be "poly-innervated". These axons "fight" for the occupancy of the synaptic territory in a "loose-win competition" termed "synaptic elimination" and this developmental process culminates with the NMJ being innervated by a single axon. The supernumerary axonal contacts at the NMJs of CAP2-KO mice represent an abnormal feature in adult animals, and I speculate that this might be consequence of failure in the mechanism of competitive synaptic elimination occurring during the post-natal development. Whether CAP2 is implicated in synaptic elimination is far from being clear, however I can hypothesize a mechanism by which CAP2 regulates MNs retraction in synaptic elimination based on existing insights. Deficiency of CAP2 impinges the mechanism of actin treadmilling, prologues the retention of immature actin isoforms within the actin-filaments, and postpones the incorporation of mature actin isoforms, thus delaying myofibril maturation[151]. The remodeling of actin network

provides driving-force for structural and morphological rearrangements in many biological process, therefore, since CAP2-defects seem to stabilize and increase rigidity of filamentous actin, as a result this might impair the dynamic events that control the "looser" axon removal from the NMJ during synaptic elimination. Other mechanisms are, however, also possible. It is known, that the neuronal activity coming from the brain could determine the "looser" and the "winner" during synaptic elimination and that often axons from neurons that fire more frequently win the process[163]. It is possible that lack of CAP2 in systemic KO mice alter brain activity resulting in delayed NMJ synaptic elimination.

5.8. Signs of premature aging in CAP2-KO NMJs

Axonal swelling, blebs situated along the motor axon and in the proximity of the junction, axonal sprouts and thin axons are structural alterations known in the field to be sign of age-related degeneration[162]. Motor axons in CAP2-KO recapitulates these features suggesting that the CAP2-deficiency might be responsible of axonal degeneration due to premature aging. Visualization of the motor axons in CAP2-KO revealed that structural defects including abnormal swelling and the presence of blebs adjacent to NMJ. Furthermore, axon sprouting represent minor axonal defects sporadically found in CAP2-KO. Despite these structural defects, the NMJs in CAP2-KO exhibit perfect alignment of the junction compartments, and the presence of SVs in correspondence to the post-synaptic machinery could indicate that the synaptic signal is preserved. Finally, it is important to mention that the dysregulation of actin dynamics has recently emerged to be involved in human neurodegenerative diseases such as Amyotrophic Lateral Sclerosis (ALS) and Spinal Muscular Atrophy (SMA), and that these diseases are characterized by motor neuron degeneration, therefore it would be interesting to study possible links of CAP2 to these conditions, whose etiology remains still not fully understood[164]. One additional sign that lack of CAP2 might be responsible of premature aging of NMJ is the presence of frequent increased fragmentation, which is an acknowledged hallmark for age-related NMJ modification[162,165]. Whether murine NMJ fragmentation observed has similar biological significance than in humans is a crucial controversy in the field of NMJ. In fact, recent findings in humans argued that human NMJ are more stable and showed lack of such age-related signs consisting of fragmentation, thus this contradicts old findings[165,166]. Furthermore, one last hint that CAP2 phenotype could be consequence of premature degeneration derives from the presence of NMJs of extremely diminished size, which I categorized "small NMJs". The small NMJ are not present at postnatal day 7, while their presence is evident later at day 21. Furthermore, small NMJs seem to be the only synapse along the entire single myofiber, thus indicating that this is the principal NMJ on that myofiber. Altogether, these results suggest that lack of CAP2 affects actin-dependent mechanisms resulting in the collapse of the synaptic area of certain synapses converging in the group of small NMJs. In summary, the NMJ is

a plastic structure undergoing remodeling events for the entire life span. Although additional investigation is needed to conclude whether NMJ phenotype in CAP2-KO is consequence of developmental delay or premature degeneration, it is important to highlight that the biological processes of development and aging exhibit common mechanisms and effector proteins, including cytoskeletal proteins and related mechanisms[167].

5.9. The cross-talk of cytoskeleton networks

The study of the role of CAP2 in motor axons has promising potential to provide missing details to a complex picture that includes the cross-talk of cytoskeleton networks. Thus far, it is known that the reorganization of MT within the axons provides driving force to assist axon withdrawal during processes of axon-pruning and the impairment of such mechanism seems to be also involved to neurodevelopmental disorders[167,168]. Furthermore, different cytoskeletal networks are intimately cross-linked and execute several cellular processes in concert. Recent studies are pointing out the importance of the cooperative action of the MT and actin networks. The role of cytoskeletal crosslinking proteins that mediate the interaction between the two individual cytoskeleton networks is also emerging[169]. Among the cytoskeletal crosslinking proteins, the Microtubule-Actin Cross-linking Factor 1 (MACF1) is a scaffolding protein that is emerging to be central in many processes of the development and maintenance of synapses of CNS including dendritic arborization and axon growth[170]. MACF1 is recently identified interactor of rapsyn at the NMJ that anchors actin and MTs at the post-synaptic membrane and organizes the AChRs at the post-synaptic terminal[53]. The muscle-specific loss of MACF1 leads to NMJ abnormalities that recapitulate the CAP2 phenotype of small and fragmented NMJs. The same study showed that MACF1 deficiency in muscle doesn't alter the MT lattice along the myofiber, thus suggesting that MTs and actin network cross-linking is particularly important at the neuromuscular synapses. The motoneuron-specific ablation of MACF1 has never been assessed raising curiosity on which impact this could have at the NMJ and if the phenotype would be similar to MN defects in CAP2-KO mice. However, it is known that MACF1 deletion in mouse brain is responsible of developmental defects leading to death of respiratory distress a few hours after birth[171]. My study showed that the lack of the actin organizer CAP2 compromises the organization of neurofilament structure, which is neuronal component of intermediate filament cytoskeletal network. Based on this finding and also on the intimate connections existing between the cytoskeletal networks, it is possible to hypothesize that the disturbances on actin-meshwork upon lack of CAP2 might also impact MTs and affect the functions at the growth cone of MNs driven by this cytoskeletal network.

5.10. Limitation of the study and future directions

My research revealed that Cap2 play important roles in NMJ development. The understanding of the underlying molecular mechanism is challenged by the fact that the key events of synaptogenesis, both at the presynaptic nerve terminal and the postsynaptic muscle machinery, rely on precise remodeling of the actin cytoskeleton. For example, at the pre-synaptic terminal the actin-dynamics support the mechanisms that drive the motor axon to take contact the post-synaptic terminal[159,171,172]. Whereas, at the opposite terminal, actin network organizes the post-synaptic apparatus by gathering and anchoring the receptors at a focal site, and promoting synaptic remodeling in response to muscle-intrinsic mechanisms and also in response to nerve-derived signaling molecules[34,37,72,89,90,97,98,173]. Also, the actin dynamics regulate physiological events of synaptic signal transmission by anchoring of synaptic vesicles at the terminal and organize their recycling, thus this mean that synaptic transmission depends on actin dynamics[168]. My findings showed that the re-expression of CAP2 in skeletal muscle fails to ameliorate the defects of NMJ in CAP2-KO suggesting that defects at NMJ derive from the nerve. However further investigations are needed. To answer this question, a future direction of my study will include full characterization of transgenic mice generated by the CRE-recombinase strategy and with tissue specific-deletion of CAP2 including: CAP2-fl/Hb9-CRE mice for MN-specific deletion and CAP2-fl/Myf5CRE CAP2-fl/Acta1CRE for muscle-specific deletion at different developmental stages[158]. Studying the actin-dynamics *in vivo* at NMJ upon CAP2-deletion would represent an interesting focus in my research, however this also represent a major technical limitation, as approaches such as fluorescence recovery after photobleaching (FRAP) are more suitable for in-vitro studies. The study of actin pools (globular *versus* filamentous) and F-actin composition (α-SKA, α-SMA and α-CAA) in muscles of CAP2-KO represents the second encountered limitation. To isolate the post-synaptic machinery along with associated proteins, a biochemistry approach was designed consisting in the immunoprecipitation of post-synaptic machinery by pull-down of AChR from muscles. This approach was useful for the immunoprecipitation of direct interactors of AChRs, such as Rapsyn. However, in the case of actin the use of beads represented a technical limitation, as actin monomers seem to interact in an aspecific way with the beads for this kind of experiment. Approaches such as laser capture microdissection represent a potential strategy to overcome the technical limitation connected to the use of beads.

5.11. Highlights of Cttn study

The DGC is a crucial transmembrane multi-protein complex to preserve the integrity of muscle fibers by linking the extracellular matrix to the intracellular cytoskeleton[173]. At the NMJ, the DCG complex is a key organizer that tethers the

AChRs also at the post-synaptic terminal and governs the rearrangement, thus the DGC is of primary importance in the maturation and maintenance of post-synaptic machinery[174]. Extensive research strived to identify the origins of a group of muscular dystrophies connected to deficiency of the DGC components, however many causes remain still unknown. Not all the disfunction of the DGC components lead to muscle damage. For example, defects in dystrophin, sarcoglicans, dystroglycans and α-dystrobrevin are all associated to muscle dystrophies, whereas mutations in α-syntrophin and utrophin exhibit no signs of such a myopathy. By contrast, the neuromuscular system is always compromised as a result of mutations in all components of DGC complex, despite to various extents[175,176]. αDB1 is a dystrophin interacting partner and intracellular component of the DGC, and loss of aDB1 in mice leads muscular dystrophies[104,176,177]. A family study reported that genetic missense variants in the coiled-coil domain of in the DTNA gene (encoding for aDB1) are associated to dominant muscular dystrophic traits of variable penetrance, thus this remarks the clinical implications of the DGC component αDB1[178]. At the murine neuromuscular system, αDB1-deficiency has a dramatic impact on the architecture of NMJ structure, that exhibits reduced depth of synaptic folds. Furthermore, αDB1-deficiency destabilizes the AChRs at the NMJ leading to decreased receptors density at the terminal and increased AChRs turnover[104, 105,176,177]. Although a consistent body of work is shedding light on the importance of αDB1 at the NMJ, the mechanism through which this protein exerts its function remains still poorly understood. Besides its structural role, αDB1 is believed to coordinate signaling events of AChRs organization at the NMJ, and thus serve as a recruitment platform for peripheral proteins that exert their function at the NMJ[105]. Our laboratory is focused on the role of αDB1 as organizer of a specific DGC microdomain and is interested in the identification and characterization of novel components recruited to the NMJ via αDB1 in response to synaptogenic signals. In the past years our research has identified the involvement of several αDB1 partners, such as Grb2 and α-catulin, in the organization of AChR, showing that αDB1 recruits DGC's peripheral partners in response to pre-synaptic stimuli[95,156,177,178]. In our screening for αDB1 partners based on mass spectrometry, Cttn emerged as a phospho-dependent interactor of αDB1, which is recruited to the Y730. Cttn is a type II NPFs that stimulates the Arp2/3 complex to polymerize branched actin filaments (details of NPFs explained in chapter 1.3.4). An accumulating body of research has linked the function of Cttn in the invadopodia formation to invasiveness and proliferation of cancer, therefore in the past decades Cttn has raised great interest in tumor diseases[179,180]. In the past decade several hints suggested that Cttn is involved in the muscle-intrinsic mechanisms of AChRs organization and in processes of post-synaptic machinery maturation during development. The most remarkable hint derives from studies in vitro from the past decade showing that the organization of AChRs is actin-dependent and linking these dynamics to the driving role of Cttn[89,157]. Furthermore, Cttn is present at the

core domain of synaptic podosomes, the highly specialized organelles appearing on cultured myotubes and essential to for the maturation of structurally complex AChR clusters, strengthening the idea that Cttn could have a role in post-synaptic machinery maturation in vitro[88,108]. The localization and function of Cttn at NMJ *in vivo* was never shown before and my studies robustly confirmed through complementary approaches based on biochemistry and *in vivo* localization, that Cttn interacts with the DGC core component αDB1, thus this suggested a specific role in this compartment of the myofiber. Furthermore, my findings provides full characterization of Cttn phenotype at the NMJ, including unbiased morphological analysis, muscle and behavioral studies in Cttn knockout animals, filling a gap in the study of the role of this protein at these synapses.

5.12. Summary of the role of Cttn at NMJ

The aim Cttn project was to provide characterization of a novel screened αDB1 interactor and peripheral component other DGC, assessing its function at NMJ in vivo. My studies showed that Cttn is enriched at the NMJ *in vivo,* confirmed that Cttn interacts with αDB1 and that the site of interaction is at the NMJ. Unbiased automated morphological analysis revealed that Cttn deficiency compromises the NMJ structure in slow-twitching muscle of Soleus, which exhibit decreased endplate size. Despite similar observation was recapitulated in fast-twitching muscle of TA, this observation remains statistically non-significant, indicating that the role of Cttn could be more important in slow- compared to fast-twitching muscle type. Muscle studies in Cttn-KO mice showed that loss of Cttn does not result in typical dystrophic phenotype, and no sign of muscle waste and myonuclei internalization was reported in both slow and fast-twitching muscles are unaffected. Last, the morphological NMJ defects observed in Sol muscle have to functional consequence on locomotor functions of mice, which perform normally both at steady state and intense exercise.

5.13. Impact of Cttn in Type I *versus* Type II contractile fibers

The most important finding from the characterization of Cttn knockout animals consists in the observation that Cttn-deficiency at the NMJ in vivo has significant impact on the synaptic size of Soleus, although mild, while NMJs from Tibialis anterior seem to be mostly unaffected. Therefore, it is important to discuss the structural and metabolic differences between these muscles. The skeletal muscles are heterogeneous tissues displaying substantial structural differences based on Myosine heavy chains (MHC) isoform expression that determines their composition and contractile speed. Thus, based on contractile properties, myofibers consisting of isoform type I (MHCI) exhibit slow contraction speed, therefore are classified as “slow”, while muscles consisting of isoforms type II (MHCIIA,

MHCIIX, MHCIIB, in order of contractile speed progression) are classified as "fast"[181]. Furthermore, differences in the metabolic properties exist in skeletal muscles fibers, which are classified as oxidative or glycolytic. As a consequence of fiber composition, skeletal muscles can serve to different purposes: Soleus predominantly is constituted by slow-oxidative fibers (MHCI and IIA), these muscles serve as movement stabilizer, display lower contractile power and higher endurance to fatigue. On the other hand, TA exhibits predominantly fast-glycolytic fibers, are rapidly recruited during the locomotion and are more rapidly fatigued. The NMJs are considered in the field to be of a single type and differences between NMJs of fast versus slow muscles are much less known. Over the past decades, the synaptic vesicle protein (SV2A) represents a single discovered component selectively expressed at the slow-motor axon terminals. Among Type I slow-twitching muscle fibers including strernomastoid (SM), gastrocnemious, and diaphragm, Sol displays the highest enrichment of SV2A at the pre-synaptic terminal180. Furthermore, SV2A is expressed at the NMJs of fast-twitching fibers of early postanal mice and lost through development. This study demonstrates that muscle activity is able to establish a muscle-to-nerve retrograde communication that seem to regulate the expression of NMJ synaptic components182. Moreover, a few proteins are known which exert differential functions in the different muscle types: for example, the deficiency at NMJ of the the Vesicular ACh Transporter (VAChT), involved in cholinergic transmission, can have different impact on slow-twitching muscles183. The shape of NMJ can differ between muscles. Therefore, this could represent a possible explanation why Cttn-deficit have differential impact in fast versus slow- twitching muscles, being dispensable for the former while leading to synaptic size shrinkage in the latter. The other possible explanation could be that fast muscles have more efficient compensatory mechanisms that obscure phenotypes in Cttn-KO mice. For instance, it is known that Cttn can be compensated by N-WAASP in stimulation of Arp2/3 complex activity. Only further research could explain observed differences between different muscle types, since experiments on N-WASP remained beyond the scope of my Ph.D. studies.

5.14. Impact of Cttn at the synapses

Cttn preferentially binds the sites of insertion of nascent F-actin branching from the pre-existing mother filament and its function as supports the Arp2/3 complex by accelerating the polymerization of F-actin branches contributing to increase the complexity of actin meshwork[147]. Although Cttn controls dynamics crucial and advantageous for the evolution of cancer, to the extent that Cttn has raised interest as a promising potential target for cancer diseases, on the other hand its role seems to be of secondary importance in other biological functions. CttnKO mice are viable and don't exhibit noticeable defects during developmental delay and later in adulthood. However, recently Cttn has been found to have a role in plasticity of

neuronal dendritic spines of CNS with spacial memory impairment connected to Cttn loss[184]. Same as for CNS, the dynamics of actin-cytoskeleton governs key events of formation, functioning, and maintenance of peripheral synapses of NMJ, and although Cttn seems to have minor role at the NMJs, it is important to take into consideration that the findings of my study on Cttn-KO mice refers to healthy animals and it would be interesting to assess the role of Cttn in cases of NMJ injury.

5.15. Conclusions

CAP2 project aimed to provide a characterization of CAP2 phenotype at NMJ and the key findings include:

- NMJs of CAP2-KO mice display defects of synaptic endplate size and disrupted architecture. A population of abnormally small, enlarged, and fragmented NMJ were identified in CAP2-KO adult animals. However, besides these alterations, the apposition of synaptic compartments is not impaired in CAP2-KO mice.

- Lack of CAP2 causes NMJ defects in both slow- and fast- twitching muscles, and this is in contrast to the findings of actin-rings formation upon CAP2 loss which affects specifically fast-twitching muscles. Therefore, the role of CAP2 at NMJ is independent from its role in the organization of contractile apparatus.

- Small NMJ are unique synapses on muscle fibers, thus excluding the hypothesis that these small AChRs fragments are additional, exuberant junctions apart from normal NMJs.

- The CAP2 phenotype at NMJ appears during development starting from postnatal day 7, suggesting that the phenotype is due to impairment in the mechanism of NMJ maturation or maintenance and not NMJ formation. Furthermore, the absence of small NMJ at P7 hints that these NMJs might result from mechanisms of early degeneration.

- The re-expression of exogenous CAP2 in muscles fails to rescue the NMJ phenotype, thus indicating that the leading cause of synaptic defects might derive from CAP2 insufficiency in the presynaptic terminal of motor axons.

- CAP2 loss is associated to motoneuron defects including swelling, blebbing, and polyinnervation of adult NMJ, and it is still not clear whether this phenotype results from developmental defects or premature aging due to the lack of CAP2.

The aim Cttn project was to provide characterization of a novel α-DB1 interactor and peripheral component other DGC, assessing its function at NMJ in vivo. The key finding include:

- Cttn is enriched at the NMJ *in vivo*

- Confirmation that Cttn interacts with αDB1 and that the site of interaction is at the NMJ *in vivo*

- Cttn deficiency causes NMJ morphological defects by decreasing post-synaptic endplate size in slow-twitching muscle of Soleus. NMJ morphology of fast-twitching muscle of TA display similar trend however the NMJ post-synaptic size is not significantly reduced, indicating that the role of Cttn is more important in slow- compared to fast-twitching muscle type.

- Cttn loss does not result in typical dystrophic phenotype including muscle waste and myonuclei internalization and that both slow and fast-twitching muscles are unaffected

- The morphological NMJ aberration have no functional consequence on locomotion that remains unaltered both at steady state and intense exercise.

6. References

1. Ji, J.L., Spronk, M., Kulkarni, K., Repovš, G., Anticevic, A. and Cole, M.W., 2019. “Mapping the human brain's cortical-subcortical functional network organization”. Neuroimage, 185, pp.35-57.

2. Bican, O., Minagar, A. and Pruitt, A.A., 2013. “The spinal cord: a review of functional neuroanatomy”. Neurologic clinics, 31(1), pp.1-18.

3. Catala, M. and Kubis, N., 2013. Gross anatomy and development of the peripheral nervous system. Handbook of clinical neurology, 115, pp.29-41.

4. Farley, A., Johnstone, C., Hendry, C. and McLafferty, E., 2014. “Nervous system: part 1”. Nursing standard, 28(31).

5. Huang, C.Y.M. and Rasband, M.N., 2018. “Axon initial segments: structure, function, and disease”. Annals of the New York Academy of Sciences, 1420(1), pp.46-61.

6. Kole, M.H., Ilschner, S.U., Kampa, B.M., Williams, S.R., Ruben, P.C. and Stuart, G.J., 2008. “Action potential generation requires a high sodium channel density in the axon initial segment”. Nature neuroscience, 11(2), pp.178-186.

7. Zhou, D., Lambert, S., Malen, P.L., Carpenter, S., Boland, L.M. and Bennett, V., 1998. “AnkyrinG is required for clustering of voltage-gated Na channels at axon initial segments and for normal action potential firing”. The Journal of cell biology, 143(5), pp.1295-1304.

8. Wu, H., Xiong, W.C. and Mei, L., 2010. “To build a synapse: signaling pathways in neuromuscular junction assembly”. Development, 137(7), pp.1017-1033.

9. Ovsepian, S.V., 2017. “The birth of the synapse”. Brain Structure and Function, 222, pp.3369-3374.

10. Cheah, M., Fawcett, J.W. and Haenzi, B., 2017. “Differential regenerative ability of sensory and motor neurons”. Neuroscience Letters, 652, pp.35-40.

11. Fogarty, M.J., Mantilla, C.B. and Sieck, G.C., 2018. “Breathing: motor control of diaphragm muscle”. Physiology, 33(2), pp.113-126.

12. Jessen, K.R., 2004. “Glial cells”. The international journal of biochemistry & cell biology, 36(10), pp.1861-1867.

13. Araque, A., Parpura, V., Sanzgiri, R.P. and Haydon, P.G., 1999. “Tripartite synapses: glia, the unacknowledged partner”. Trends in neurosciences, 22(5), pp.208-215.

14. Perea, G., Navarrete, M. and Araque, A., 2009. “Tripartite synapses: astrocytes process and control synaptic information”. Trends in neurosciences, 32(8), pp.421-431.

15. Durkee, C.A. and Araque, A., 2019. “Diversity and specificity of astrocyte–neuron communication”. Neuroscience, 396, pp.73-78.

16. Guerra-Gomes, S., Sousa, N., Pinto, L. and Oliveira, J.F., 2018. “Functional roles of astrocyte calcium elevations: from synapses to behavior”. Frontiers in cellular neuroscience, 11, pp.427.

17. Li, L., Xiong, W.C. and Mei, L., 2018. “Neuromuscular junction formation, aging, and disorders”. Annual review of physiology, 80, pp.159-188.

18. Lepore, E., Casola, I., Dobrowolny, G. and Musarò, A., 2019. “Neuromuscular junction as an entity of nerve-muscle communication”. Cells, 8(8), pp.906.

19. Batool, S., Raza, H., Zaidi, J., Riaz, S., Hasan, S. and Syed, N.I., 2019. “Synapse formation: from cellular and molecular mechanisms to neurodevelopmental and neurodegenerative disorders”. Journal of neurophysiology, 121, pp.1381–1397.

20. Slater, C.R., 2017. “The structure of human neuromuscular junctions: some unanswered molecular questions”. International journal of molecular sciences, 18(10), pp.2183.

21. Sanes, J.R. and Lichtman, J.W., 1999. Development of the vertebrate neuromuscular junction. Annual review of neuroscience, 22(1), pp.389-442.

22. Südhof, T.C., 2012. “The presynaptic active zone”. Neuron, 75(1), pp.11-25.

23. Nelson, N., 1993. “Presynaptic events involved in neurotransmission”. Journal of Physiology-Paris, 87(3), pp.171-178.

24. Schiavo, G., Stenbeck, G., Rothman, J.E. and Söllner, T.H., 1997. “Binding of the synaptic vesicle v-SNARE, synaptotagmin, to the plasma membrane t-SNARE, SNAP-25, can explain docked vesicles at neurotoxin-treated synapses”. Proceedings of the National Academy of Sciences, 94(3), pp.997-1001.

25. Rizo, J., 2010. “Synaptotagmin-SNARE coupling enlightened”. Nature Structural & Molecular Biology, 17(3), pp.260-262.

26. Südhof, T.C., 2013. “Neurotransmitter release: the last millisecond in the life of a synaptic vesicle”. Neuron, 80(3), pp.675-690.

27. Brunger, A.T., Choi, U.B., Lai, Y., Leitz, J., White, K.I. and Zhou, Q., 2019. “The pre-synaptic fusion machinery”. Current opinion in structural biology, 54, pp.179-188.

28. Salzer, J.L., 2015. Schwann cell myelination. Cold Spring Harbor perspectives in biology, 7(8), a020529.

29. Hartline, D.K. and Colman, D.R., 2007. “Rapid conduction and the evolution of giant axons and myelinated fibers”. Current Biology, 17(1), R29-R35.

30. Nave, K.A. and Salzer, J.L., 2006. “Axonal regulation of myelination by neuregulin 1”. Current opinion in neurobiology, 16(5), pp.492-500.

31. Alvarez-Suarez, P., Gawor, M. and Prószyński, T.J., 2020. “Perisynaptic schwann cells-The multitasking cells at the developing neuromuscular junctions”. In Seminars in Cell & Developmental Biology, 104, pp.31-38.

32. Lanuza, M.A., Garcia, N., González, C.M., Santafé, M.M., Nelson, P.G. and Tomas, J., 2003. “Role and expression of thrombin receptor PAR-1 in muscle cells and neuromuscular junctions during the synapse elimination period in the neonatal rat”. Journal of neuroscience research, 73(1), pp.10-21.

33. Yang, J.F., Cao, G., Koirala, S., Reddy, L.V. and Ko, C.P., 2001. “Schwann cells express active agrin and enhance aggregation of acetylcholine receptors on muscle fibers”. Journal of Neuroscience, 21(24), pp.9572-9584.

34. Nishimune, H., Valdez, G., Jarad, G., Moulson, C.L., Müller, U., Miner, J.H. and Sanes, J.R., 2008. “Laminins promote postsynaptic maturation by an autocrine mechanism at the neuromuscular junction”. The Journal of cell biology, 182(6), pp.1201-1215.

35. Werle, M.J., 2009. “Neuromuscular Junction (NMJ): Postsynaptic Basal Lamina”, Encyclopedia Neuroscience, pp.595–600.

36. Patton, B.L., 2000. “Laminins of the neuromuscular system”. Microscopy research and technique, 51(3), pp.247-261.

37. Samuel, M.A., Valdez, G., Tapia, J.C., Lichtman, J.W. and Sanes, J.R., 2012. “Agrin and synaptic laminin are required to maintain adult neuromuscular junctions”. PLoS One 7, e46663.

38. Katz, N.K. and Barohn, R.J., 2021. “The history of acetylcholinesterase inhibitors in the treatment of myasthenia gravis”. Neuropharmacology, 182, pp.108303.

39. English, B.A. and Webster, A.A., 2012. “Acetylcholinesterase and its inhibitors”. In Primer on the autonomic nervous system. Academic Press. Chapter 132, pp.631-633.

40. Aldunate, R., Casar, J.C., Brandan, E. and Inestrosa, N.C., 2004. “Structural and functional organization of synaptic acetylcholinesterase”. Brain research reviews, 47(1-3), pp.96-104.

41. Sigoillot, S.M., Bourgeois, F., Lambergeon, M., Strochlic, L. and Legay, C., 2010. “ColQ controls postsynaptic differentiation at the neuromuscular junction”. Journal of Neuroscience, 30(1), pp.13-23.

42. Karmouch, J., Dobbertin, A., Sigoillot, S. and Legay, C., 2013. “Developmental consequences of the ColQ/MuSK interactions”. Chemico-biological interactions, 203(1), pp.287-291.

43. Sigoillot, S.M., Bourgeois, F., Karmouch, J., Molgó, J., Dobbertin, A., Chevalier, C., Houlgatte, R., Léger, J. and Legay, C., 2016. “Neuromuscular junction immaturity and muscle atrophy are hallmarks of the ColQ-deficient mouse, a model of congenital myasthenic syndrome with acetylcholinesterase deficiency”. The FASEB Journal, 30(6), pp.2382-2399.

44. Tintignac, L.A., Brenner, H.R. and Rüegg, M.A., 2015. “Mechanisms regulating neuromuscular junction development and function and causes of muscle wasting”. Physiological reviews, 95(3), pp.809-852.

45. Sanes, J.R. and Lichtman, J.W., 2001. “Induction, assembly, maturation and maintenance of a postsynaptic apparatus”. Nature Reviews Neuroscience, 2(11), pp.791-805.

46. Wonnacott, S., Bermudez, I., Millar, N.S. and Tzartos, S.J., 2018. “Nicotinic acetylcholine receptors”. British journal of pharmacology, 175(11), pp.1785-1788.

47. Cetin, H., Beeson, D., Vincent, A. and Webster, R., 2020. “The structure, function, and physiology of the fetal and adult acetylcholine receptor in muscle”. Frontiers in molecular neuroscience, 13, pp.581097.

48. Papke, R.L. and Lindstrom, J.M., 2020. “Nicotinic acetylcholine receptors: conventional and unconventional ligands and signaling”. Neuropharmacology, 168, pp.108021.

49. Slater, C.R., 2008. Structural factors influencing the efficacy of neuromuscular transmission. Annals of the New York Academy of Sciences, 1132(1), pp.1-12.

50. Noakes, P.G., Phillips, W.D., Hanley, T.A., Sanes, J.R. and Merlie, J.P., 1993. 43K protein and acetylcholine receptors colocalize during the initial stages of neuromuscular synapse formation in vivo. Developmental biology, 155(1), pp.275-280.

51. Xing, G., Xiong, W.C. and Mei, L., 2020. “Rapsyn as a signaling and scaffolding molecule in neuromuscular junction formation and maintenance”. Neuroscience Letters, 731, pp.135013.

52. Gautam, M., Noakes, P.G., Mudd, J., Nichol, M., Chu, G.C., Sanes, J.R. and Merlie, J.P., 1995. “Failure of postsynaptic specialization to develop at neuromuscular junctions of rapsyn-deficient mice”. Nature, 377(6546), pp.232-236.

53. Oury, J., Liu, Y., Töpf, A., Todorovic, S., Hoedt, E., Preethish-Kumar, V., Neubert, T.A., Lin, W., Lochmüller, H. and Burden, S.J., 2019. “MACF1 links Rapsyn to microtubule-and actin-binding proteins to maintain neuromuscular synapses”. Journal of Cell Biology, 218(5), pp.1686-1705.

54. Martínez-Martínez, P., Phernambucq, M., Steinbusch, L., Schaeffer, L., Berrih-Aknin, S., Duimel, H., Frederik, P., Molenaar, P., De Baets, M.H. and Losen, M., 2009. "Silencing rapsyn in vivo decreases acetylcholine receptors and augments sodium channels and secondary postsynaptic membrane folding". Neurobiology of disease, 35(1), pp.14-23.

55. Mohler, P.J., Gramolini, A.O. and Bennett, V., 2002. "Ankyrins". Journal of cell science, 115(8), pp.1565-1566.

56. Bailey, S.J., Stocksley, M.A., Buckel, A., Young, C. and Slater, C.R., 2003. "Voltage-gated sodium channels and ankyrinG occupy a different postsynaptic domain from acetylcholine receptors from an early stage of neuromuscular junction maturation in rats". Journal of Neuroscience, 23(6), pp.2102-2111.

57. Zhang, C., Joshi, A., Liu, Y., Sert, O., Haddix, S.G., Teliska, L.H., Rasband, A., Rodney, G.G. and Rasband, M.N., 2021. "Ankyrin-dependent Na+ channel clustering prevents neuromuscular synapse fatigue". Current Biology, 31(17), pp.3810-3819.

58. Gawor, M. and Prószyński, T.J., 2018. "The molecular cross talk of the dystrophin–glycoprotein complex". Annals of the New York Academy of Sciences, 1412(1), pp.62-72.

59. Wood, S.J. and Slater, C.R., 2001. "Safety factor at the neuromuscular junction". Progress in neurobiology, 64(4), pp.393-429.

60. Gromova, A. and La Spada, A.R., 2020. "Harmony lost: cell–cell communication at the neuromuscular junction in motor neuron disease". Trends in Neurosciences, 43(9), pp.709-724.

61. Al-Qusairi, L. and Laporte, J., 2011. "T-tubule biogenesis and triad formation in skeletal muscle and implication in human diseases". Skeletal muscle, 1(1), pp.1-11.

62. Nelson, B.R., Wu, F., Liu, Y., Anderson, D.M., McAnally, J., Lin, W., Cannon, S.C., Bassel-Duby, R. and Olson, E.N., 2013. "Skeletal muscle-specific T-tubule protein STAC3 mediates voltage-induced Ca2+ release and contractility". Proceedings of the National Academy of Sciences, 110(29), pp.11881-11886.

63. Squire, J., 2019. The actin-myosin interaction in muscle: Background and overview. International Journal of Molecular Sciences, 20(22), pp.5715.

64. Shi, L., Fu, A.K. and Ip, N.Y., 2012. "Molecular mechanisms underlying maturation and maintenance of the vertebrate neuromuscular junction". Trends in neurosciences, 35(7), pp.441-453.

65. Biressi, S., Molinaro, M. and Cossu, G., 2007. "Cellular heterogeneity during vertebrate skeletal muscle development". Developmental biology, 308(2), pp.281-293.

66. Langlois, S. and Cowan, K.N., 2017. Regulation of skeletal muscle myoblast differentiation and proliferation by pannexins. Protein Reviews, 17, pp.57-73.

67. Yang, X.L., Huang, Y.Z., Xiong, W.C. and Mei, L., 2005. “Neuregulin-induced expression of the acetylcholine receptor requires endocytosis of ErbB receptors”. Molecular and Cellular Neuroscience, 28(2), pp.335-346.

68. Lin, W., Burgess, R.W., Dominguez, B., Pfaff, S.L., Sanes, J.R. and Lee, K.F., 2001. “Distinct roles of nerve and muscle in postsynaptic differentiation of the neuromuscular synapse”. Nature, 410(6832), pp.1057-1064.

69. Schneider, V.A. and Granato, M., 2003. “Motor axon migration: a long way to go”. Developmental biology, 263(1), pp.1-11.

70. Yang, X., Arber, S., William, C., Li, L., Tanabe, Y., Jessell, T.M., Birchmeier, C. and Burden, S.J., 2001. “Patterning of muscle acetylcholine receptor gene expression in the absence of motor innervation”. Neuron, 30(2), pp.399-410.

71. Vock, V. M., Ponomareva, O. N. & Rimer, M., 2008. “Evidence for muscle-dependent neuromuscular synaptic site determination in mammals”. J. Neurosci. 28, pp.3123–3130.

72. Daniels, M.P., 2012. “The role of agrin in synaptic development, plasticity and signaling in the central nervous system”. Neurochemistry international, 61(6), pp.848-853.

73. Bezakova, G. and Ruegg, M.A., 2003. “New insights into the roles of agrin”. Nature Reviews Molecular Cell Biology, 4(4), pp.295-309.

74. Ruegg, M.A. and Bixby, J.L., 1998. “Agrin orchestrates synaptic differentiation at the vertebrate neuromuscular junction”. Trends in neurosciences, 21(1), pp.22-27.

75. Hopf, C. and Hoch, W., 1998. Dimerization of the muscle-specific kinase induces tyrosine phosphorylation of acetylcholine receptors and their aggregation on the surface of myotubes. Journal of Biological Chemistry, 273(11), pp.6467-6473.

76. Lee, Y., Rudell, J., Yechikhov, S., Taylor, R., Swope, S. and Ferns, M., 2008. “Rapsyn carboxyl terminal domains mediate muscle specific kinase–induced phosphorylation of the muscle acetylcholine receptor”. Neuroscience, 153(4), pp.997-1007.

77. DePew, A.T. and Mosca, T.J., 2021. Conservation and innovation: versatile roles for LRP4 in nervous system development. Journal of Developmental Biology, 9(1), p.9.

78. Okada, K., Inoue, A., Okada, M., Murata, Y., Kakuta, S., Jigami, T., Kubo, S., Shiraishi, H., Eguchi, K., Motomura, M. and Akiyama, T., 2006. “The muscle protein Dok-7 is essential for neuromuscular synaptogenesis”. Science, 312(5781), pp.1802-1805.

79. Bergamin, E., Hallock, P.T., Burden, S.J. and Hubbard, S.R., 2010. "The cytoplasmic adaptor protein Dok7 activates the receptor tyrosine kinase MuSK via dimerization". Molecular cell, 39(1), pp.100-109.

80. Inoue, A., Setoguchi, K., Matsubara, Y., Okada, K., Sato, N., Iwakura, Y., Higuchi, O. and Yamanashi, Y., 2009. "Dok-7 activates the muscle receptor kinase MuSK and shapes synapse formation". Science signaling, 2(59), pp.ra7.

81. Arnold, A.S., Gill, J., Christe, M., Ruiz, R., McGuirk, S., St-Pierre, J., Tabares, L. and Handschin, C., 2014. "Morphological and functional remodelling of the neuromuscular junction by skeletal muscle PGC-1α". Nature communications, 5(1), pp.3569.

82. Li, X.M., Dong, X.P., Luo, S.W., Zhang, B., Lee, D.H., Ting, A.K., Neiswender, H., Kim, C.H., Carpenter-Hyland, E., Gao, T.M. and Xiong, W.C., 2008. "Retrograde regulation of motoneuron differentiation by muscle β-catenin". Nature neuroscience, 11(3), pp.262-268.

83. Todd, K.J., Darabid, H. and Robitaille, R., 2010. "Perisynaptic glia discriminate patterns of motor nerve activity and influence plasticity at the neuromuscular junction". Journal of Neuroscience, 30(35), pp.11870-11882.

84. Lee, Y.I., Li, Y., Mikesh, M., Smith, I., Nave, K.A., Schwab, M.H. and Thompson, W.J., 2016. "Neuregulin1 displayed on motor axons regulates terminal Schwann cell-mediated synapse elimination at developing neuromuscular junctions". Proceedings of the National Academy of Sciences, 113(4), pp.479-487.

85. Missias, A.C., Chu, G.C., Klocke, B.J., Sanes, J.R. and Merlie, J.P., 1996. "Maturation of the Acetylcholine Receptor in Skeletal Muscle: Regulation of the AChR γ-to-ϵ Switch". Developmental biology, 179(1), pp.223-238.

86. Yumoto, N., Wakatsuki, S. and Sehara-Fujisawa, A., 2005. "The acetylcholine receptor γ-to-ε switch occurs in individual endplates". Biochemical and biophysical research communications, 331(4), pp.1522-1527.

87. Rudolf, R. and Straka, T., 2019. "Nicotinic acetylcholine receptor at vertebrate motor endplates: Endocytosis, recycling, and degradation". Neuroscience letters, 711, pp.134434.

88. Bernadzki, K.M., Rojek, K.O. and Prószyński, T.J., 2014. „Podosomes in muscle cells and their role in the remodeling of neuromuscular postsynaptic machinery". European journal of cell biology, 93(10-12), pp.478-485.

89. Dai, Z., Luo, X., Xie, H. and Peng, H.B., 2000. "The actin-driven movement and formation of acetylcholine receptor clusters". The Journal of cell biology, 150(6), pp.1321-1334.

90. Cartaud, A., Stetzkowski-Marden, F., Maoui, A. and Cartaud, J., 2011. “Agrin triggers the clustering of raft-associated acetylcholine receptors through actin cytoskeleton reorganization”. Biology of the cell, 103(6), pp.287-301.

91. Zou, S. and Pan, B.X., 2022. “Post-synaptic specialization of the neuromuscular junction: junctional folds formation, function, and disorders”. Cell & Bioscience, 12(1), pp.93.

92. Hughes, B.W., Kusner, L.L. and Kaminski, H.J., 2006. “Molecular architecture of the neuromuscular junction”. Muscle & Nerve: Official Journal of the American Association of Electrodiagnostic Medicine, 33(4), pp.445-461.

93. Serra, A., Ruff, R.L. and Leigh, R.J., 2012. “Neuromuscular transmission failure in myasthenia gravis: decrement of safety factor and susceptibility of extraocular muscles”. Annals of the New York Academy of Sciences, 1275(1), pp.129-135.

94. Belhasan, D.C. and Akaaboune, M., 2020. “The role of the dystrophin glycoprotein complex on the neuromuscular system”. Neuroscience letters, 722, 134833.

95. Gingras, J., Gawor, M., Bernadzki, K.M., Grady, R.M., Hallock, P., Glass, D.J., Sanes, J.R. and Proszynski, T.J., 2016. “α-Dystrobrevin-1 recruits Grb2 and α-catulin to organize neurotransmitter receptors at the neuromuscular junction”. Journal of cell science, 129(5), pp.898-911.

96. Jacobson, C., Côté, P.D., Rossi, S.G., Rotundo, R.L. and Carbonetto, S., 2001. “The dystroglycan complex is necessary for stabilization of acetylcholine receptor clusters at neuromuscular junctions and formation of the synaptic basement membrane”. The Journal of cell biology, 152(3), pp.435-450.

97. Gee, S.H., Montanaro, F., Lindenbaum, M.H. and Carbonetto, S., 1994. “Dystroglycan-α, a dystrophin-associated glycoprotein, is a functional agrin receptor”. Cell, 77(5), pp.675-686.

98. Montanaro, F., Gee, S.H., Jacobson, C., Lindenbaum, M.H., Froehner, S.C. and Carbonetto, S., 1998. “Laminin and α-dystroglycan mediate acetylcholine receptor aggregation via a MuSK-independent pathway”. Journal of Neuroscience, 18(4), pp.1250-1260.

99. Taniguchi, M., Kurahashi, H., Noguchi, S., Fukudome, T., Okinaga, T., Tsukahara, T., Tajima, Y., Ozono, K., Nishino, I., Nonaka, I. and Toda, T., 2006. “Aberrant neuromuscular junctions and delayed terminal muscle fiber maturation in α-dystroglycanopathies”. Human molecular genetics, 15(8), pp.1279-1289.

100. Tinsley, J., Deconinck, N., Fisher, R., Kahn, D., Phelps, S., Gillis, J.M. and Davies, K., 1998. “Expression of full-length utrophin prevents muscular dystrophy in mdx mice”. Nature medicine, 4(12), pp.1441-1444.

101. Guiraud, S., Roblin, D. and Kay, D.E., 2018. “The potential of utrophin modulators for the treatment of Duchenne muscular dystrophy”. Expert Opinion on Orphan Drugs, 6(3), pp.179-192.

102. Aittaleb, M., Martinez-Pena y Valenzuela, I. and Akaaboune, M., 2017. “Spatial distribution and molecular dynamics of dystrophin glycoprotein components at the neuromuscular junction in vivo”. Journal of cell science, 130(10), pp.1752-1759.

103. Zhao, K., Shen, C., Li, L., Wu, H., Xing, G., Dong, Z., Jing, H., Chen, W., Zhang, H., Tan, Z. and Pan, J., 2018. “Sarcoglycan alpha mitigates neuromuscular junction decline in aged mice by stabilizing LRP4”. Journal of Neuroscience, 38(41), pp.8860-8873.

104. Peters, M.F., Sadoulet-Puccio, H.M., Mark Grady, R., Kramarcy, N.R., Kunkel, L.M., Sanes, J.R., Sealock, R. and Froehner, S.C., 1998. “Differential membrane localization and intermolecular associations of α-dystrobrevin isoforms in skeletal muscle”. The Journal of cell biology, 142(5), pp.1269-1278.

105. Grady, R.M., Akaaboune, M., Cohen, A.L., Maimone, M.M., Lichtman, J.W. and Sanes, J.R., 2003. “Tyrosine-phosphorylated and nonphosphorylated isoforms of α-dystrobrevin: roles in skeletal muscle and its neuromuscular and myotendinous junctions”. The Journal of cell biology, 160(5), pp.741-752.

106. Kummer, T.T., Misgeld, T., Lichtman, J.W. and Sanes, J.R., 2004. “Nerve-independent formation of a topologically complex postsynaptic apparatus”. The Journal of cell biology, 164(7), pp.1077-1087.

107. Pęziński, M., Daszczuk, P., Pradhan, B.S., Lochmüller, H. and Prószyński, T.J., 2020. “An improved method for culturing myotubes on laminins for the robust clustering of postsynaptic machinery”. Scientific Reports, 10(1), pp.4524.

108. Proszynski, T.J., Gingras, J., Valdez, G., Krzewski, K. and Sanes, J.R., 2009. “Podosomes are present in a postsynaptic apparatus and participate in its maturation”. Proceedings of the National Academy of Sciences, 106(43), pp.18373-18378.

109. Thompson, O., Kleino, I., Crimaldi, L., Gimona, M., Saksela, K. and Winder, S.J., 2008. “Dystroglycan, Tks5 and Src mediated assembly of podosomes in myoblasts”. PloS one, 3(11), e3638.

110. Murphy, D.A. and Courtneidge, S.A., 2011. “The'ins' and'outs' of podosomes and invadopodia: characteristics, formation and function”. Nature reviews Molecular cell biology, 12(7), pp.413-426.

111. Fletcher, D.A. and Mullins, R.D., 2010. “Cell mechanics and the cytoskeleton”. Nature, 463(7280), pp.485-492.

112. Desai, A. and Mitchison, T.J., 1997. “Microtubule polymerization dynamics” Annual review of cell and developmental biology, 13(1), pp.83-117.

113. Herrmann, H. and Aebi, U., 2016. “Intermediate filaments: structure and assembly”. Cold Spring Harbor Perspectives in Biology, 8(11), pp.018242.

114. Fuchs, E. and Weber, K., 1994. “Intermediate filaments: structure, dynamics, function and disease”. Annual review of biochemistry, 63(1), pp.345-382.

115. Pollard, T.D., 2017. “What we know and do not know about actin”. The actin cytoskeleton, pp.331-347.

116. Dominguez, R. and Holmes, K.C., 2011. “Actin structure and function”. Annual review of biophysics, 40, pp.169-186.

117. Cheever, T.R. and Ervasti, J.M., 2013. “Actin isoforms in neuronal development and function”. International review of cell and molecular biology, 301, pp.157-213.

118. Perrin, B.J. and Ervasti, J.M., 2010. “The actin gene family: function follows isoform”. Cytoskeleton, 67(10), pp.630-634.

119. Papponen, H., Kaisto, T., Leinonen, S., Kaakinen, M. and Metsikkö, K., 2009. “Evidence for γ-actin as a Z disc component in skeletal myofibers”. Experimental Cell Research, 315(2), pp.218-225.

120. Nakata, T., Nishina, Y. and Yorifuji, H., 2001. “Cytoplasmic γ actin as a Z-disc protein”. Biochemical and biophysical research communications, 286(1), pp.156-163.

121. Sonnemann, K.J., Fitzsimons, D.P., Patel, J.R., Liu, Y., Schneider, M.F., Moss, R.L. and Ervasti, J.M., 2006. “Cytoplasmic γ-actin is not required for skeletal muscle development but its absence leads to a progressive myopathy”. Developmental cell, 11(3), pp.387-397.

122. Belyantseva, I.A., Perrin, B.J., Sonnemann, K.J., Zhu, M., Stepanyan, R., McGee, J., Frolenkov, G.I., Walsh, E.J., Friderici, K.H., Friedman, T.B. and Ervasti, J.M., 2009. “γ-Actin is required for cytoskeletal maintenance but not development”. Proceedings of the National Academy of Sciences, 106(24), pp.9703-9708.

123. Hanft, L.M., Rybakova, I.N., Patel, J.R., Rafael-Fortney, J.A. and Ervasti, J.M., 2006. “Cytoplasmic γ-actin contributes to a compensatory remodeling response in dystrophin-deficient muscle”. Proceedings of the National Academy of Sciences, 103(14), pp.5385-5390.

124. Henderson, C.A., Gomez, C.G., Novak, S.M., Mi-Mi, L. and Gregorio, C.C., 2018. “Overview of the muscle cytoskeleton”. Comprehensive Physiology, 7(3), pp.891–944.

125. Wang, Z., Grange, M., Wagner, T., Kho, A.L., Gautel, M. and Raunser, S., 2021. “The molecular basis for sarcomere organization in vertebrate skeletal muscle”. Cell, 184(8), pp.2135-2150.

126. Hitchcock-DeGregori, S.E. and Barua, B., 2017. “Tropomyosin structure, function, and interactions: a dynamic regulator”. Fibrous proteins: structures and mechanisms, Sub-Cellular Biochemistry book series, 82, pp.253–284.

127. Loong, C.K., Badr, M.A. and Chase, P.B., 2012. “Tropomyosin flexural rigidity and single Ca2+ regulatory unit dynamics: implications for cooperative regulation of cardiac muscle contraction and cardiomyocyte hypertrophy”. Frontiers in Physiology, 3, pp.80.

128. Farah, C.S. and Reinach, F.C., 1995. “The troponin complex and regulation of muscle contraction”. The FASEB Journal, 9(9), pp.755-767.

129. Tobacman, L.S., 2021. “Troponin revealed: uncovering the structure of the thin filament on-off switch in striated muscle”. Biophysical Journal, 120(1), pp.1-9.

130. Pollard, T.D., 2007. “Regulation of actin filament assembly by Arp2/3 complex and formins”. Annual Reviews of Biophysics and Biomolecular Structure, 36, pp.451-477.

131. Jégou, A. and Romet-Lemonne, G., 2021. “Mechanically tuning actin filaments to modulate the action of actin-binding proteins”. Current Opinion in Cell Biology, 68, pp.72-80.

132. Goley, E.D. and Welch, M.D., 2006. “The ARP2/3 complex: an actin nucleator comes of age”. Nature reviews Molecular cell biology, 7(10), pp.713-726.

133. Helgeson, L.A. and Nolen, B.J., 2013. “Mechanism of synergistic activation of Arp2/3 complex by cortactin and N-WASP”. Elife, 2, pp.00884.

134. Schnoor, M., Stradal, T.E. and Rottner, K., 2018. “Cortactin: cell functions of a multifaceted actin-binding protein”. Trends in cell biology, 28(2), pp.79-98.

135. Ammer, A.G. and Weed, S.A., 2008. “Cortactin branches out: roles in regulating protrusive actin dynamics”. Cell motility and the cytoskeleton, 65(9), pp.687-707.

136. Weed, S.A., Karginov, A.V., Schafer, D.A., Weaver, A.M., Kinley, A.W., Cooper, J.A. and Parsons, J.T., 2000. “Cortactin localization to sites of actin assembly in lamellipodia requires interactions with F-actin and the Arp2/3 complex”. The Journal of cell biology, 151(1), pp.29-40.

137. Jeannot, P. and Besson, A., 2020. “Cortactin function in invadopodia”. Small GTPases, 11(4), pp.256-270.

138. Li, T., Zhang, C., Hassan, S., Liu, X., Song, F., Chen, K., Zhang, W. and Yang, J., 2018. “Histone deacetylase 6 in cancer”. Journal of hematology & oncology, 11(1), pp.1-10.

139. Kim, J.Y., Hwang, H.G., Lee, J.Y., Kim, M. and Kim, J.Y., 2020. “Cortactin deacetylation by HDAC6 and SIRT2 regulates neuronal migration and dendrite morphogenesis during cerebral cortex development”. Molecular Brain, 13, pp.1-15.

140. Osseni, A., Ravel-Chapuis, A., Thomas, J.L., Gache, V., Schaeffer, L. and Jasmin, B.J., 2020. “HDAC6 regulates microtubule stability and clustering of AChRs at neuromuscular junctions”. Journal of Cell Biology, 219(8).

141. Rust, M.B., Khudayberdiev, S., Pelucchi, S. and Marcello, E., 2020. “CAPt’n of actin dynamics: Recent advances in the molecular, developmental and physiological functions of cyclase-associated protein (CAP)”. Frontiers in cell and developmental biology, 8, pp.586631.

142. Ono, S., 2013. “The role of cyclase-associated protein in regulating actin filament dynamics–more than a monomer-sequestration factor”. Journal of cell science, 126(15), pp.3249-3258.

143. Fedor-Chaiken, M., Deschenes, R.J. and Broach, J.R., 1990. “SRV2, a gene required for RAS activation of adenylate cyclase in yeast”. Cell, 61(2), pp.329-340.

144. Freeman, N.L., Chen, Z., Horenstein, J., Weber, A. and Field, J., 1995. “An actin monomer binding activity localizes to the carboxyl-terminal half of the Saccharomyces cerevisiae cyclase-associated protein”. Journal of Biological Chemistry, 270(10), pp.5680-5685.

145. Hubberstey, A.V. and Mottillo, E.P., 2002. “Cyclase-associated proteins: CAPacity for linking signal transduction and actin polymerization”. The FASEB Journal, 16(6), pp.487-499.

146. Jansen, S., Collins, A., Golden, L., Sokolova, O. and Goode, B.L., 2014. “Structure and mechanism of mouse cyclase-associated protein (CAP1) in regulating actin dynamics”. Journal of Biological Chemistry, 289(44), pp.30732-30742.

147. Kotila, T., Wioland, H., Enkavi, G., Kogan, K., Vattulainen, I., Jégou, A., Romet-Lemonne, G. and Lappalainen, P., 2019. “Mechanism of synergistic actin filament pointed end depolymerization by cyclase-associated protein and cofilin”. Nature Communications, 10(1), pp.5320.

148. Kotila, T., Kogan, K., Enkavi, G., Guo, S., Vattulainen, I., Goode, B.L. and Lappalainen, P., 2018. “Structural basis of actin monomer re-charging by cyclase-associated protein”. Nature communications, 9(1), pp.1892.

149. Bertling, E., Hotulainen, P., Mattila, P.K., Matilainen, T., Salminen, M. and Lappalainen, P., 2004. “Cyclase-associated protein 1 (CAP1) promotes cofilin-induced actin dynamics in mammalian nonmuscle cells”. Molecular biology of the cell, 15(5), pp.2324-2334.

150. Colpan, M., Iwanski, J. and Gregorio, C.C., 2021. “CAP2 is a regulator of actin pointed end dynamics and myofibrillogenesis in cardiac muscle”. Communications Biology, 4(1), pp.365.

151. Kepser, L.J., Damar, F., De Cicco, T., Chaponnier, C., Prószyński, T.J., Pagenstecher, A. and Rust, M.B., 2019. “CAP2 deficiency delays myofibril actin cytoskeleton differentiation and disturbs skeletal muscle architecture and function”. Proceedings of the National Academy of Sciences, 116(17), pp.8397-8402.

152. Peche, V.S., Holak, T.A., Burgute, B.D., Kosmas, K., Kale, S.P., Wunderlich, F.T., Elhamine, F., Stehle, R., Pfitzer, G., Nohroudi, K. and Addicks, K., 2013. “Ablation of cyclase-associated protein 2 (CAP2) leads to cardiomyopathy”. Cellular and molecular life sciences, 70, pp.527-543.

153. Xiong, Y., Bedi, K., Berritt, S., Attipoe, B.K., Brooks, T.G., Wang, K., Margulies, K.B. and Field, J., 2019. “Targeting MRTF/SRF in CAP2-dependent dilated cardiomyopathy delays disease onset”. JCI insight, 4(6), pp.124629.

154. Kepser, L.J., Khudayberdiev, S., Hinojosa, L.S., Macchi, C., Ruscica, M., Marcello, E., Culmsee, C., Grosse, R. and Rust, M.B., 2021. “Cyclase-associated protein 2 (CAP2) controls MRTF-A localization and SRF activity in mouse embryonic fibroblasts”. Scientific Reports, 11(1), pp.4789.

155. Kumar, A., Paeger, L., Kosmas, K., Kloppenburg, P., Noegel, A.A. and Peche, V.S., 2016. “Neuronal actin dynamics, spine density and neuronal dendritic complexity are regulated by CAP2”. Frontiers in Cellular Neuroscience, 10, pp.180.

156. Oh, H.J., Abraham, L.S., van Hengel, J., Stove, C., Proszynski, T.J., Gevaert, K., DiMario, J.X., Sanes, J.R., Van Roy, F. and Kim, H., 2012. “Interaction of α-catulin with dystrobrevin contributes to integrity of dystrophin complex in muscle”. Journal of Biological Chemistry, 287(26), pp.21717-21728.

157. Madhavan, R., Gong, Z.L., Ma, J.J., Chan, A.W. and Peng, H.B., 2009. “The function of cortactin in the clustering of acetylcholine receptors at the vertebrate neuromuscular junction”. PLoS One, 4(12), e8478.

158. Braun, T. and Arnold, H.H., 1995. Inactivation of Myf-6 and Myf-5 genes in mice leads to alterations in skeletal muscle development. The EMBO journal, 14(6), pp.1176-1186.

159. Schneider, F., Metz, I., Khudayberdiev, S. and Rust, M.B., 2021. “Functional redundancy of cyclase-associated proteins CAP1 and CAP2 in differentiating neurons”. Cells, 10(6), pp.1525.

160. Pelucchi, S., Vandermeulen, L., Pizzamiglio, L., Aksan, B., Yan, J., Konietzny, A., Bonomi, E., Borroni, B., Rust, M., Marino, D.D. and Mikhaylova, M., 2019. “CAP2

is a novel regulator of Cofilin in synaptic plasticity and Alzheimer's disease". bioRxiv, 789552.

161. Bremer, A., Schoumans, J., Nordenskjöld, M., Anderlid, B.M. and Giacobini, M., 2009. "An interstitial deletion of 7.1 Mb in chromosome band 6p22. 3 associated with developmental delay and dysmorphic features including heart defects, short neck, and eye abnormalities". European journal of medical genetics, 52(5), pp.358-362.

162. Taetzsch, T. and Valdez, G., 2018. "NMJ maintenance and repair in aging". Current opinion in physiology, 4, pp.57-64.

163. Bernstein, B.W., Maloney, M.T. and Bamburg, J.R., 2011. "Actin and diseases of the nervous system". Neurobiology of Actin: From Neurulation to Synaptic Function, pp.201-234.

164. Jones, R.A., Harrison, C., Eaton, S.L., Hurtado, M.L., Graham, L.C., Alkhammash, L., Oladiran, O.A., Gale, A., Lamont, D.J., Simpson, H. and Simmen, M.W., 2017. "Cellular and molecular anatomy of the human neuromuscular junction". Cell reports, 21(9), pp.2348-2356.

165. Oda, K., 1984. "Age changes of motor innervation and acetylcholine receptor distribution on human skeletal muscle fibres". Journal of the neurological sciences, 66(2-3), pp.327-338.

166. Brill, M.S., Kleele, T., Ruschkies, L., Wang, M., Marahori, N.A., Reuter, M.S., Hausrat, T.J., Weigand, E., Fisher, M., Ahles, A. and Engelhardt, S., 2016. "Branch-specific microtubule destabilization mediates axon branch loss during neuromuscular synapse elimination. Neuron", 92(4), pp.845-856.

167. Cingolani, L.A. and Goda, Y., 2008. "Actin in action: the interplay between the actin cytoskeleton and synaptic efficacy". Nature Reviews Neuroscience, 9(5), pp.344-356.

168. Pacheco, A. and Gallo, G., 2016. "Actin filament-microtubule interactions in axon initiation and branching". Brain research bulletin, 126, pp.300-310.

169. Cammarata, G.M., Bearce, E.A. and Lowery, L.A., 2016. "Cytoskeletal social networking in the growth cone: How+ TIPs mediate microtubule-actin cross-linking to drive axon outgrowth and guidance". Cytoskeleton, 73(9), pp.461-476.

170. Ka, M. and Kim, W.Y., 2016. "Microtubule-actin crosslinking factor 1 is required for dendritic arborization and axon outgrowth in the developing brain". Molecular neurobiology, 53, pp.6018-6032.

171. Ervasti, J.M. and Campbell, K.P., 1993. "A role for the dystrophin-glycoprotein complex as a transmembrane linker between laminin and actin". The Journal of cell biology, 122(4), pp.809-823.

172. Grady, R.M., Zhou, H., Cunningham, J.M., Henry, M.D., Campbell, K.P. and Sanes, J.R., 2000. “Maturation and maintenance of the neuromuscular synapse: genetic evidence for roles of the dystrophin–glycoprotein complex”. Neuron, 25(2), pp.279-293.

173. Belhasan, D.C. and Akaaboune, M., 2020. “The role of the dystrophin glycoprotein complex on the neuromuscular system”. Neuroscience letters, 722, pp.134833.

174. Valenzuela, I.M.P.Y., Chen, P.J., Barden, J., Kosloski, O. and Akaaboune, M., 2022. “Distinct roles of the dystrophin–glycoprotein complex: α-dystrobrevin and α-syntrophin in the maintenance of the postsynaptic apparatus of the neuromuscular synapse”. Human Molecular Genetics, 31(14), pp.2370-2385.

175. Grady, R.M., Grange, R.W., Lau, K.S., Maimone, M.M., Nichol, M.C., Stull, J.T. and Sanes, J.R., 1999. “Role for α-dystrobrevin in the pathogenesis of dystrophin-dependent muscular dystrophies”. Nature cell biology, 1(4), pp.215-220.

176. Nascimento, A., Bruels, C.C., Donkervoort, S., Foley, A.R., Codina, A., Milisenda, J.C., Estrella, E.A., Li, C., Pijuan, J., Draper, I. and Hu, Y., 2023. “Variants in DTNA cause a mild, dominantly inherited muscular dystrophy”. Acta Neuropathologica, 145(4), pp.479-496.

177. Bernadzki, K.M., Gawor, M., Pęziński, M., Mazurek, P., Niewiadomski, P., Rędowicz, M.J. and Prószyński, T.J., 2017. “Liprin-α-1 is a novel component of the murine neuromuscular junction and is involved in the organization of the postsynaptic machinery”. Scientific reports, 7(1), pp.9116.

178. Bernadzki, K.M., Daszczuk, P., Rojek, K.O., Pęziński, M., Gawor, M., Pradhan, B.S., De Cicco, T., Bijata, M., Bijata, K., Włodarczyk, J. and Prószyński, T.J., (2020). “Arhgef5 binds α-dystrobrevin 1 and regulates neuromuscular junction integrity”. Frontiers in Molecular Neuroscience, 13, pp.104.

179. Yin, M., Ma, W. and An, L., 2017. “Cortactin in cancer cell migration and invasion”. Oncotarget, 8(50), pp.88232.

180. Ji, R., Zhu, X.J., Wang, Z.R. and Huang, L.Q., 2020. “Cortactin in Epithelial–Mesenchymal Transition”. Frontiers in Cell and Developmental Biology, 8, pp.585619.

181. Bloemberg, D. and Quadrilatero, J., 2012. “Rapid determination of myosin heavy chain expression in rat, mouse, and human skeletal muscle using multicolor immunofluorescence analysis”. PloS one, 7(4), pp.35273.

182. Chakkalakal, J.V., Nishimune, H., Ruas, J.L., Spiegelman, B.M. and Sanes, J.R., 2010. “Retrograde influence of muscle fibers on their innervation revealed by a novel marker for slow motoneurons”. Development, 137(20), pp.3489-3499.

183. Magalhaes-Gomes, M.P., Motta-Santos, D., Schetino, L.P., Andrade, J.N., Bastos, C.P., Guimarães, D.A., Vaughan, S.K., Martinelli, P.M., Guatimosim, S., Pereira, G.S.

and Coimbra, C.C., 2018. “Fast and slow-twitching muscles are differentially affected by reduced cholinergic transmission in mice deficient for VAChT: A mouse model for congenital myasthenia”. Neurochemistry international, 120, pp.1-12.

184. Cornelius, J., Rottner, K., Korte, M. and Michaelsen-Preusse, K., 2021. “Cortactin contributes to activity-dependent modulation of spine actin dynamics and spatial memory formation”. Cells, 10(7), pp.1835.